Lehrstuhl für Fluidmechanik und Prozessautomation
der Technischen Universität München

# High Pressure Inactivation of Bacteria: Mathematical and Microbiological Aspects

Klaus Valentin Kilimann

Vollständiger Abdruck der von der Fakultät Wissenschaftszentrum Weihenstephan für Ernährung, Landnutzung und Umwelt der Technischen Universität München zur Erlangung des akademischen Grades eines

**Doktor-Ingenieurs (Dr.-Ing.)**

genehmigten Dissertation.

Vorsitzender:

Univ.-Prof. Dr.-Ing. Eberhard Geiger

Prüfer der Dissertation:

1. Assistant Prof. Dr.rer.nat. Michael Gänzle,
   University of Alberta, Edmonton / Kanada
2. Univ.-Prof. Dr.-Ing. habil. Antonio Delgado
3. Prof. Dr.-Ing. Christoph Hartmann,
   The German University in Cairo / Ägypten (schriftl. Beurteilung)

Die Dissertation wurde am 27.07.2005 bei der Technischen Universität München eingereicht und durch die Fakultät Wissenschaftszentrum Weihenstephan für Ernährung, Landnutzung und Umwelt am 30.08.2005 angenommen.

Meinen Großeltern

*Hans Kilimann* † 19.04.2004

*Sophie Kilimann* † 29.08.2004

*Veronika Thomann* † 02.07.2005

# CONTENTS

# PUBLICATIONS

REVIEWED PAPERS

Kilimann KV, Hartmann C, Delgado A, Vogel RF, Gänzle MG. 2005. A Fuzzy logic based model for the multi-stage high pressure inactivation of *Lactococcus lactis* ssp. *cremoris* MG 1363, **International Journal of Food Microbiology** 98 (1) 89-108

Kilimann KV, Hartmann C, Vogel RF, and Gänzle MG. 2005. Differential inactivation of glucose- and glutamate dependent acid resistance of *Escherichia coli* TMW 2.497 by high-pressure treatments, accepted in **Systematic and Applied Microbiology**

Kilimann KV, Hartmann C, Delgado A, Vogel RF, Gänzle MG. 2005. Combined high pressure and temperature induced lethal and sublethal injury of *Lactococcus lactis* - application of multivariate statistical analysis, submitted to **International Journal of Food Microbiology**

Gänzle MG, Kilimann KV, Hartmann C, Vogel RF, Delgado A. 2005. Data Mining and Fuzzy Modelling of high pressure inactivation pathways of *Lactococcus lactis*, submitted to **Innovative Food Science and Emerging Technologies**

Kilimann KV, Kitsubun P, Delgado A, Gänzle MG, Chapleau N, Le Bail A, Hartmann C. 2005. Experimental and numerical study of heterogeneous pressure-temperature induced lethal and sublethal injury of *Lactococcus lactis* in a medium scale high pressure autoclave, submitted to **Biotechnology and Bioengineering**

Kilimann KV, Hartmann C, Delgado A, Vogel RF, Doster W, Gänzle MG. 2005. A FT-IR spectroscopical study of the inactivation of *Lactococcus lactis* – correlations between FT-IR data and lethal and sublethal injury, **to be submitted**

REVIEWED CONFERENCE CONTRIBUTIONS

Kilimann KV, Hartmann C, Gänzle MG. 2004. Application of Fuzzy Logic and Statistical Analysis for modelling high-pressure microbial inactivation, In: (P. Neittaanmäki, T. Rossi, K. Majava, O. Pironneau) **4th European Congress on Computational Methods in Applied Sciences and Engineering ECCOMAS 2004**, Jyvaskyla, Finland, 24.-28.07.2004 (ISBN 951-39-1868-8)

Kilimann KV, Hartmann C, Gänzle MG. 2004. Application of Multivariate Statistical Analysis and Human Expert Knowledge in Fuzzy Logic Modelling of the Multi-Stage High-Pressure Inactivation of *Lactococcus lactis* ssp. *cremoris* MG 1363, **3rd International Conference on Simulation in Food and Bio Industries FOODSIM 2004**, Wageningen, Netherlands, 16.-18.06.2004 (ISBN 90-77381-11-2)

Kilimann KV, Hartmann C, Gänzle MG. 2003. Fuzzy based description of multi-stage high- pressure inactivation of *Lactococcus lactis* ssp. *cremoris* MG 1363, **4th International Conference on Predictive Modelling in Foods**, 15-19.06.2003, Quimper, France (ISBN 90-5682-400-7)

CONFERENCE CONTRIBUTIONS

Kilimann KV, Hartmann C, Delgado A, Gänzle MG. 2005. Non-linear modelling and statistical anlaysis of multi-stage high-pressure inactivation of lactic acid bacteria. **76. Jahrestagung der Gesellschaft für Angewandte Mathematik und Mechanik**, Université du Luxembourg, Luxembourg, 28.03.-01.04.2005

Kilimann KV, Hartmann C, Delgado A, Gänzle MG. 2004. Data mining and fuzzy modelling of high pressure inactivation pathways of *Lactococcus lactis*. **High pressure Bioscience and Biotechnology**, Rio de Janeiro, Brasil, 27.-30.9.2004

Kilimann KV, Hartmann C, Gänzle MG (Poster). 2004. Synergistic or antagonistic effects of combined high pressure pH inactivation of *E. coli*: Intracellular pH versus cell death. **High pressure Bioscience and Biotechnology**, Rio de Janeiro, Brasil, 27.-30.9.2004

Eberhard M, Benning R, Kilimann K, Petermeier H, Delgado A. 2004. Betriebsdatenbasierende Optimierung des Filtrationsprozesses mittels Data Mining. **Filtrationstechnisches Symposium**, Freising, Germany, 13-14.09.2004

Kilimann KV, Hartmann C, Delgado A, Vogel RF, Gänzle MG (Poster). 2003. Modellierung der mehrstufigen Inaktivierung von *Lactococcus lactis* ssp. *cremoris* MG 1363 durch hohen hydrostatischen Druck mit Hilfe eines Fuzzy-Logik Ansatzes, **GVC Jahrestagung der Biotechnologen**, Mannheim, Germany, 16.-18.09.2003

Eberhard M, Benning R, Kilimann K, Petermeier H, Delgado A (Poster). 2005. Optimisation of the filtration process by application of data mining. **30th International EBC Congress**, Praha, Czech Republic, 14.-19.5.2005

# ABBREVIATIONS

| | |
|---|---|
| Adi | arginine decarboxylase |
| arg | arginine |
| $a_w$ | water activity |
| CFU | viable cell counts |
| CFUsub | stress resistant cell counts |
| COG | center of gravity method |
| D/H | hydrogen-deuterium |
| $D_2O$ | deuterium oxide |
| E | error matrix |
| EB | ethidium bromide |
| EHEC | enterohemorrhagic |
| em | emission |
| ex | excitation |
| exp | experiment |
| FT-IR | fourier transform infrared spectroscopy |
| g | relative centrifugal force |
| GABA | glutamate-γ-aminobutyrate antiporter |
| GAD | glutamate decarboxylase |
| GFP | green fluorescent protein |
| Glu | glutamate |
| h | hour |
| HD-CFD | high pressure computer fluid dynamics |
| HP | high pressure |
| INT | 2-(4-iodophenyl)-3-(-4-nitrophenyl)-5-phenyltetrazolium chloride |

| | |
|---|---|
| k | rate constant |
| K | equilibrium constant |
| l | litre |
| L-B | luria-bertani |
| LmrP | secondary drug transporter located in the membrane of *Lactococcus lactis* |
| m | growth rate constant |
| $m_R$ | growth rate constant of the resistant fraction |
| $m_S$ | growth rate constant of the sensitive fraction |
| M(t) | inactivated fraction of the population |
| $M_{max}$ | maximal possible inactivated population |
| MA | metabolic activity |
| MDR | multidrug resistance transporter |
| MES | 2-(N-morpholino)ethanesulfonic acid |
| MI | membrane integrity |
| min | minute |
| ml | milliliter |
| OD | optical density |
| p | pressure |
| PBO | phosphate buffer |
| $pH_{ex}$ | extracellular pH |
| $pH_{in}$ | intracellular pH |
| PI | propidium iodide |
| PCA | principal component analysis |
| PCs | principal components |
| PCR | polymerase chain reaction |

| | |
|---|---|
| R | gas constant |
| RFI | relative fluorescence intensity |
| S | score matrix |
| s | second |
| Sim | simulation |
| SST | shear stress transport |
| t | time |
| $t_0$ | half-life-period |
| $t_R$ | half-life-period of the resistant fraction |
| $t_S$ | half-life-period of the sensitive fraction |
| T | absolute temperature |
| $T_m$ | melting temperature |
| $T_0$ | temperature dependent point of inflection |
| TUM | Technische Universität München |
| V | loading matrix |
| V(r*) | residual variance |
| $\Delta V$ | reaction volume |
| $\Delta V^*$ | activation volume |
| vol | volume |
| w. d. | without publishing date |
| X | data matrix |
| yjde | agmatin antiporter |
| $\varepsilon$ | limit of convergence |
| $\mu$ | dependency of the fuzzy classifiers |

# 1. Introduction

Most preserved foods are thermally processed by subjecting the food to a temperature of 60°C to 121°C from a few seconds to several minutes (Kessler, 1996). Elevated process times and temperatures are used resulting from the resistance of bacteria. This resistance strongly depends on several indicators. First, the stage of the growth cycle at which the organisms were subjected to the heat treatment plays a major role for its resistance magnitude. Cells out of stationary phase are more resistant than cells out of exponential phase due to *de novo* protein synthesis occuring by entering stationary phase. Second, the medium composition affects the inactivation in different ways (pH, $a_w$, osmolytes). Bacteria exhibit a maximal resistance against temperature treatment at optimal pH compared to optimal growth pH. Furthermore, a reduction of the $a_w$ may result in a higher resistance to thermal treatment, due to the fact, that heat is transmitted by exisiting water in food. Protective additives like fatty acids, proteins, carbohydrates, or osmolytes in molar concentrations may also prevent bacterial inactivation from thermal treatment. The protectants work in that way, that they surround cells in the manner of protection colloids. Due to the reduced heat conductivity, heat transfer is hampered and the inactivation of the bacteria will not take place or occurs with certain time delay (Krämer, 1997). A differentiation of different types of heat treatment like pasteurisation or sterilisation is given in Kessler (1996) and Schlegel (1997). Differences were found in the temperature level and/or the treatment time. In terms of process induced sensorial, nutritional, and chemical reactions due to heat, a mild process with a maxima of food safety is desired to obtain minima of temperature related changes.

Because of the fact that not only the shelf life but also the quality of food is becoming increasingly important to consumers, the concept of non-thermal methods for food preservation has gained increased attention during the last decade. Alternative methods such as high pressure (HP) preservation of food are developed to reduce the quality degradation of foods resulting from thermal processing (Knorr, 1996; Hendrickx et al., 1998; Butz et al., 2002; Harte et al., 2002; Krebbers et al., 2002). Alternatives for thermal processes may also include oscillating magnetic fields, high intensity pulsed electric fields, intense light pulses, irradiation, chemicals and biochemicals (Ulmer et al., 2002a; Port et al., 2003; Kim et al., 2004; Devlieghere et al., 2004).

The application area of HP in food industry may additionally range from the inactivation of enzymes, the extraction of useful food ingredients, HP-induced expression of useful genes as

well as freezing and thawing of food which may result in a higher prevention of process-induced damage of structural food components.

## 1.1. General Principle of High Pressure Treatment

Two physical principles govern HP-processing. First, due to its high propagation velocity (3000 m $s^{-1}$ in $H_2O$), high pressure acts instantaneously throughout a mass of food independent of size, shape and food composition (isostatic principle). Nevertheless, package size, shape and composition should be taken into account as factors in process definition, because temperature- or pH-heterogeneity may appear in complex food matrices (Pehl et al., 2000; Pehl and Delgado, 2002; Hartmann and Delgado, 2002; de Heij, 2003; Hartmann and Delgado; 2003, Hartmann et al.; 2004). Secondly, every pressure induced phenomenon (phase transition, change in molecular configuration, chemical reaction) is related to a change in volume (Cheftel, 1995; Stippl, 2005). At equilibrium in homogeneous systems, a decrease of volume is enhanced by pressure application and vice versa. Relations between equilibrium constant and volume change of this reaction is given by the equation of Planck (Planck, 1887)

$$\left(\frac{\partial \ln K}{\partial p}\right)_T = -\frac{\Delta V}{RT} \tag{1}$$

where K is the equilibrium constant, p the pressure, T the absolute temperature and R the gas constant. ΔV represents the difference between the final and the initial volume.

In formal analogy, the dependence of the rate constant k on pressure can be written as

$$\left(\frac{\partial \ln k}{\partial p}\right)_T = -\frac{\Delta V^*}{RT} \tag{2}$$

where $\Delta V^*$ represents the activation volume and k the rate constant of a chemical or enzymatical reaction. Both equations include the solute and the surrounding solvent of the system. Thus, any balanced state connected with a non-zero volume change will be shifted to a more compact state by pressure application; any reaction connected with a positve or negative activation volume will be slowed down or forced by pressure (Evans, 1935; Gross und Jaenicke, 1994). A review about activation and reaction volumes is given by Asano and Le Noble (1978).

Further on, the work of compression during pressure treatment will increase the temperature depending on the composition of the food,. e.g. 2-3 K per 100 MPa in pure $H_2O$. On the contrary, it is observed in foods that contain a higher amount of fat (e.g. butter, cream, mayonnaise), that the temperture increase will be larger than the above mentioned one (Rasanayagam et al., 2003). This increase of temperature induces an increase of volume through dilation. Thus, an increase of temperature will affect the rate of reaction according to Arrhenius law as well as the equilibrium constant.

## 1.2. High Pressure Treatment of Biological Systems

Of particular significance is the behaviour of biological systems during or after the process. The effect of HP in combination with different environmental conditions such as different pressure levels, different temperatures, different medium compositions (either baroprotecive or bactericidals ones) has to be analysed. For this purpose, Figure 1 represents schematically the influence of combined pressure-temperature treatment on the denaturation behaviour of proteins. In the presence of baroprotective or bactericidal co-solvents, the elliptical phase boundary may be shifted.

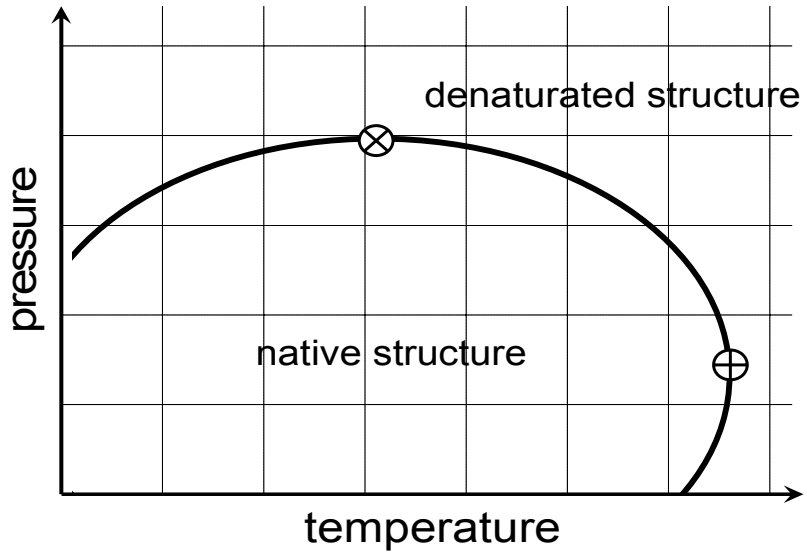


**Figure 1**: Schematic diagram of pressure-temperature dependent denaturation of proteins (Hawley, 1971; Buchner, 2005). The symbols representing either ⊗ a temperature- or ⊕ a pressure-optimum of denaturation.

The phase equilibrium between the native and the denatured state (free energy difference between native and unfolded state) is often described in literature by an elliptical phase boundary. Therefore, a natural explanation could be applied for the phase behaviour of heat and cold denaturation of proteins. If moderate pressure levels are applied, the temperature of heat denaturation increases slightly with pressure. Otherwise, pressure may drive the protein back to the native state if thermally denatured proteins are regarded. A similar behaviour is found if the temperature is changed at an elevated pressure level. Further on, the phase boundary may also be described by a parabolic or hyperbolic shape (Buchner, 2005).

Considering the denaturation of proteins, a temperature optimum exists, with a maximum of pressure resistance as well as a pressure optimum, with a maximum of temperature resistance as it is shown exemplary in Figure 1. The presented elliptical boundary represents just the simplest possible case describing one inactivation mechanism. Specifically, if microorganisms are regarded as containing a many proteins, the elliptical phase boundary may be deformed due to overlapping effects of the analysed system. Furthermore, by adding bactericidals or protectants, the area describing the native structure will be shifted towards higher (protectants) or lower (bactericidals) pressure-temperature configurations. Due to the fact that then microorganisms may be highly resistant to adverse environmental conditions (in the presence of protectants) and will cause human disease through the consumption of insufficiently pasteurised food, the analysis of these phenomena is of technical interest in order to obtain an optimal process configuration. The process should be designed to treat food as gentle as possible, minimising nutritional and chemical changes as well as avoiding any risk for human health.

### 1.2.1. Influence of High Pressure on Proteins

The primary structure of proteins remains intact during the whole HP treatment (Mozhaev et al., 1994). On the other hand, changes in the secondary structure of proteins occur if very high pressure levels are applied. Through treatment at these pressure levels, hydrogen bonds are ruptured. In turn, this leads to irreversible denaturation (Balny and Masson, 1993). Further on, pressure-induced changes in the tertiary structure of proteins under HP conditions are maintained by hydrophobic and ionic interactions (Balny and Masson, 1993). Multimeric proteins, held together by non-covalent bonds, dissociate at pressures lower than 150 MPa, thereby disrupting quaternary structures (Penniston, 1971). Finally, the disruption of the

secondary and tertiary structure of proteins is considered to be major cause of cell death, due to the stopped supply of microorganisms with essential substances like amino acids.

### 1.2.2. Influence of High Pressure on Microorganisms

The efficiency of HP-preservation is influenced by a number of microorganism and environmental related factors. Significant factors are the type and form of microorganisms, the genus, the species and the strain of microorganisms. Additionally, the efficiency of inactivation of microorganisms is strongly influenced by the growth stage, the environmental stress selection mechanisms and the presence of different co-solvents which may act either as baroprotectants or synergistic bactericides.

**Incubation versus Adaptation.** The successful inactivation of microorganisms strongly depends on their anamnesis prior to pressure application. Cells treated with HP show different responses with respect to their state of growth. Cells grown to an exponential phase were more pressure sensitive than cells grown to a stationary phase. HP treatment of cells grown to an exponential phase results in physical damage to the membrane which results in an inability to be resealed. Such a catastrophic loss of membrane integrity results in a loss to the maintenace of homeostasis and leads to cell death (Pagan and Mackey, 2000; McClements et al., 2001; Manas and Mackey, 2004).

Contrariwise, stationary phase *E. coli* strains exhibit a large variation in their resistance to pressure and the most resistant strains are reduced by less than 2 log even after treatments with 800 MPa (Hauben et al., 1997; Alpas et al., 1999; Benito et al., 1999; Pagan et al., 2000). In case of high pressure treatment, current performance standards require a 5D reduction in food production (Anonymous, 2003). Food products are a relevant route of transmission with pathogenic strains of *Escherichia coli*. Especially enterohemorrhagic *E. coli* (EHEC) strains are a major public health concern because the organism has a low infectious dose, is highly resistant to adverse environmental conditions, and causes severe disease symptoms ranging from a mild diarrhea to hemorrhagic colitis and the life threatening hemolytic-uremic syndrome. Outbreaks of *E. coli* were linked to the consumption of meats, apple juice and insufficiently pasteurised milk (Cody et al., 1999; MacDonald et al., 1999; Goh et al., 2002).

For this microorganism, the alternative sigma factor $\sigma^S$ encoded by *rpoS* plays a decisive role for the pressure resistance and the heterogeneity of *rpoS*-alleles contributes to the variation of

pressure resistance of *E. coli* strains (Abee and Wouters, 1999; Robey et al., 2001). The $\sigma^S$ regulon comprises more than 40 genes, and genes activated by $\sigma^S$ specifically contribute to the resistance of *E. coli* to starvation, oxidative stress, low pH, and high osmolarity (Hengge-Aronis, 2002).

Moreover, one of the basic principles of microbial genetics is that incubation in extreme environments such as cold, osmotic, acidic, and heat shock treatments result in the selection of mutants resistant to severe conditions. Increasing high pressure resistance was observed in *Lactobacillus plantarum* after preincubation at elevated temperatures and increasing thermotolerance of *Lactobacillus rhamnosus* GG was found after pre-pressurisation (Ulmer et al., 2002b; Ananta and Knorr, 2003). The change to sublethal environmental growth conditions will induce protection mechanisms resulting in a *de novo* synthesis of general "stress" proteins and in unusual higher durability to preservation (Noma and Hayakawa, 2003; Motshwene et al., 2004; Scheyhing et al., 2004). Additionally, similarities between pressure resistance and heat resistance of *E. coli* strains have been found to be triggered by the constitutive expression of heat shock genes (Aertsen et al., 2004). This stress induced enhanced resistance of microorganisms has to be considered seriously regarding the process design of HP application in the food industry.

**Lethality versus sublethal injury.** Pressure ranging from 200 to 800 MPa at ambient temperature is lethal to vegetative cells of bacteria and higher organisms (Knorr, 1996). Therefore, the magnitude of pressure treatment strongly depends on the pressure level and the pressure application time (Cheftel, 1995; Gervilla et al., 1997). Moreover, temperature during HP processing may influence the lethality of the method significantly if the microbial cells are pressurised at temperatures away from their optimal temperature of growth (Kalchayanand et al., 1998; Ulmer et al., 2002b; Lanza et al., 2004).

Damage to bacterial membranes and membrane bound enzyme systems are assumed to be a major cause of pressure induced sublethal injury (Wouters et al., 1998; Gänzle and Vogel, 2001; Chilton et al., 2001; Smelt et al., 2002). By the use of moderately high pressures, sublethally injured cells fail to survive or thrive in adverse environmental conditions, for example low pH (Garcia-Graells et al., 1998), in the presence of antimicrobial agents such as nisin or lysozyme (Masschalck et al., 2001a and 2001b), or in the presence of high NaCl concentration (Ulmer et al., 2000; Wuytack et al., 2003). Many foods are selective media due to their particular properties such as pH-value and presence of antimicrobial compounds as

well as their thermal history. In those foods, pressure inactivation of specific resistance mechanisms required for growth or survival is sufficient for preservation (Garcia-Graells, 1998; Molina-Gutierrez et al., 2002; Ulmer et al., 2002b). Sublethal pressure treatment reverses the permeability of the membrane to potassium and protons and hence reduces the membrane potential (Molina-Gutierrez et al., 2002; Vogel et al., 2003). Sublethal injury is triggered by the inactivation of membrane bound enzymes involved in pH homeostasis, which accounts for the loss of acid resistance in lactic acid bacteria and *Escherichia coli* (Wouters et al., 1998; Molina-Gutierrez et al., 2002; Kilimann et al., 2005b). Furthermore, sublethal pressure application eliminates the resistance of *E. coli* to various environmental stressors as it compromises outer membrane function (Gänzle and Vogel, 2001), sensitises the cells to the lactoperoxidase system (Van Opstal et al., 2003), and eliminate their acid resistance (Pagan et al., 2001). A sublethal treatment of *E. coli* at a pressure level of 500 MPa, followed by incubation at pH-values of 4.0 or below eliminates *E. coli* in various fruit juices (Garcia-Graells et al., 1998; Jordan et al., 2001). However, the acid tolerance of *E. coli* is strongly dependent on acid inducible stress proteins and the availability of amino acids in the substrate. The acid tolerance of *E. coli* is increased by the $\sigma^S$-regulated alteration of the cytoplasmic membrane (Chang and Cronan, 1999) the overexpression of proteins that prevent DNA-damage (Choi et al., 2000), as well as the induction of enzymes that extrude protons from the cytoplasm to maintain a high intracellular pH (Diez-Gonzalez and Karaibrahimoglu, 2004). The maintenance of a high internal pH is a prerequisite for the survival of microorganisms during acid challenge because it provides a favourable environment for cytoplasmic enzymes and macromolecules, and because the transmembrane pH gradient provides metabolic energy.

Furthermore, it has been shown that sublethal pressure treatments inactivate HorA, an ATP-dependent MDR transport enzyme involved in hop resistance and $F_oF_1$-ATPase of *Lactobacillus plantarum* respectively (Wouters et al., 1998; Ulmer et al., 2002b). HP also affects the metabolic activity and induces morphological modifications. Ribosomal destruction in *E. coli* and *Listeria monocytogenes* results in metabolic malfunctions contributing to cell death (Isaacs et al., 1995). In *Lactobacillus viridescens* cavities between cytoplasmic membrane and outer cell wall were observed after HP at 400 MPa (Park et al., 2001).

**Bactericides versus baroprotectants.** Successful preservation of food by HP treatment is significantly influenced by co-solvents which are available as food ingredients. Therefore, the different co-solvents may act either as baroprotectants or synergistic bactericides.

A protective effect against pressure inactivation was observed by using different molar masses of sucrose and sodium chloride. For this purpose, the inactivation of microorganisms as well as the denaturation of proteins was investigated using HP. A protective effect of sucrose and glucose was reported for the $F_0F_1$-ATPase and for the orange pectinesterase in the presence of sucrose and $Ca^{2+}$ (Van den Broeck et al., 1999; Saad-Nehme et al., 2001). Compatible solutes accumulated by bacteria as a response to osmotic upshock also provide protection towards pressure-induced cell death. No inactivation of *Lactococcus lactis* was observed using 1.5M of sucrose, 600 MPa at 20°C, as well as by the use of 4M NaCl, 400 MPa, 20°C over one hour of pressure application (Molina-Höppner et al., 2004). Significant baroprotective effects on the inactivation of *Escherichia coli* have been obeserved in the presence of calcium as well as in the presence of sucrose (Hauben et al., 1998; Van Opstal et al., 2003).

On the contrary, the studies of microbial inactivation in the presence of bactericidal environment will support the inactivation of microorganisms. It is reported, that low pH would cause a progressive increase of cell sensitivity under pressure (Mackey et al., 1995). An additional 3 log cycle reduction of *Listeria monocytegenes* CA was reported by the use of pH 4.0 in comparison to cells treated at a pH of 6.0 (Stewart et al., 1997) and a reduction of 1.2-3.9 log cycles in the presence of citric or lactic acid at pH 4.5 for four foodbourne pathogens (Alpas et al., 2000). Beyond this, in the presence of antimicrobial compounds such as bacteriocins, lysozyme, and nisin, the intensities of pressure treatment can be reduced (ter Steeg et al., 1999; Masschalck et al., 2001a and 2001b; Karatzas et al., 2001).

### 1.2.3. Physiological Response of Microorganisms During the Inactivation Process

Microbial inactivation caused by thermal or non thermal inactivation techniques can exhibit different kinds of inactivation patterns. Therefore, a subset of characterisitic inactivation curves is shown in Figure 2. Biphasic, concave, biphasic with a shoulder and convex trends have been observed while studying microbial inactivation (Cheftel, 1995; Xiong et al., 1999; Lee et al., 2001; Mafart et al., 2002).

In the case of different inactivation processes, different types of microbial inactivation may be observed depending on the strain as well as on the composite of the food matrix. First-order kinetics (linear) describe a linear decrease of the measurand. Two- or three phase inactivation curves have also been observed. First, two phase inactivation curves result in a quick

inactivation followed by a base describing a fraction of the population which appears to be resistant against the applied process parameters (linear with tailing). Second, a preeceding shoulder followed by linear decrease may also be observed (shoulder with linear). In the presence of protective compounds or in the presence of baroresistant strains of microorganisms, characteristics may change to no inactivation (shoulder). Additionally, a three-phase sigmoidal characteristic may be observed, concerning shoulder, linear inactivation as well as a resistant subpopulation. For the use of preservation processing in the food industry, it is of special interest to detect process parameter relations resulting in decreased microbial risk over a period of time. Therefore, all modifications of parameters (strain, food compounds, process temperature or pressure) have to be analysed in terms of either successful or ineffective inactivation to reduce the huge amount of microbial data to human understanding. This increased knowledge base concerning the various effects of process parameters (pressure, pressure holding time, temperature, additives, ….) is a prerequisite for predictive models of bacterial inactivation during the process and its application in the food industry.

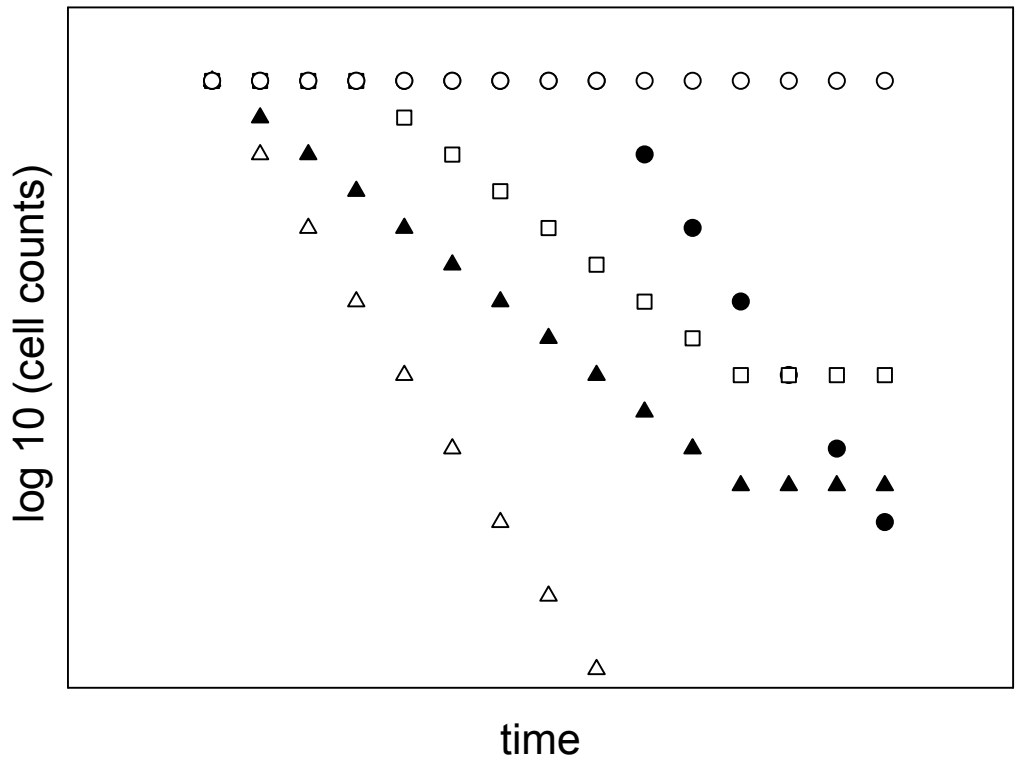


**Figure 2**: Commonly observed types of inactivation curves: shoulder (○), linear with a preceeding shoulder (●), sigmoidal like (□), linear with tailing (▲) and linear (Δ).

## 1.3. Data Analysis

Model based approaches are increasingly applied in the food and bioprocess industries. A major purpose of model application is to increase the productivity, profitability and/or efficiency of an analysed process. Considerable research efforts have been devoted to model improvement via computer aided process engineering methods. In this way, mathematical modelling, optimisation and control have become fundamental tools for optimally designed and operated processes in food industry.

Data analysis is required to process very large data sets. Normally, most information is readily available to the average person and can be extracted through analytical means. If a data base grows, the extraction of the required informations become difficult. The principle objective of the data analysis is the extraction of implicit, previously unknown and potentially useful information from complex and huge data sets. Additionally, hidden coherences between measured variables in a data set can be detected, resulting in an elimination of redundant information. Generated models represent a partial simplified image of the analysed real system that shows analogous behavior in the important properties and that allows a prediction of the behaviour of the original system within a limited region. Therefore, the generated systems shall be less complex. Thus, a transparent structure of complex mechanisms can be reached. Such models may be used to reduce experimental studies and research costs. A functional and validated model will work faster and cheaper than the original system (Heijnen, 1996; Bellgardt, 2000; Becker, 2002).

### 1.3.1. Principle Objectives of Data Analysis

The principle objective of data analysis is to extract knowledge out of aquired data sets. In general, the common procedure is given in Figure 3. The first step is the selection of a set of data which should be studied in detail. Therefore, all data which are measured for the description of one process should be gathered in one database. This data base can be preprocessed using different statistical tools. In general, preprocessing is necessary to remove “noise” and to let analysis and modelling tools work on “clean” data. This data must be transformed to that style, which allows them to take legal action of modelling. Additionally, the transformation of data variables covering different scales to a single scale enables one to compare these variables and may end in a reduction of dimensionality (Vandeginste et al., 1998).

After selection, preprocessing, and transformation, data analysis tools have to be used to analyse the data in detail. For this purpose, different types of tools are known which have been seperated into either black box, transparent, or hybrid approaches. Transparent approaches represent mathematical models describing relationships through analysing the operating mechanisms using known laws, theorems, and principles, such as chemical kinetics or physical laws (Esterl et al., 2003; Hartmann and Delgado, 2004). On the other hand, black box approaches have been widely used when relationships between variables are difficult to describe or to implement by theoretical models. To extract valuable and relevant information from these kind of data, decision trees, Fuzzy technologies or neural network tools are used to obtain insights into information hidden within the data (Geeraerd et al., 1998; Arnold et al., 2002; Chen and Mynett, 2003; Kilimann et al., 2005a).

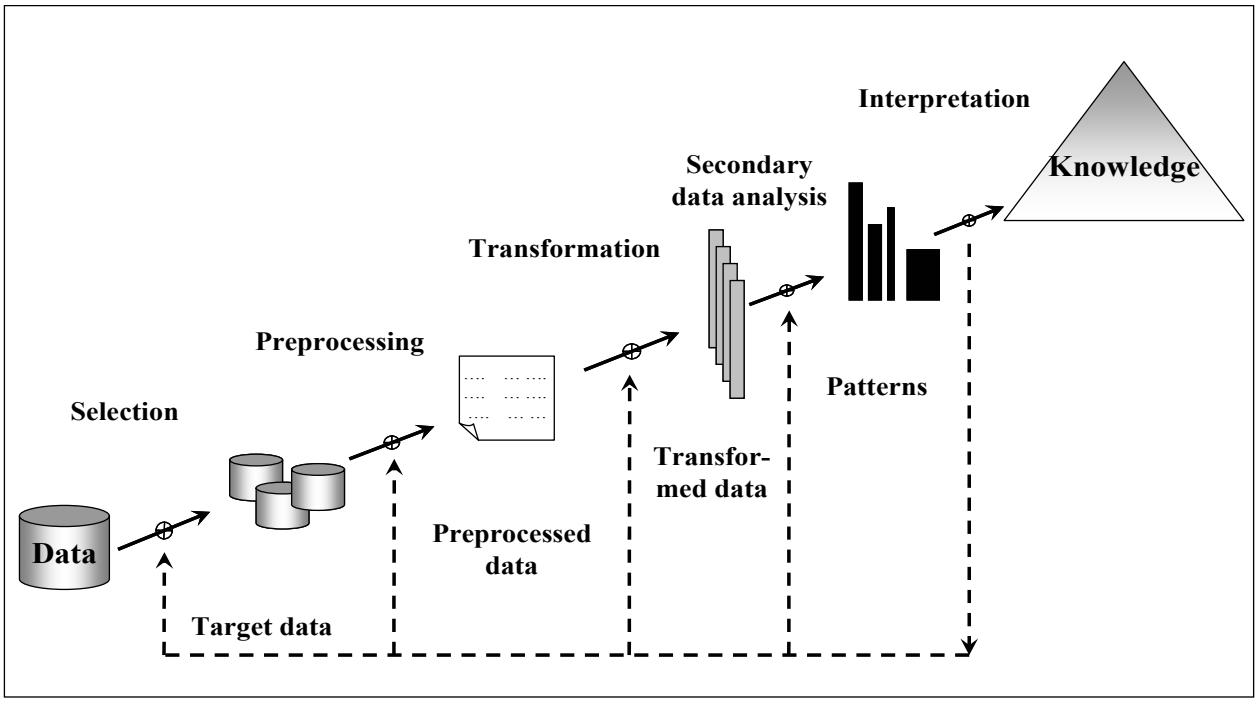


**Figure 3**: Process configuation of data analysis (Fayyad, 1996).

### 1.3.2. **Modelling of Microbial Inactivation**

Microbial inactivation induced by several process types like high pressure, temperature, chemicals, etc. may end in different shapes of inactivation depending on the applied process combinations (e.g. pressure, time, temperature level) as well as on the complexity of the food matrix (bactericidals or baroprotectants). First, inactivation kinetics can be described in the

simplest case by first order kinetics, where log linear inactivation occurs (Hartmann and Delgado, 2002; Deboosere et al., 2004). If non-log-linear kinetics occur, first order kinetics fail to describe the inactivation correctly. Therefore, higher order polynomials are used to describe the inactivation in dependence on the process parameters. For this purpose, multiple regression techniques are widely used for the prediction of the inactivation of organisms as well as the inactivation of important enzymes (Periago et al., 1998; Mafart et al., 2001; Diels et al., 2003). Furthermore, kinetics can be described by vitalistic models which also use empirical equations. Predicted parameters of the bacterial inactivation profile versus time can then described by means of polynomials of the used environmental factors in order to adjust the parameters as functions of process factors (Cole et al., 1993; Stephens et al., 1994; Gänzle et al., 2001). Additionally, differential equation models are used to describe the inactivation of biological matter. The integration of further knowledge into these models requires the formulation of further differential equations with additional parameters, that have to be quantified by experimental investigations (Ludikhuyze et al., 1997; Erkmen, 2001; Lee et al., 2001; Fachin et al., 2002). Complex models are also used that are derived from reaction mechanisms consisting of two or three-reaction steps and include the Arrhenius equation for temperature dependency on the parameters as well as the temperature change in an initial heating period (Illeova et al., 2003). The formulation of the dependency on kinetic parameters by Arrhenius relationships sometimes fails. This has promoted the use of a kinetic parameter prediction based on artificial neural networks or Fuzzy Logic. The knowledge derived from data analysis promises good predictability. The drawback of these tools is the black box approach, which does not allow for the detection of biological and physiological mechanisms of microorganisms during HP as well as the extrapolation of data (Murnleitner et al.,2002; Ewald et al., 2003; Bryjak et al., 2004).

If the inactivation is not only characterised by surviving kinetics but also by multiple measurands in order to account for lethal and sublethal effects due to the treatment, a more detailed mathematical and statistical knowledge concerning both, lethal and sublethal cellular damage is required. Therefore, multivariate statistical analysis is a powerful tool to process very large data sets. Multivariate analysis of biological data is frequently applied in biochemistry or bioengineering (Wollenweber et al., 1997; Becker and Schmidt, 2000; Huang et al., 2002; Stippl et al., 2002; O'Sullivan et al., 2003; Vaidyanathan et al., 2003). For the predictive modelling of these complex and non-linear systems, a reduction of the amount of measured data has to be achieved by making complex relationships between the measurands

accessible to human understanding. For this purpose, chemometrics are appropriate (Jolliffe, 1986; Martens and Næs, 1989; Henrion and Henrion, 1995; Vandeginste et al., 1998). Correlations derived by chemometrics can then be used to introduce a multi-layer structure into a model, providing at least one layer of autonomous variables. The suggested model structure then results in using either one type of modelling tool or the application of more than one tool ending in a construction of a hybrid. Hybrid models are often used to combine transparent and black box approaches to reduce computational capacities and to simplify the entire model. For this purpose, hybrid models are suitable tools for the correct description of these complex and non-linear biological systems, even in systems where the single and the combined effects of important input variables on the system output remain unknown (Petermeier et al., 2002; Yoo et al., 2003).

Furthermore, the applied tools must be validated. Validation represents an important step in the modelling process and helps to assess the reliability of models before they can be used as decision support systems. In general, validation typically involves the comparison of model predictions with corresponding observations of experiments not used to develop the model or using data generated from literature. The main idea behind this step is that models can not be used with confidence until such a validation is made. Hence, validation is an essential step allowing researchers to understand the applicable range of the model as well as the limit of its performance. Furthermore, the model originally used for predictive modelling now becomes an information resource, which contributes to the understanding of important relations in complex and non-linear systems.

## 1.4. Aim of the Thesis

The aim of the thesis was to study and to describe the effect of different inactivation processes on the lethal and sublethal behaviour of *Lactococcus lactis* ssp. *cremoris* MG 1363 and of *Escherichia coli* TMW 2.497.

First, the temperature induced inactivation in the presence of protective co-solvents of *L. lactis* is studied. In addition, informations about the structural changes of proteins in *L. lactis* are collected by in-situ FT-IR spectroscopy. Therefore, a cumulative research of all proteins of *L. lactis* (located in the membrane or cytoplasm) and their behaviour in relation to the increased temperature level were analysed and will be discussed. The motivation of this part

is based on the possible informations concerning protein denaturation and its influence on cell death and sublethal injury of the bacteria.

Second, the combined effects of pressure, baroprotective co-solvents, and temperature were analysed on the viability and the physiological response of *L. lactis* using five physiological states (describing lethal and sublethal injury), namely viable cell counts, stress resistant cell counts, metabolic activity, membrane integrity and LmrP-activity. Moreover, the use of Principal Component Analysis (PCA) aimed to detect correlations between these five physiological states in order to facilitate the interpretation of the experimental data and to reduce the amount of measurands for future applied mathematical and microbiological studies.

In terms of *E. coli,* it was the aim of this thesis to determine the effect of glutamate, glucose, and arginine on the survival during pressure treatment, and during post-pressure acid challenge. To obtain insight on the mechanisms of protection provided by acid survival pathways, the consumption of arginine and glutamate as well as their effect on the intracellular pH of *E. coli* during pressure treatment and post-pressure acid challenge were determined in addition to the viable cell counts. The intracellular pH was determined by using the pH-dependent fluorescence of the green fluorescent protein, GFP.

Third, the generated data set describing pressure-temperature-co-solvent induced inactivation of *L. lactis* will be extended. Therefore, an existing inactivation data set was used as a function of pressure level, pressure holding time and several substrate additives, which is based on experimental data covering the pressure range of 200 to 600 MPa, pH-values between 4.0 and 6.5, and the presence of additives known to exert a protective effect towards pressure induced inactivation. The analysed data set was divided roughly in two equal parts to obtain a data subset for model establishment, and a data subset for model valiadation. This data combined with the results out of PCA may be used to define a multi-layer Fuzzy model which shall predict the data correctly as well as to validate the correlations detected by PCA. For this purpose, the suitability of the definition of autonomous variables in the Fuzzy rulebase will be evaluated.

Finally, this work will analyse the effects of process induced non-uniformity on the inactivation of *L. lactis* in a medium size high pressure autoclave experimentally and numerically. Thus, differences in the inactivation behaviour will be analysed experimentally by the detection of lethal and sublethal injury of *L. lactis* at different locations in the

autoclave. Afterwards, a predictive microbial model for the inactivation of *L. lactis* will be generated, which take into account: pressure, temperature, protective additives as well as the shoulder and tailing effects of the bacteria. Subsequently, this model should be suitable to combine it with the High Pressure Computer Fluid Dynamics (HD-CFD) technique in order to investigate the heterogeneity of the inactivation process of *L. lactis* numerically. This part of the study is in coorperation with Kitsubun (2005).

# 2. Material and Methods

In this work, different inactivation techniques and their influence on the inactivation behaviour of *L. lactis* and *E. coli* were analysed. Therefore, the focus was set on high pressure processing on liquid food, with packaging and an operating range between 0.1 MPa to 600 MPa and process temperatures ranging from 278 K to 348 K. The used biological and statistical/mathematical tools are described briefly in subsequent chapter.

## 2.1. Technical Equipment

High-pressure experiments were done using two different kind of pressure chambers. First, the pressure chamber at Technische Mikrobiologie Weihenstephan was used with a specific volume of 10 ml, TUM, Germany (Dunze Hochdrucktechnik, Hamburg, Germany). The compression/decompression rate was set to 200 MPa $min^{-1}$ for each experiment. The system was equipped with an internal temperature control and a thermostatic jacket connected to a water bath. A maximum operating pressure of 600 MPa in a temperature range from 278 K to 323 K was used. The pressure level, time, and temperature of pressurisation were controlled by a computer program. Despite the small volume of the pressure chamber, a heterogeneous temperature distribution was determined. Due to its voulume, the decay time to re-equilibrate is about 100 s and this was found to have no influence on the inactivation. Ethylenglycole was used as experimental fluid.

Second, a pressure chamber (CIP 6000, Alsthom, Nantes, France) at ENITIAA-GEPEA, Nantes, France, was used with a specific volume of 3.3 litres. The compression/decompression rate was 200 MPa $min^{-1}$. The system had a maximum operating pressure of 600 MPa and a temperature range from 303 K to 323 K was used. The desired temperature level was adjusted with a thermostat jacket connected to a water bath. A JULABO High Precision Thermostat is used for tempering the cooling fluid. Pressure is built up with a pressure amplifier, which is fed by a pre-pump generating a pressure of 0.5 MPa. Water is tempered in the supply tank of the pre-pump by adding cold or hot water. The pipe leading from the high pressure pump to the vessel is approximately 3 m long and exposed to the local environmental conditions. Furthermore, the temperature, measured at 6 different locations, and the pressure have been registered by a data logger (SA 32, AOiP, France). The tubes were fixed at two different locations in the pressure chamber. Figure 4 illustrates the geometry of the chamber

as well as the location of the thermocouples of type K and the tubes incorporating microbiological probes.

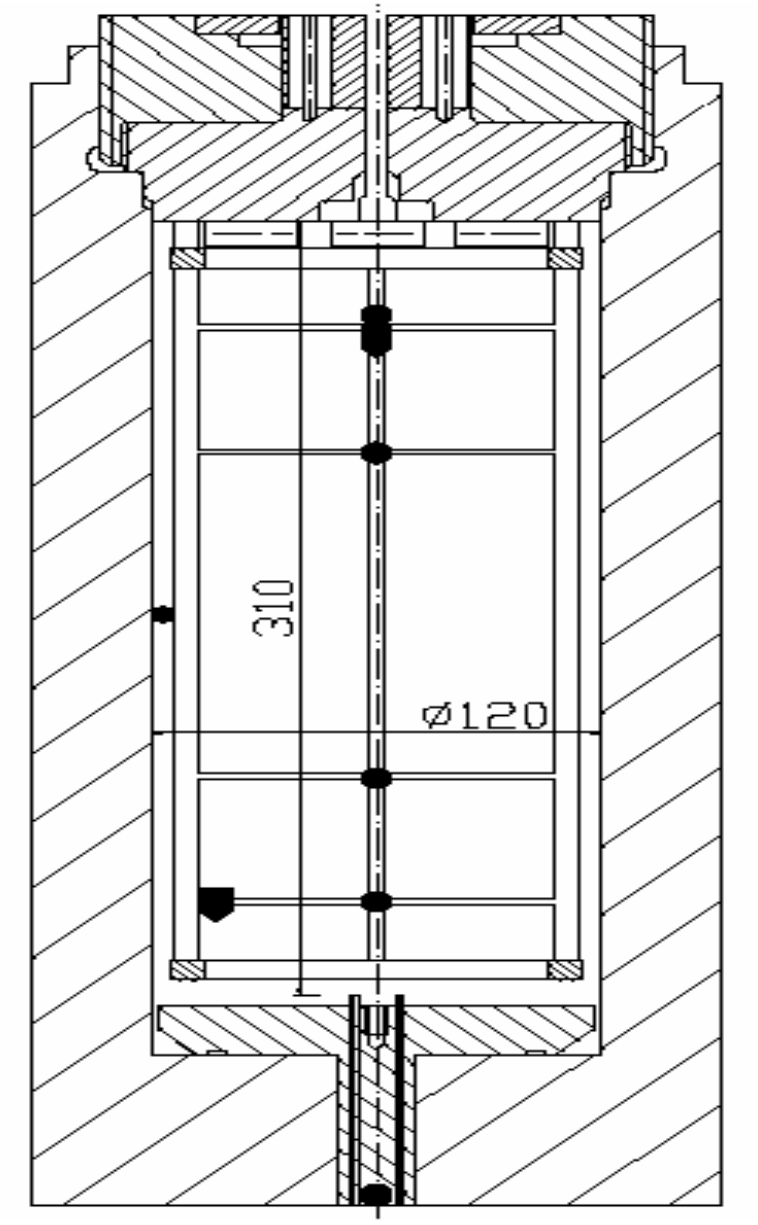


**Figure 4**: Setup of the 3.3l autoclave (Institut ENITIAA, Nantes). Used symbols represent the location of the tubes (♥) and the thermo couples (●).

## 2.2. Chemicals

MES [2-(N-morpholino)ethanesulfonic acid] (Gerbu Biotechnik GmbH, Gaiberg, Germany), DL-Arginine, L-Glutamate, Valinomycin, Nigericin, Polymixin from Sigma-Aldrich

(Steinheim, Germany), L-Glutamic acid test kit for the determination of glutamate (Boehringer Mannheim/R-Biopharm/Enzymatic BioAnalysis, Germany), LIVE/DEAD® BacLight™ from Molecular probes, Eugene, U.S.A. All other chemicals and M17 broth were analytical grade from Merck (Darmstadt, Germany).

## 2.3. Methods for Characterisation of Combined High Pressure-Temperature Induced Inactivation on Cells of *Lactococcus lactis*

*Lactococcus lactis* ssp. *cremoris* MG 1363 was grown at 30°C in M17 broth supplemented with 1% glucose. Cells of an overnight culture were harvested by centrifugation, washed and resuspended in buffer to cell counts of about $10^9$ cells $ml^{-1}$. This buffer was designated as "milk buffer" because it was intentionally set up to resemble whey (Molina-Höppner, 2002) and contained the following compounds (g $l^{-1}$): KCl, 1.1; $MgSO_4 \cdot 7H_2O$, 0.7110; $NaH_2PO_4 \cdot 2H_2O$, 1.874; $CaSO_4 \cdot 2H_2O$, 1.0; $CaCl_2 \cdot 2H_2O$, 0.99; citric acid, 2.0; lactose, 52.0. The pH was adjusted to pH 6.5. Where indicated, the following compounds were added to the buffer: 1.5 M sucrose or 4 M NaCl.

### 2.3.1. Determination of Viable Cell Counts and Stress Resistant Cell Counts

After pressure treatment, cell suspensions of each vial were diluted and plated on M17 agar supplemented with 1% of glucose or M17 agar containing 3% NaCl for determination of viable and stress resistant cell counts, respectively. The plates were incubated for 24 h at 30°C under aerobic conditions to assess viable cell counts (CFU), and for 48 h to assess stress resistant cell counts (CFUsub) under same conditions as described above.

### 2.3.2. Determination of Metabolic Activity

The determination of metabolic activity of pressure treated *L. lactis* was carried out as described (Ulmer et al., 2000). Cells from pressure treated cultures were harvested and resuspended in 1 vol. of phosphate buffer (PBO (g/l), $H_2KPO_4$, 6.8; $MgSO_4 \cdot 7H_2O$, 0.1; $MnSO_4 \cdot 1H_2O$, 0.05). An equal volume of a stock solution of 4 mM 4-iodonitrotetrazolium violet (INT, 2-(4-iodophenyl)-3-(-4-nitrophenyl)-5-phenyltetrazolium chloride) and 20 mM glucose in PBO was added to the bacterial cell suspension and incubated at 30°C for 1h.

During incubation, the absorbance was measured at 590 nm with a spectrafluor microtiter plate reader (TECAN, Grödig, Austria). A calibration curve was established for each inactivation kinetic by using the calibration samples described above and the results are reported as a percentage of the metabolic activity of untreated cells (MA).

### 2.3.3. Determination of Membrane Integrity

The determination of membrane integrity of pressure treated *L. lactis* was carried out with the LIVE/DEAD® BacLight™ kit with propidium iodide as membrane-impermeant probe essentially according to the instructions of the manufacturer. 1 ml pressurised cell suspension was harvested by centrifugation. The supernatant was removed and the pellet resuspended in 1 ml PBO. A stock solution of LIVE/DEAD® BacLight™ was prepared, the final concentration of each dye was 33.4 µM Syto®9 and 200 µM propidium iodide. 100 µl of each of the bacterial cell suspensions were mixed in 100 µl of the stock solution, mixed thoroughly and incubated for 5 minutes in the dark at 30°C. The fluorescence intensities of Syto®9 and PI were measured with excitation and emission wavelengths of 485 nm and 520 nm, and 485 nm and 635 nm, respectively, using a spectrafluor microtiter plate reader (TECAN, Grödig, Austria). The ratio of Syto®9 to PI fluorescence intensity was used as a measure for membrane integrity. A calibration curve was established for each inactivation kinetic using the calibration samples described above and the results are reported as as a percentage of intact membrane (MI).

### 2.3.4. Determination of LmrP-Activity

Ethidium bromide is a substrate for the membrane bound enzyme LmrP and other multi drug resistance MDR-transport enzymes. *L. lactis* MG 1363 contains at least four drug extrusion activities (Yokota et al., 2000). Because extrusion of EB by *L. lactis* MG 1363 occurs predominantly by the LmrP transporter and is fully inhibited by ionophores that dissipate the proton motive force (Bolhuis et al., 1994; Bolhuis et al.,1995; Bolhuis et al., 1996), EB efflux activity was reported as LmrP activity. EB stock solutions were prepared by dissolving 40 µmol $l^{-1}$ of EB in PBO. Cells were washed, harvested by centrifugation and resuspended in a stock solution of PBO and EB, the final concentration was 20 µmol $l^{-1}$. After this treatment, the cell suspension was stained for 2 hours at 30°C in the dark without an energy source. Then glucose was added to a final concentration of 20 g $l^{-1}$. Cells re-energised with glucose export

EB, resulting in a lower fluorescence of the EB-DNA complex. Immediately after glucose addition, the fluorescence of the EB-DNA complex was measured over 30 min in a spectrafluor microtiter plate reader (TECAN, Grödig, Austria) using excitation and emission wavelengths of 485 nm and 595 nm. The initial rate of EB efflux as measured by the decrease of EB fluorescence intensity upon glucose addition was calculated as described by (Ulmer et al., 2002b) and reported as LmrP-activity (LmrP).

## 2.4. Measurement of Conformational Changes in the Protein Structure and of the Membrane Phase State of *L. lactis* by FT-IR Spectroscopy

Conformational changes in proteins and internal vibrational modes of lipid acyl chains of the membrane of *L. lactis* due to elevated temperatures were measured by an in-situ technique Fourier transformed infrared (FT-IR) spectroscopy. The cells of an overnight culture were harvested by centrifugation (5 min at 10,000×g [relative centrifugal force]), washed twice in milk buffer or milk buffer 1.5M sucrose (sucrose) and incubated for 45 min in the buffer system which was subsequently analysed. After incubation, the cells were harvested and washed in triplicate in Deuterium oxide ($D_2O$) or $D_2O$-sucrose. This step was performed so that easily accessible $H^+$ ions were exchanged by the Deuterium ones. Following this step, it was possible to detect the amide bands which would be otherwise overlapped by the dominating spectra of water. Afterwards, cells were poured into a 20-µm-thick infrared cell equipped with $CaF_2$-windows. $CO_2$ was removed and air moisture inside the chamber was dried. The FT-IR spectra were recorded with an Equinox 55 spectrometer (Bruker, Ettlingen, Germany) equipped with a DTGs detector. Twenty scans were averaged for each temperature point. The scan was started if the averaged temperature measured over the diagonal of the $CaF_2$-windows was equal to the desired temperature level. Spectra were recorded between 6 and 75°C and the temperature was adjusted by an external water thermostat. Using this detection method, the membrane phase of *L. lactis* as well as characteristics of amide A + HOD, amide I', amide II, and amide II' were detected. The presented data were out of two independent experiments. The error of this method is within the overall error of the setup.

An overview of all detected bands, their declaration, the location of their absorption maxima as well as their wave number range is given in Table 1. The data from literature were compared with the obtained spectra. Results for *L. lactis* were in agreement with the findings of Linders et al. (1997) and Barth and Zscherp (2002).

**Table 1**: Common range of the characteristical bands of the secondary structure of the proteins detected by FT-IR in *L. lactis*.

| band | wave number ($cm^{-1}$) | range of value ($cm^{-1}$) |
|---|---|---|
| amide A + HOD | ~3400 | 3200-2800 |
| symmetric $CH_2$ | ~2852 | - |
| amide I' | ~1652 | 1600-1700 |
| amide II | ~1550 | - |
| Tyrosine | ~1515 | - |
| side chains | - | 1500-1600 |
| amide II' | ~1455 | 1500-1350 |

In this work, FT-IR-spectroscopy has been used to detect the behaviour of the characteristics named above. Therefore, the temperature range was varied between 6°C and 75°C and the surrounding $D_2O$ was used as a pure system or supplemented with 1.5M sucrose. The shown spectra in Figure 5 were reduced about the dominant $D_2O$ peak ranging from 2800 $cm^{-1}$ to 2100 $cm^{-1}$. Figure 5 represents data which were recorded using 30°C and 75°C and sucrose as an additive to $D_2O$. The spectra measured in pure $D_2O$ comprised the same characteristics as the presented one. Due to the temperature induced shift of the spectra, it is possible to gain informations about the structures named above and their behaviour while using extreme temperature conditions (Table 1; Linders et al., 1997; Barth and Zscherp, 2002). Informations about the membrane phase behaviour were gained from the temperature shift of the peak-maxima of the symmetric $CH_2$. The characteristic changes of the amide bands allow to draw conclusions about conformational changes (amide II, amide II') in the proteins as well as the secondary structure (amide I') of the proteins of *L. lactis*. Data shown in Figure 5 represent data of a fully inactivated population (75°C) and a vital population (30°C) of *L. lactis*.

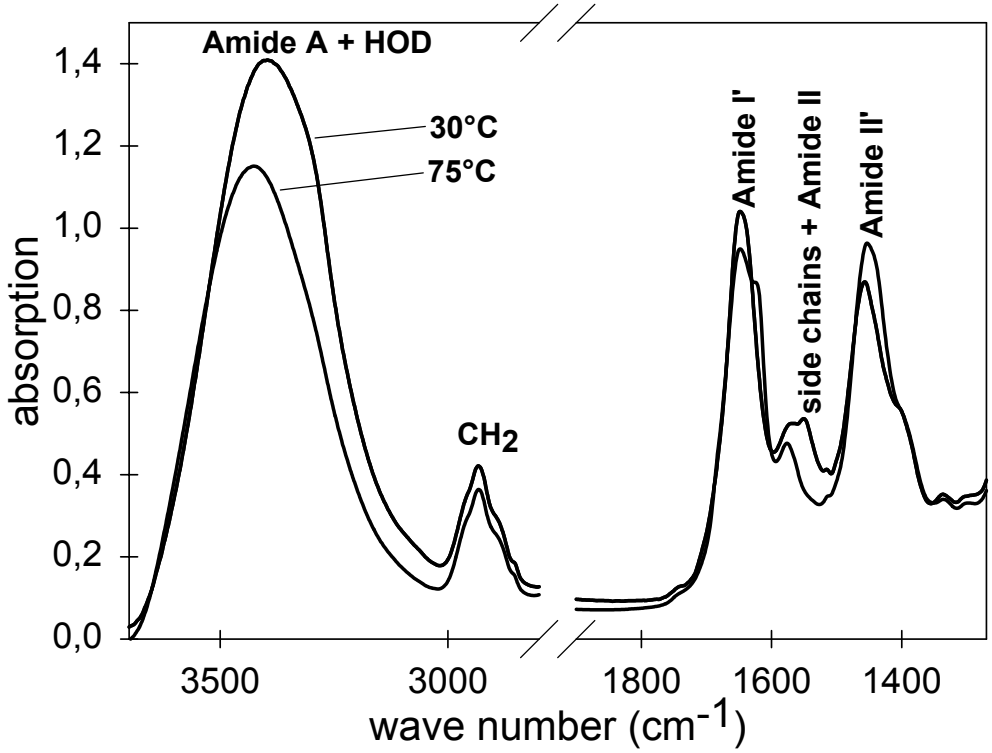


**Figure 5**: Parts of the FT-IR spectra of *L. lactis* supplemented in $D_2O$-sucrose using a temperature of 30°C and 75°C. Shown are relevant regions of the spectra describing amide A +HOD, $CH_2$, amide I', side chains and amide II, and amide II'.

The membrane-phase behaviour was detected by the information of the symmetric $CH_2$ absorbance peak at wave numbers near 2852 $cm^{-1}$ (Figure 6A). The internal vibrational modes of the lipid acyl chains were assigned on the basis of studies of polymethylenes and polymethylene chain compounds (Snyder, 1961; Reis et al., 1996). In the region from 2800 $cm^{-1}$ to 3100 $cm^{-1}$, there are infrared absorption bands due to symmetric and antisymmetric modes of the methylene chain at about 2850 $cm^{-1}$ and 2.920 $cm^{-1}$, respectively. The wave numbers of these bands are conformation sensitive and thus respond to temperature induced changes of the *trans*/*gauche* ratio in acyl chains. The vibration mode (asymmetric stretch) of the terminal $CH_3$ group occurs at about 2.960 $cm^{-1}$.

Figure 6B represents the spectral information about amide A and HOD-stretching band. Amide A is almost described by the N-H-stretching vibration band at wave numbers ranging from 3300 $cm^{-1}$ to 3400 $cm^{-1}$ (Barth und Zscherp, 2002; imb Jena, w.d.). Due to the fact, that the analysis took place in a liquid environment, the HOD-stretching band behaviour is dominant and no prediction about amide A behaviour was possible. Therefore, the peak was

just used to quantify the surrounding temperature due to the fact, that the peak maxima is shifted to lower wave numbers in case of elevated temperatures (compare Figure 6B).

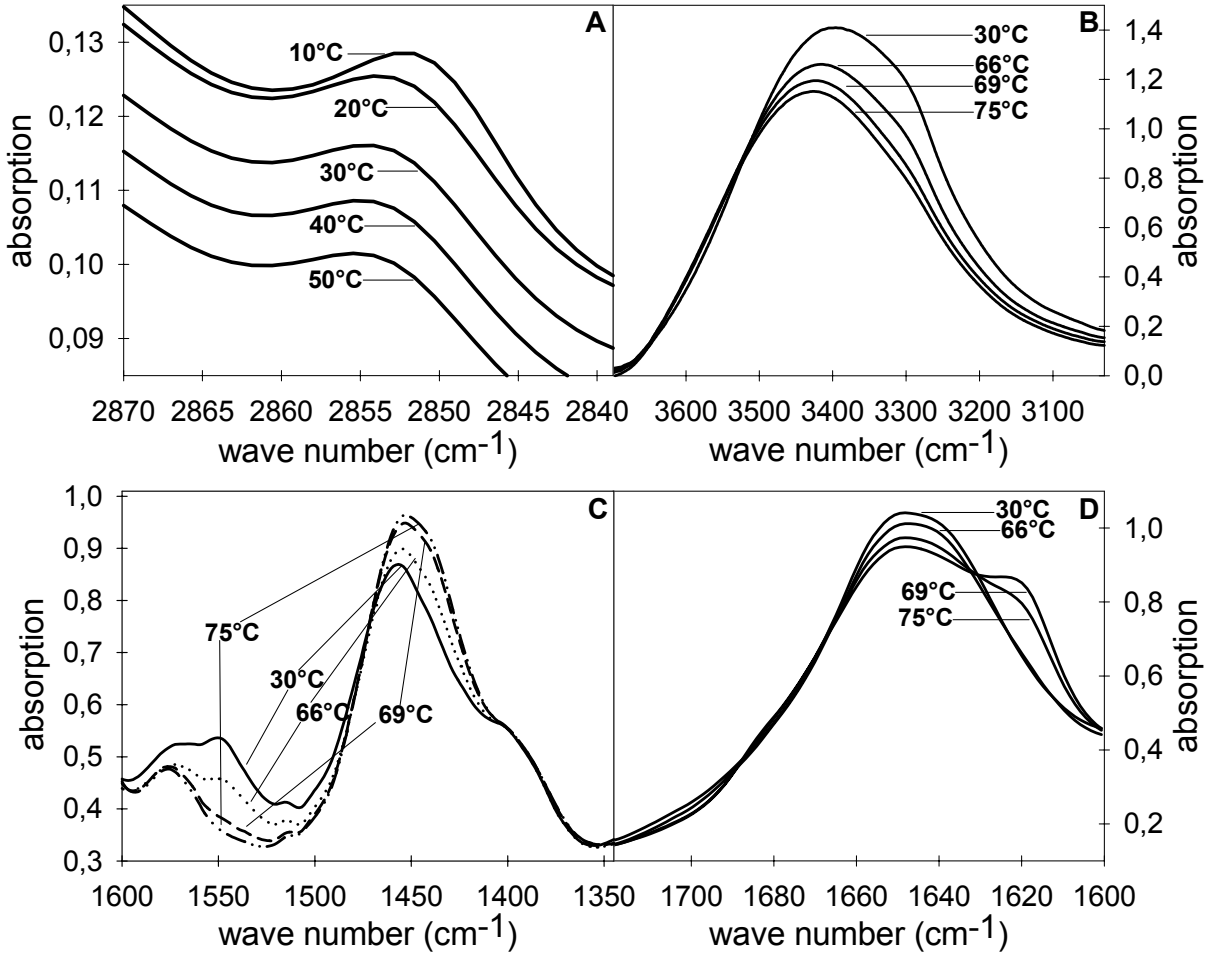


**Figure 6**: Fragments of the complete FT-IR spectra of the secondary structure analysis of proteins and the lipid acyl chains of *L. lactis*. A: temperature induced shift of $CH_2$, B: temperature induced shift of amide A + HOD, C: temperature induced shift of amide II' and amide II, D: temperature induced shift of amide I'.

In case of amide II (~1550 $cm^{-1}$, nondeuterated) and its corresponding amide II' (~1455 $cm^{-1}$, deuterated), a sensitive indicator of hydrogen-deuterium-(D/H) exchange in proteins was found (Figure 6C). This peak represents the combined measurement of in-plane N-H-bending-vibration, C-C-stretching and C-N-stretching-vibration that occurs in proteins (imb Jena, w.d.). The shown area is highly sensitive for the detection of conformational changes in proteins and therefore represents an indicator for the upcoming exchange of D/H protons due to the elevated temperature (Linders et al. 1997; Smeller et al. 2000; Smeller et al. 2002). The

idea was, that the intensity of the amide II' band will increase (~1455 $cm^{-1}$), the greater the D/H-exchange took place. On the other side, the intensity of the corresponding amide II peak (~1550 $cm^{-1}$) is decreasing with increasing temperature (compare Figure 6C). In conclusion, the amide II band is shifted about 100 wave numbers to the lower waver numbers of amide II' region. This was found by Smeller et al. (2002). and was significantly proved by our data (Figure 6C).

Figure 6D describes the amide I' band in dependence on different temperatures (1600 $cm^{-1}$ - 1700 $cm^{-1}$). In this range, it is possible to gain important informations about the secondary structure of the proteins. Therefore, 70-85% are originating from the C=O-stretching vibration and 10-20% are resulting from the C-N-stretching vibration (imb Jena, w.d.). The lower the wave number of amide I', the higher is the binding of the proton relating to C=O of the peptide (Takeda et al., 1995a and 1995b). Using the second derivative spectra of the shown absorbance spectra, a classification of characteristics in the secondary structure of proteins is possible. Therefore, ordered structres are shifted by thermal treatment to an unordered behaviour describing conformational changes in the proteins due to the process.

This part of the work was done at Lehrstuhl für Experimentalphysik IV at TUM. Further on, the data analysis was done using Sigma Plot 8.0 as well as OPUS.

## 2.5. Methods for Characterisation of High Pressure Induced Inactivation on Cells of *Escherichia coli*

*Escherichia coli* TMW2.497 was grown at 37°C in Luria-Bertani (LB) medium containing the following compounds per litre: peptone, 10 g; NaCl, 5 g; yeast extract, 5 g. The pH was adjusted to pH 7.0 with 1M HCl. Ampicillin to a level of 50 ppm was furthermore added unless otherwise stated. 15 g $l^{-1}$ agar-agar were added to obtain solid media. Plates were incubated aerobically and liquid cultures were generally agitated at 240 rpm. *E. coli* TMW2.497 is a derivative of *E. coli* JM109 (DE3) carrying the gene coding for red-shift green fluorescent protein (GFP) on plasmid pQBI-63 (Ehrmann et al., 2001). In preparation of *E. coli* TMW2.497 for pressure treatments, the strain was inoculated in 50 ml LB-broth without ampicilline in a 250 ml Erlenmeyer-flask and incubated for 16 h. The cell suspension were subcultured with a 5% inoculum for 3 – 4 h to obtain a culture with an optical density ($OD_{590nm}$) of 1.0, corresponding to cells in their late exponential growth phase.

### 2.5.1. MES-Buffer

For all pressure treatments, cells were suspended in buffer containing 50 mM 2-(N-morpholino)ethanesulfonic acid (MES) and 10 mM glucose (MES-buffer) or MES-buffer arg/glu additionally containing 10 mM each of DL-arginine and L-glutamate. The pH of each buffer was adjusted to 5.4 with 1M HCl. MES was chosen as a buffering salt because the effect of pressure in the range of 0.1 – 400 MPa on the $pK_A$ of MES is negligible (Kitamura et al., 1987).

### 2.5.2. Pressure Treatement of *E. coli*

*E. coli* cells were harvested by centrifugation, washed twice in MES buffer or MES buffer arg/glu as indicated, resuspended in the corresponding buffer, transferred to 2 ml tubes with screw cap, and stored at room temperature until use. Pressure treatments were performed in the 10 ml pressure autoclaves that were maintained at 30°C. The compression/decompression rates were 200MPa $min^{-1}$. Cells were exposed to a pressure of 200, 300 or 400 MPa for various time intervals (0 to 120 min). A pressure holding time of 0 min indicates compression to 200, 300 or 400 MPa immediately followed by decompression, equivalent to the exposure to above ambient pressure for a total of 2, 3, and 4 min, respectively. The viable cell counts of pressure treated cultures were determined by plating appropriate dilutions of the samples on LB-agar and an incubation for 24h.

### 2.5.3. Determination of the Intracellular pH ($pH_{in}$) of Untreated and Pressure Treated *E. coli*

The assay system for the determination of the $pH_{in}$ was based on the pH-dependence of GFP fluorescence (Kneen et al., 1998; Olsen et al., 2002). To calibrate the GFP fluorescence in strain *E. coli* TMW2.497 to the $pH_{in}$, cells were washed with buffers with pH values ranging from 4.0 to 7.0, and resuspended in the corresponding buffer. 50 mM buffers were prepared from citric acid (pH 4.0 and 5.0) or MES (pH 5.4, 6.0 and 7.0). The pH was adjusted with either NaOH or HCl. The $pH_{in}$ of *E. coli* was equilibrated to the external pH by addition of polymyxin B (1µM), valinomycin (1µM) and nigericin (1µM), and the GFP-fluorescence in the various buffers was measured with a fluorescence spectrometer (LS-50B, Perkin Elmer, Überlingen, Germany) at the excitation wavelengths of 410 nm (pH-independent

fluorescence) and 485 nm (pH dependent fluorescence) and an emission wavelength of 520 nm. The bandwidth of the excitation and emission monochromators were set to 5 nm. The ratio of the relative fluorescence intensities (RFI) was calculated as ($RFI_{ex.\ 485nm,\ em.\ 520\ nm}$)/($RFI_{ex.\ 410\ nm,\ em.\ 520\ nm}$) and plotted against the buffer pH. A calibration curve was established for experiments performed on a single day. It was verified that pressure treatment with 200 or 300 MPa did not affect the fluorescence ratio of GFP (Figure 7).

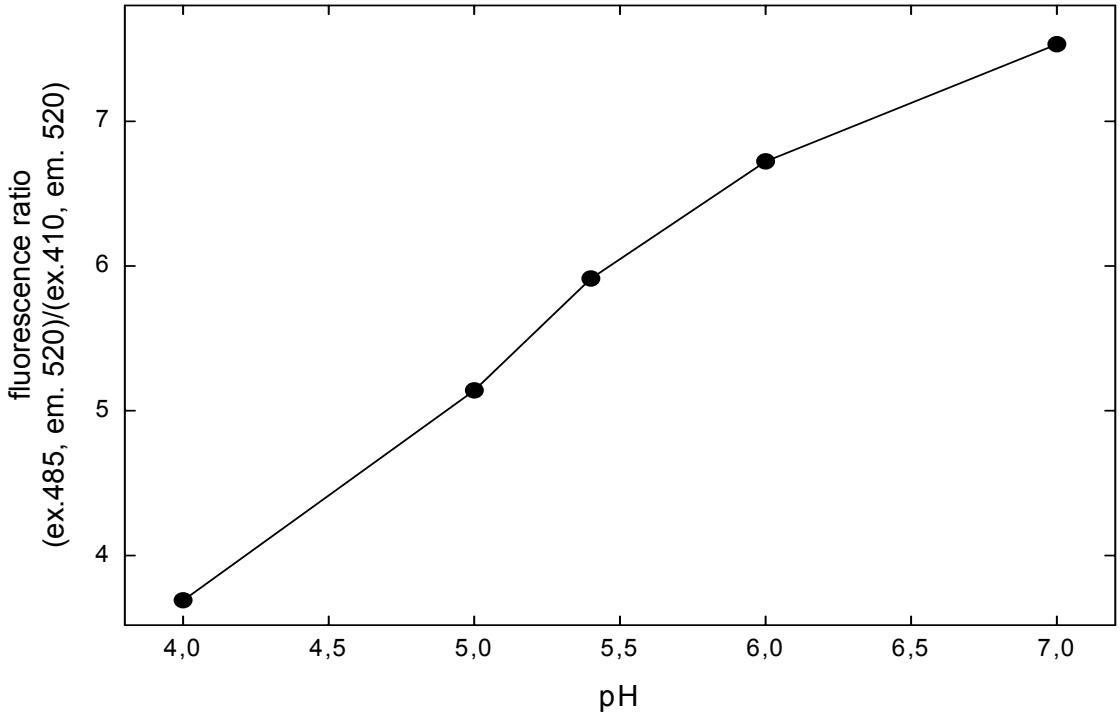


**Figure 7**: Calibration curve to determine the $pH_{in}$ of *E. coli* TMW2.497 expressing GFP based on the GFP fluorescence. *E. coli* was suspended in buffers with an pH of 4.0, 5.0, 5.4, 6.0 or 7.0 and the internal and the external pH-values were equilibrated by addition of polymyxin B, valinomycin, and nigericin to a level of 1 µM each. The GFP fluorescence was determined at the excitation and emission wavelength of 410 and 520 nm (pH independent fluorescence), and at the excitation and emission wavelength of 485 and 520 nm (pH dependent fluorescence) and the fluorescence ratios were plotted against the pH.

To determine the ability of pressure treated cells of *E. coli* to restore a transmembrane ΔpH after pressure treatment, cells were treated in MES-buffer or MES-buffer arg/glu for 0, 1, 2, 4, 8, 16 or 20 min at 200 or 300 MPa. After pressure treatment, the cells were incubated for 30 min at 30°C and the $pH_{in}$ was determined by measurement of the GFP fluorescence as described above. Untreated cells were used as control.

### 2.5.4. In Situ Determination of the Intracellular pH ($pH_{in}$) at High Pressure

For the determination of the internal pH during high pressure treatment, the pressure autoclave was equipped with an optical window and the fluorescence of the sample in the pressure autoclave was measured by means of an optical fibre connected to the fluorescence spectrometer as described (Gänzle and Vogel, 2001; Molina-Gutierrez et al., 2002). Three milliliters of cell suspension were placed in the pressure chamber and the GFP fluorescence intensities were measured at two excitation wavelengths (410 and 485 nm) and an emission wavelength of 520 nm before and during pressure treatment. The bandwidth of the excitation and emission monochromators were set at 15 nm. The fluorescence was monitored over a period of 10 minutes: 4 min incubation in the pressure autoclave at ambient pressure, 1 min compression to 200 MPa, and 5 min of incubation at 200 MPa. For experiments prepared on a single day, two calibration curves were determined as described in the previous paragraph: one calibration curve was measured at 0.1 MPa and the second calibration curve was measured at 200 MPa.

### 2.5.5. Post Pressure Acid Survival of *E. coli*

*E. coli* TMW 2.497 was treated at 200 or 300 MPa for 0 – 20 min in MES-buffer or MES-buffer arg/glu and the cell counts in the pressure-treated samples were determined. Furthermore, pressure treated cells were harvested by centrifugation and samples were resuspended in three different buffers: 50 mM citrate (pH 4.0) with 10 mM glucose, 50 mM citrate (pH 4.0) with 10 mM glucose and 10 mM each of arginine and glutamate, or 50 mM MES (pH 5.4) with 10 mM glucose. Samples that were pressure treated in the absence of amino acids were resuspended in citrate- or MES-buffer in the absence of amino acids, and samples that were pressure-treated in the presence of amino acids were stored in citrate- or MES-buffer arg/glu. Cells from a pressure treated sample were incubated in these three buffers for 24 h at ambient temperature. After 24 h of incubation, the viable cell counts were determined by plating appropriate dilutions on LB-agar. For those samples that were treated at 200 MPa and stored in buffer with arginine and glutamate, the arginine and glutamate levels in the samples were determined by HPLC. The cells were removed by centrifugation and the supernatant was injected on a Spherimage-80 ODS-2 column as described (Anonymous, 1997).

A second experiment was carried out with cells treated at 200 MPa for 0, 4, 8, and 20 min, and post-pressure incubation in citrate buffer, pH 4.0, in the presence of arginine and glutamate. To determine the kinetics of glutamate turnover during post-pressure incubation, 8 samples were taken after 0 to 24h of post pressure incubation and the glutamate levels in the cell-free supernatants of these samples were determined by using an enzymatic test kit for L-glutamate (R-Biopharm, Mannheim, Germany) according to the instructions of the supplier.

### 2.5.6. Effect of Acid Adaptation on Post Pressure Acid Survival

Cells were adapted to mild acid conditions by incubation for 100 min in MES-buffer pH 5.4 at 30°C prior to pressure treatment. The pressure treatment at 200 MPa and the determination of the post-pressure acid survival of acid adapted cells was carried out as described for the non-adapted cells.

## 2.6. Data Analysis of High Pressure Inactivation on *L. lactis*

For the formulation and the validation of a Fuzzy model, previously measured data sets were used (Molina-Höppner, 2002) in addition to the pressure-temperature-co-solvent dependent inactivation kinetics that were determined in preparation of this work. The inactivation kinetics were previously analysed using the same strain of *L. lactis*, the same media for cultivation and pressure treatment, the same pressure equipment, and the same methods for analysis of pressure treated cells. An overview on all data sets used for Fuzzy modelling is provided in Table 2.

**Table 2**: Parameter combinations used for data analysis. Data were taken from Molina-Höppner (2002) as indicated by [a)] or obtained in this work.

| temperature | pressure | analysed parameters | additive |
|---|---|---|---|
| 5°C | 200 MPa | CFU, CFUsub, MI, MA, LmrP | none, 1.5M sucrose, 4M NaCl |
| 10°C | 200 MPa | CFU, CFUsub, MI, MA, LmrP | none, 1.5M sucrose, 4M NaCl |
| 15°C | 200 MPa | CFU, CFUsub, MI, MA, LmrP | none, 1.5M sucrose, 4M NaCl |
| 20°C | 200 MPa [a)] | CFU, CFUsub, MI, MA, LmrP | None |
| 20°C | 200 MPa [a)] | CFU, LmrP | 0.5M sucrose |

| temperature | pressure | analysed parameters | additive |
|---|---|---|---|
| 20°C | 200 MPa [a)] | CFU, CFUsub | 1M mannitol |
| 20°C | 200 MPa [a)] | CFU, CFUsub, LmrP | 4M NaCl |
| 20°C | 200 MPa | CFU, CFUsub | pH 4, pH 5, pH 6, pH 6.5 |
| 30°C | 200 MPa | CFU, CFUsub, MI, MA, LmrP | None |
| 40°C | 200 MPa | CFU, CFUsub, MI, MA, LmrP | none, 1.5M sucrose, 4M NaCl |
| 45°C | 200 MPa | CFU, CFUsub, MI, MA, LmrP | none, 1.5M sucrose, 4M NaCl |
| 50°C | 200 MPa | CFU, CFUsub, MI, MA, LmrP | none, 1.5M sucrose, 4M NaCl |
| 20°C | 250 MPa | CFU, CFUsub, MI, MA, LmrP | None |
| 20°C | 250 MPa | MI, MA | 4M NaCl |
| 5°C | 300 MPa | CFU, CFUsub, MA | none, 1.5M sucrose, 4M NaCl |
| 20°C | 300 MPa [a)] | CFU, CFUsub, MI, MA, LmrP | None |
| 20°C | 300 MPa [a)] | CFU, CFUsub | pH 6.0 |
| 20°C | 300 MPa [a)] | CFU, CFUsub | pH 5.0 |
| 20°C | 300 MPa [a)] | CFU, CFUsub | pH 4.0 |
| 20°C | 300 MPa [a)] | CFU, CFUsub | 0.5M sucrose |
| 20°C | 300 MPa [a)] | CFU, CFUsub | pH 6.0 and 0.5M sucrose |
| 20°C | 300 MPa [a)] | CFU, CFUsub | pH 5.0 and 0.5M sucrose |
| 20°C | 300 MPa [a)] | CFU, CFUsub | pH 4.0 and 0.5M sucrose |
| 20°C | 300 MPa [a)] | CFU | 1M NaCl |
| 20°C | 300 MPa [a)] | CFU, LmrP | 4M NaCl |
| 20°C | 300 MPa [a)] | CFU, MI, MA | milk serum |
| 30°C | 300 MPa | CFU, CFUsub, MA | none, 1.5M sucrose, 4M NaCl |
| 50°C | 300 MPa | CFU, CFUsub, MA | none, 1.5M sucrose, 4M NaCl |
| 20°C | 350 MPa | CFU, CFUsub, MI, MA | 0.5M sucrose |
| 20°C | 400 MPa [a)] | CFU | 3M NaCl, 4M NaCl |
| 20°C | 400 Mpa [a)] | CFU | None |
| 20°C | 400 MPa [a)] | CFU | 0.5M sucrose |
| 20°C | 400 MPa [a)] | CFU | 1M sucrose |
| 20°C | 400 MPa [a)] | CFU | 1.5M sucrose |

| temperature | pressure | analysed parameters | additive |
|---|---|---|---|
| 20°C | 400 MPa [a)] | CFU | 1M NaCl |
| 20°C | 400 MPa [a)] | CFU | 2M NacCl |
| 20°C | 400 MPa [a)] | CFU | 1M NaCl and 2.5mM glycine betaine |
| 20°C | 400 MPa [a)] | CFU | 2M NaCl and 2.5mM glycine betaine |
| 20°C | 400 MPa [a)] | CFU | 3M NaCl and 2.5mM glycine betaine |
| 5°C | 500 MPa | CFU, CFUsub, MA | none, 1.5M sucrose, 4M NaCl |
| 20°C | 500 MPa | MI, MA, LmrP | 1.5M sucrose |
| 20°C | 500 MPa | MI, MA | 4M NaCl |
| 30°C | 500 MPa | CFU, CFUsub, MA | none, 1.5M sucrose, 4M NaCl |
| 50°C | 500 MPa | CFU, CFUsub, MA | none, 1.5M sucrose, 4M NaCl |
| 20°C | 600 MPa [a)] | CFU | None |
| 20°C | 600 MPa [a)] | CFU | 0.5M sucrose |
| 20°C | 600 MPa [a)] | CFU | 1M sucrose |
| 20°C | 600 MPa [a)] | CFU, MI, MA, LmrP | 1.5M sucrose |
| 20°C | 600 MPa [a)] | CFU | 1M NaCl |
| 20°C | 600 MPa [a)] | CFU | 2M NaCl |
| 20°C | 600 MPa [a)] | CFU | 3M NaCl |
| 20°C | 600 MPa [a)] | CFU, MI, MA, LmrP | 4M NaCl |
| 20°C | 600 MPa [a)] | CFU | 2M NaCl and 2.5mM glycine betaine |

The experimental raw data were processed as illustrated in Figure 8 for further analysis by PCA, and for the formulation of the Fuzzy model. The first step of the data processing consisted of averaging multiple raw data obtained from duplicate, triplicate or quadruplicate experiments at identical experimental conditions. The numerical values for viable cell counts and stress resistant cell counts (CFU and CFUsub) were averaged after log-transformation. Second, a normalisation was carried out to scale the data from their original range to a range between zero and one.

Fuzzy C-means clustering was done by the use of Data Engine. The method allowed the identification of data clusters and gave the cluster-centres necessary for the fuzzyfication.

These centres were analysed with respect to transfer functions and analysis of sensitivity in order to define the range of values of the linguistic variables necessary for the fuzzyfication. Furthermore, the automatic generation of the Fuzzy rules was done by WinROSA (both MIT GmbH, Aachen, Germany), an evolutionary search algorithm. These rules were checked by an expert on validity and the rule set was possibly enhanced in case where the algorithm failed. The Fuzzy Logic calculation was performed using Fuzzy-Studio (Gimbio mbH, München, Germany). This software tool allowed the generation of the necessary multi-layer structure of the model. To define the layer of the autonomous variables in the Fuzzy model, a Principal Component Analysis was carried out using MATLAB version 6.5 (The MathWorks, Inc. Natick, MA, USA).

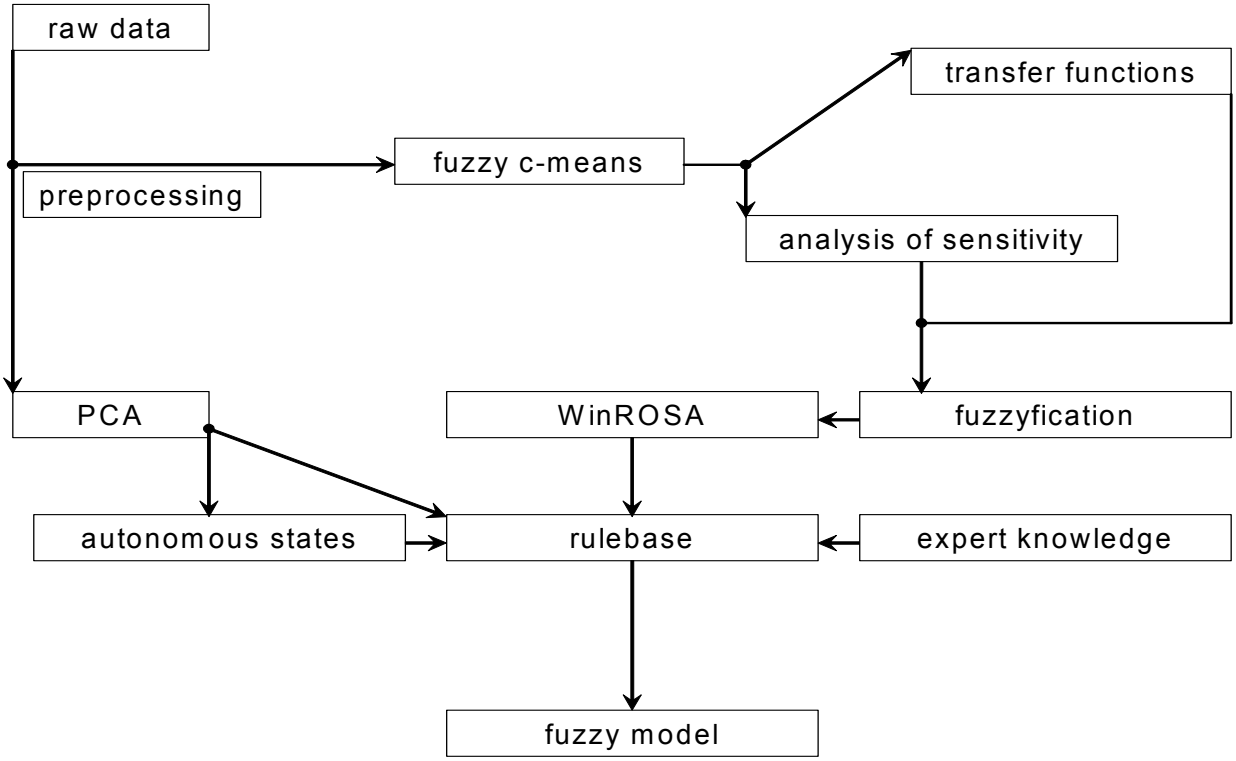


**Figure 8**: Schematic diagram of data-based tools and multivariate statistical analysis that were used in this work for the formulation of a Fuzzy model.

### 2.6.1. Principal Component Analysis

The main purpose of the use of Principal Component Analysis (PCA) was to assess the question whether the major information derived from the 5 different physiological states

(variables) determined experimentally of the data matrix X can be expressed through a reduced number of variables. The data matrix X was defined as

$$X = \left[ x_1, x_2, ..., x_i, ..., x_n \right]^T \left( n \times m \right) \tag{3}$$

where n was the total number of kinetic data sets $x_i$ from a kinetic determined at a specific parameter combination, at specific pressure holding times i. The column vector $x_i$ contains m different components (variables).

Principal components (PC), subsequently denoted as loadings, represent eigenvectors of the matrix X and are obtained by the determination of the eigenvalues and eigenvectors of the correlation matrix $X^T \cdot X \cdot (n-1)^{-1}$. Since the data matrix X can be reconstructed from a linear combination of the eigenvectors, a transformation between the matrix containing the loadings V and the original data matrix X must exist and is supposed to have the form

$$\underset{n\times m}{X} = \underset{n\times m}{S} \cdot \underset{m\times m}{V}^{T} \tag{4}$$

where S is the score matrix containing the coefficients for the linear combination of the loadings.

Thus, PCA performs a rotation of the axes of a coordinate system in a multivariate space defined by the original variables to a coordinate system with orthogonal directions of maximal variance. Hence, a new space was defined by the loadings, each of them being characterised by a percentage of variance of the data.

In order to reduce the amount of data to the significant variables, the number of loadings is reduced to $k < n$, which engenders a reduction of the score matrix to a dimension $k \times m$. Consequently, above mentioned linear combination of the reduced set of loadings can be written as

$$\underset{n\times m}{X} = \underset{n\times k}{S} \cdot \underset{m\times k}{V}^{T} + \underset{n\times m}{E} \tag{5}$$

where the error generated by the reduction of employed number of loadings is represented by the error matrix E.

The number k can be chosen by the modeller. A good estimate for an appropriate number k can be obtained from the scree-plot representing the residual variance as a function of the number of eigenvectors that were calculated. The residual variance V of the $r^*$-th eigenvector was defined as

$$V\left(r^*\right) = \sum_{k=r+1}^{r} \lambda_k^2 \text{ with } 1 \le r^* < r \tag{6}$$

where r represented the number of nontrivial eigenvalues.

To investigate correlations in data, it is useful to project the initial variables into the subspace defined by the reduced number of loadings. The graphical representation of this operation is called “loading-plot”. Each component of PC 1 was plotted against its corresponding component of PC 2. The interpretation was based on the direction in which the points lie on this plot as seen from its origin. If two or more vectors in the loading plot indicate (almost) the same direction they reveal a redundancy in the number of the vector components, thus in the number of measured variables. In this case, the cosine of the angle included by the vectors is approximately 1. Generally, the cosine of the angle between the vectors represents the correlation coefficient for both variables. For further details on PCA, the reader is referred to (Jolliffe, 1986; Martens and Næs, 1989; Henrion and Henrion, 1995; Vandeginste et al., 1998).

### 2.6.2. Fuzzy Logic

In this work, the objective of Fuzzy modelling was to create a multi-step rulebase, which is able to predict all 5 physiological variables of *L. lactis* determined experimentally in dependence on the parameter combinations (input variables) pressure, temperature, pressure holding time and additives. To simplify the rulebase, PCA was carried out to identify those 2 of the 5 variables which can be used as “autonomous output variables” in the Fuzzy model and are predicted in dependence on the input variables. The remaining 3 variables are then predicted by use of the autonomous output variables. If the prediction quality of those variables was not adequate in specific cases, the output autonomous state was omitted. Figure 9 illustrates the structure of the model.

Principal objective of Fuzzy modelling was the definition of a rule base, that is able to predict autonomous output variables as a function of independent input variables by application of Fuzzy (non-binary) logic. Using the results of autonomous output variables, dependent output variables should be predicted. In the case of total error of this prediction tool, dependent output variables could also be predicted by the use of independent input variables (compare Figure 9).

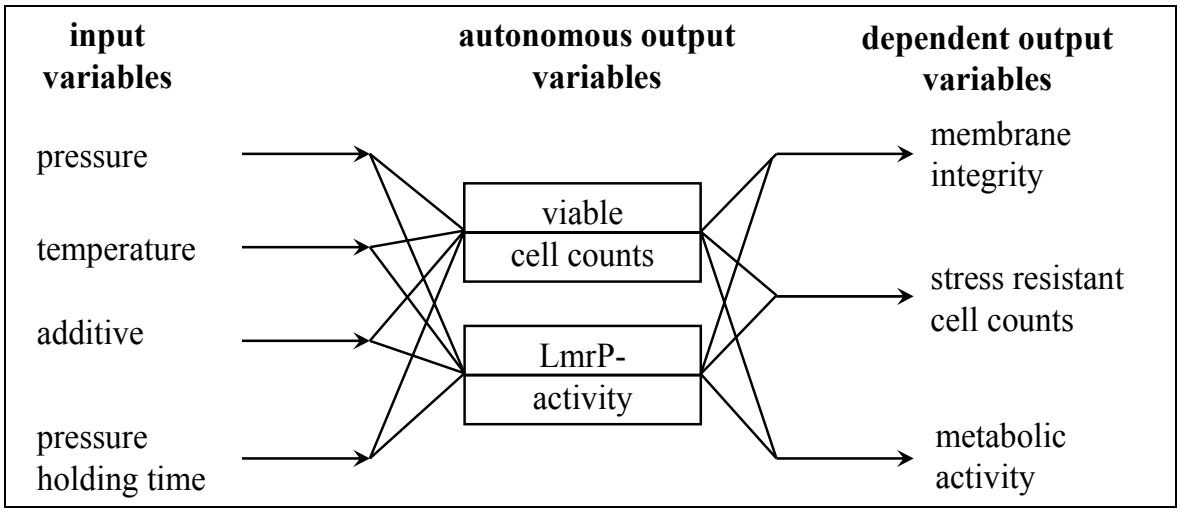


**Figure 9**: Graphical representation of the Fuzzy model.

The first step of the determination of the rule base was the “fuzzyfication”. Sharp data were described with linguistic variables. For example, in the current context pressure values between 50 MPa and 300 MPa were described with the linguistic variable "low", while the linguistic variable "high" was associated to the pressure range between 300 MPa and 600 MPa. The association of linguistic variables to a variable range was achieved by the use of a membership function that took on values larger than zero if the pressure value was located completely within this range and equals zero if the pressure value was completely out of this range. Several membership functions were used to associate linguistic variables to the complete range of the variable. This procedure was applied to all dependent and independent variables. In order to avoid gaps in the parameter definition, the ranges of the individual Fuzzy classifiers were overlapping.

The geometrical form of the membership functions and their definition range may be determined intuitively by the experienced modeller. A more sophisticated method to identify

structures in complex data is the Fuzzy C-means clustering, which has been employed in the current work (Anonymous, 2001). The method allowed the identification of data clusters and gave the cluster-centres as well as a class-membership-value for each data point as result.

To start the algorithm, a number of classes was estimated. At the beginning of the search, classes were chosen randomly by the algorithm and once defined classes were enhanced by application of the algorithm. The method stopped if a predefined difference between the membership value of the previous and of the present iteration was smaller than a given limit of convergence ε. The obtained class-centres and membership values represented typical clusters of measurands.

The obtained cluster membership values were further analysed with respect to their dependency on the in- and output-variables. From the characteristics of these transfer- and sensitivity functions the geometrical shape of the Fuzzy classifiers μ(x) was obtained for all input and output variables (Zimmermann, 1993).

The next step in the set-up of the Fuzzy Logic model was the detection and formulation of rules for the dependency of output parameters on the input parameters. The Fuzzy ROSA algorithm (Fuzzy Rule Oriented Statistic Analysis) was used, which represented an evolutionary search algorithm that allows the automatic generation of Fuzzy rules from data. Therefore, the previously obtained Fuzzyfication must be imported into the software, which then found correlations between data and fuzzyfication. The results were Fuzzy rules having an IF-THEN-structure (see examples below). The Fuzzy "IF"-part described the premise, the Fuzzy "THEN"-part the conclusion of the rule. A validity value is between 0 and 1 and was automatically associated to a rule describing the validity of the rule with respect to the investigated data. The obtained rules were checked by an expert on plausibility and further rules were introduced based on (human) expert knowledge when the set of rules generated by Fuzzy ROSA algorithm failed to adequately described the experimental data. All rules together represented the rulebase of the Fuzzy Logic model (Krone and Kiendl, 1996).

The evaluation of the rule sets requires the combination of rules that apply to a given set of input variables. This was done in a step denominated the inference. For a given parameter set of sharp (input) data, the membership function values to the corresponding linguistic variables were determined by evaluation of the Fuzzy classifiers. These values were associated with the premise of each rule that applies to the present input parameters (aggregation). From the rule and evaluation of the classifiers of the output variable, the membership value of the

conclusion was obtained. This value was always one in the present case, but might adopt other values in general. Both membership values were combined (activation) and weighted by the validity function of the rule (accumulation). One obtains a value for each of the rules representing the degree of application of the rule for the specific set of parameter values.

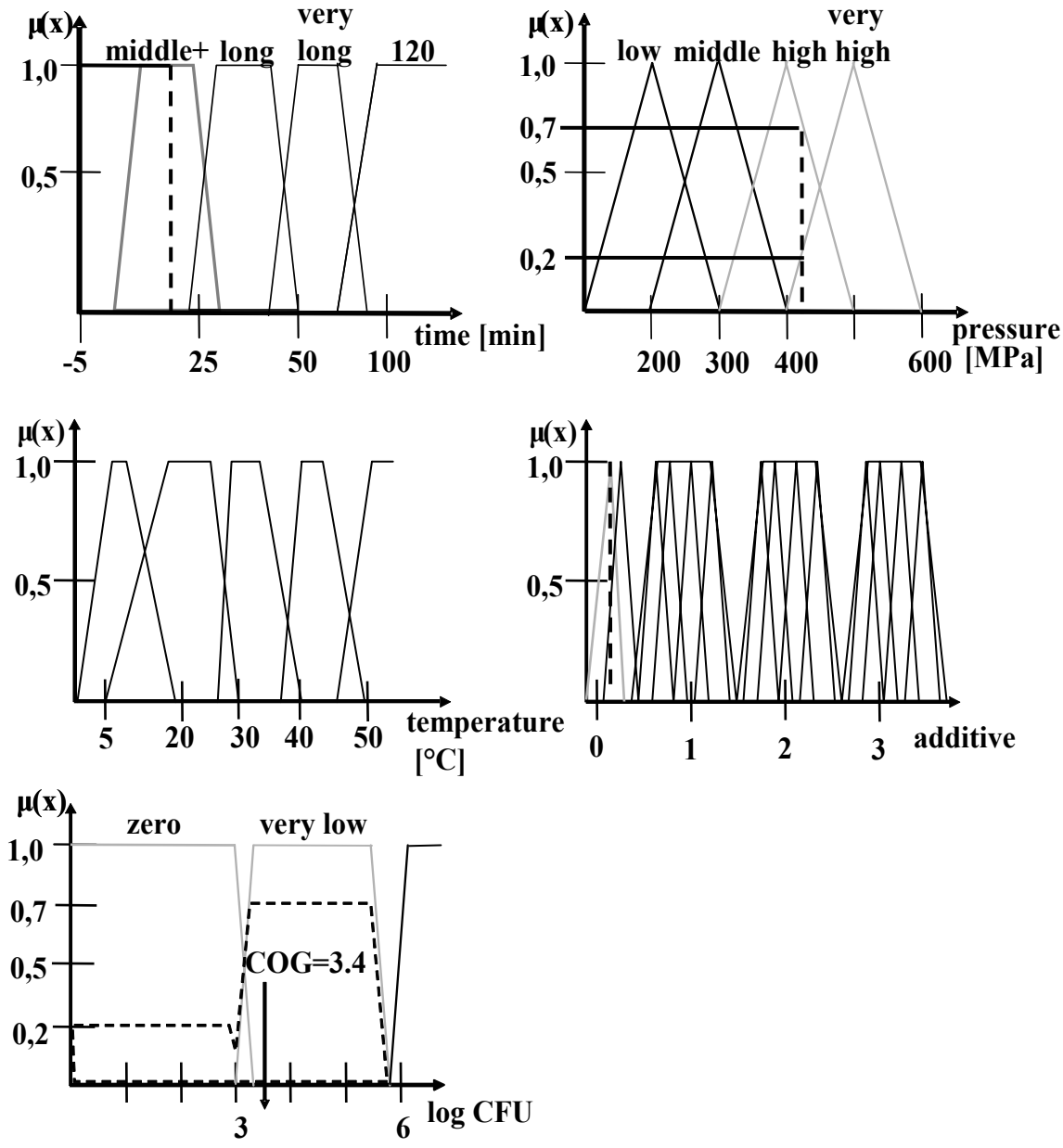


**Figure 10**: Fuzzyfication of the Fuzzy variables. Defuzzyfication (COG-method) of the rules for the present case: number of viable cell counts were detected.

The values of all rules referring to a specific output value were collected and analysed with its classifier function. Each rule addresses a specific linguistic variable of the output variable.

The value of the rule was used to weight the linguistic variable. In order to obtain a sharp value of the output variable the centre of gravity method was applied (Kiendl, 1997). The following example illustrates the operation of the Fuzzy rulebase (Figure 10). The sharp input data consists of a value for the pressure of 430 MPa, a pressure holding time of 20 min and no substrate additive (pure milk buffer). From the rule base, only two rules apply to this case of input parameter values:

*Rule 1: IF "pressure" is "high" AND "time" is "middle+" AND "additive" is "milk buffer" THEN "cell count" is "very low" with a validity of 1.0*

*Rule 2: IF "pressure" is "very high" AND "additive" is "milk buffer" THEN "cell count" is "zero" with a validity of 1.0*

In terms of the classifiers , pressure is “high” with a truth value of 0.7 and “very high” with a truth value of 0.2. The pressure holding time is “middle+” with a truth value of 1.0. The additive is “zero” with a validity function of 1.0 as well. Both involved rules have a previously determined validity value of 1.0.

Thus, rule 1 applies with a truth value of 0.7 and rule 2 applies with a truth value of 0.2. Both truth values are then applied as a weight factor to the Fuzzy classifiers of the conclusion. This leads to a membership function with a maximum value of 0.2 for "zero" viable cell counts and a maximum value of 0.7 for "very low" viable cell counts. In order to obtain a sharp value for the logarithmic cell count to be expected for the above mentioned parameters, the centre of gravity (COG) is determined to 3.4 log cycles and taken as the result of the variable viable cell count.

### 2.6.3. The Logistic Equation

One of the most fundamental models of growth in a closed environment is the Logistic equation also called the Verhulst or Verhulst-Pearl model (Brown and Rothery, 1993). In this work, the function is used as a “mirror” function to describe pressure induced cell death. It can be written as

$$M(t) = \frac{M_{Max}}{1 + \exp\left(-m\left(t - t_0\right)\right)} \tag{7}$$

where M(t) represents the inactivated fraction of the population, $M_{Max}$ is the maximal possible fraction of the inactivated population, m denotes the growth rate constant, and $t_0$ is the time to reach 50% of $M_{Max}$.

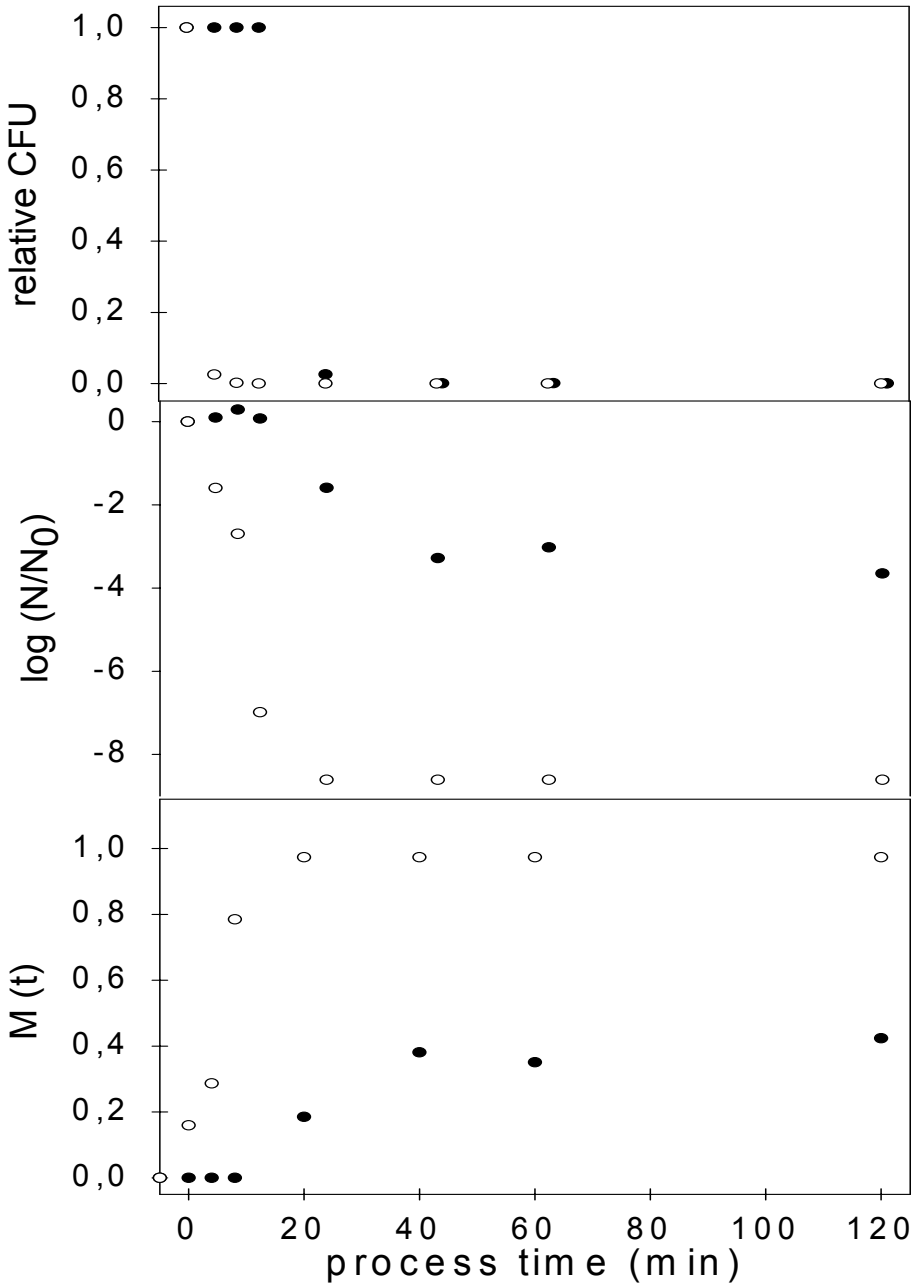


**Figure 11**: Graphical explanation of the used transformation of microbiological inactivation data to obtain growth data. Symbols represent averaged data at 200 MPa and either 30°C (●) resulting in a pronounced tailing or at 50°C (○), where no tailing was visible.

The transformed inactivation data of *L. lactis* were fitted using this Logistic equation. It has been used in this work, because it allows to predict all presented types of inactivation being

shown in Figure 2. The pressure, temperature and additive dependent constants $M_{Max}$, m, and $t_0$ where calculated using either Gauss distribution function or sigmoid functions with four parameters to determine the influence of the environment. Therefore, Sigma Plott 2002 for Windows 8.0 was used.

For the above described purpose, microbiological inactivation data was transformed in the following steps. First, all control values of the same buffer system were averaged. This control value was used for all measured data belonging to one used buffer system. This data set was divided through its averaged control value. As a result of this step, data were set between 0 and 1 (Figure 11A). However, with this kind of data, no prediction of the residual population can be done. Therefore, data were logarithmised (Figure 11B) and then log-linearised. Due to this linearisation, growth functions have been calculated representing the originally data (Figure 11C).

### 2.6.4. Inactivation Process Modelling Using a 3.3-Litre-Medium-Size-Autoclave

In order to investigate the fluid motion, the temperature distributions and the inactivation process of *L. lactis* inside of the 3.3-litre autoclave during the high pressure treatment, experiments were carried out as well as numerical simulations using the code ANSYS CFX 5.7$^{TM}$, which solves the conservation equations of mass, momentum, and energy (Rohsenow, 1973; Jischa, 1982; Spurk, 2004), and user defined transport equations using the Finite Volume Techniques. Furthermore, this code was enhanced with own Fortran 90 codes to describe thermofluiddynamical properties of water under high pressure, e.g. density, specific thermal capacity, viscosity, and the inactivation process of the lactic acid bacteria. Several contributions discussed the solution methods of these equations under high pressure and showed validated results (Hartmann, 2002; Hartmann et al., 2004; Kowalczyk et al., 2004). Furthermore, in larger high-pressure autoclaves with higher compression rates, inflow turbulence can occur. For the high pressure application, both the turbulent inflow conditions and the heat transfer at the inner wall of the autoclave must be taken into account. Thus, the Shear Stress Transport (SST) turbulence model, which accounts for both phenomena, is the most suitable turbulence model for this application. This model gives highly accurate predictions under adverse pressure gradients and ensures accurate solutions of the flow near the wall with the wall scale equation of this turbulence model, making it suitable for the

numerical simulations of the thermofluiddynamics inside a high pressure autoclave (Menter, 1994). An overview on all data prepared for this part of the thesis is provided in Table 3.

**Table 3**: Parameter combinations used for the detection of inactivation kinetics due to their location. Each combination of pressure level, process time and temperature were characterised at least in duplicate or triplicate.

| $T_{Start}$ | analysed parameters | pressure holding time (s) | pressure medium |
|---|---|---|---|
| 301K | CFU, CFUsub | 480, 720 | milk buffer |
| 304K | CFU, CFUsub | 240, 480, 720 | milk buffer |
| 311K | CFU, CFUsub | 480, 720 | sucrose, NaCl |
| 316K | CFU, CFUsub | 240, 480, 720 | sucrose |
| 316K | CFU, CFUsub | 480, 720 | NaCl |
| 321K | CFU, CFUsub | 240, 480 | sucrose, NaCl |

The calculated temperature and pressure simulations inside the autoclave were linked to the inactivation process due to the fact that it strongly depends on these distributions. Since the temperature and pressure distributions are transient and spatial, the inactivation kinetics is a function of time and space. For the calculation of the inactivation process of *L. lactis*, equation (8) was employed to implement the Logistic equation for the description of pressure-temperature effects on microbial cell death of *L. lactis* in industrial applications. The first order differential equation can be written as

$$\frac{\partial M}{\partial t} = \left(1 - \frac{M(\vec{x},t)}{M_{Max}}\right) \cdot m \cdot M(\vec{x},t) \qquad (8).$$

The calculation of the inactivation of *L. lactis* according to the mentioned differential equation above is carried out using the numerical temperature and pressure data at both locations, where the PCR-tubes were placed. First, the cubic splines for temperature and pressure according to both measurement locations were created. Second, a FORTRAN 90

program was written containing the subroutine for the calculation of the inactivation (equation 8). Linking this program with the created splines, the amount of inactivation was achieved at both locations. The inactivation can then be retransformed using the averaged control as the reduction of the cell counts $\log(N/N_0)$. The results in all of the three food matrices are discussed. Overall, for this part of the work, more than 40 GBytes of data were created, mostly for the calculation of the thermofluiddynamical parameters. More than 50 simulations were carried out over a period of three computational months with four computers running in serial or parallel mode.

## Statement

The work presented in the current chapter (2.6.4), in chapter 3.7.3 and in chapter 4.5.2 was carried out as a collaboration between Mr. Panit Kitsubun and the author. Therefore, I would like to thank him for the perfect work and good cooperation. Data belonging to the microbial inactivation as well as the formulation of the mathematical model was done by myself. Mr. Kitsubun incoorporated the equations as subroutines and calculated the inactivation of *L. lactis* in dependence of temperature, pressure, additive and time. For further information, the reader is refered to Kitsubun (2005).

# 3. Results

This work provides a closer analysis of microbial behaviour using different inactivation techniques like temperature-co-solvent and/or pressure/temperature- and/or pressure-pH-dependent inactivation methods.

*L. lactis* has been chosen to describe the influence of temperature or pressure/temperature inactivation in the presence of protective food ingredients like sucrose or sodium chloride in molar concentrations on its inactivation behaviour by the use of different detection techniques describing lethal and sublethal injury of the bacteria as well as the unfolding behaviour of the protein-pool of *L. lactis*. In addition, data based and chemomotric tools were used to detect correlations between the different measurement techniques which described the physiology of the microorganism during or after the treatment. Finally, redundant measurement variables were eliminated and the inactivation behaviour of *L. lactis* is described using two different kind of modelling systems - a data based as well as a determministic tool. The Logistic equation was used to describe the influence of spatiotemporal heterogeneities on the inactivation behaviour of *L. lactis* in a 3.3-litre-medium-size high pressure autoclave.

Furthermore, pressure-pH-dependent inactivation was analysed using *E. coli* to detect correlations between cell death and the behaviour of the intracellular pH during and after the pressure treatment. For this case, the focus was set on three *rpoS* induced stress proteins which were involved in the stabilisation of pH homeostasis of *E. coli*.

## 3.1. Temperature Induced Lethal and Sublethal Injury of *L. lactis*

The effect of time-temperature dependent inactivation as well as the addition of 1.5M sucrose (sucrose) or 4M sodium chloride (NaCl) to milk buffer on *L. lactis* was analysed in this work using indicators of lethal (viable cell counts, CFU) and sublethal injury (stress resistant cell counts, CFUsub). Therefore, a temperature range of 40°C-75°C was chosen with an increment of 5°C as well as process times ranging from 2 min to 120 min. All temperature inactivation kinetics were performed at least in duplicate and the results are reported as mean ± standard deviation.

Figure 12 presents all data for temperature inactivation of *L. lactis* in milk buffer within a range of 40°C-75°C for CFU (Figure 12A) and CFUsub (Figure 12B). If a temperature level below 50°C was used, no substantial reduction of CFU was observed. Contrarely, a reduction

of CFUsub was obvious at a temperature of 45°C resulting in a Δ-2-log-reduction of *L. lactis* after 42 min. Using 50°C, the reduction of CFU started slightly after process time longer than 30 min and ends after 62 min of temperature treatment in a Δ-6-log-reduction of *L. lactis*. The reduction of CFUsub at this temperature started after 4 min and ends in a total inactivation of the population after 62 min.

Furthermore, an increasing temperature resulted in a more efficient process characterised by a more effective inactivation of the bacteria as well as a reduced time for both physiological states. In case of CFU, the use of 65°C ended in a complete inactivation of the population after a tratment of 4 min. Using 70°C and 75°C, no CFU was detected after 2 min. Data concerning CFUsub indicated, that the whole population is affected by a process temperature of 65°C and a process time of 2 min. Using these parameters, no stress resistant cell counts of *L. lactis* were detected.

The protective effect of adding sucrose or NaCl to milk buffer is shown in Figure 13 and Figure 14. In general, a protective effect for both physiological states was detected compared to the inactivation behaviour of *L. lactis* in milk buffer, e.g. using 60 min, sucrose, and 50°C, a difference of 6 log is visible. Furthermore, by the application of higher temperatures, a more efficient inactivation was reached in both systems. Nevertheless, no CFU was detectable after 2 min at 75°C despite of the presence of NaCl or sucrose.

Further on, differences of the additive induced protection between sucrose and NaCl have been detected. NaCl protected the CFU of *L. lactis* at higher temperatures more efficient than sucrose. Differences were observed at 65°C, when a treatment time of 10 min was used (Δ-5-log) and at 70°C, when 2 min (Δ-2-log) or 6 min (Δ-3-log) of the above mentioned temperature was applied.

Comparing the results from CFU with those of CFUsub similiar observations were made. NaCl is more efficient in protecting *L. lactis* against the temperature treatment,whereas differences of Δ-1-log were visible using temperatures of 60°C, 65°C and 70°C after 2 min of temperature treatment. Concluding, sucrose and NaCl protects *L. lactis* against temperature inactivation. Furthermore, NaCl provides stronger protection than sucrose for both CFU and CFUsub if higher temperatures were used.

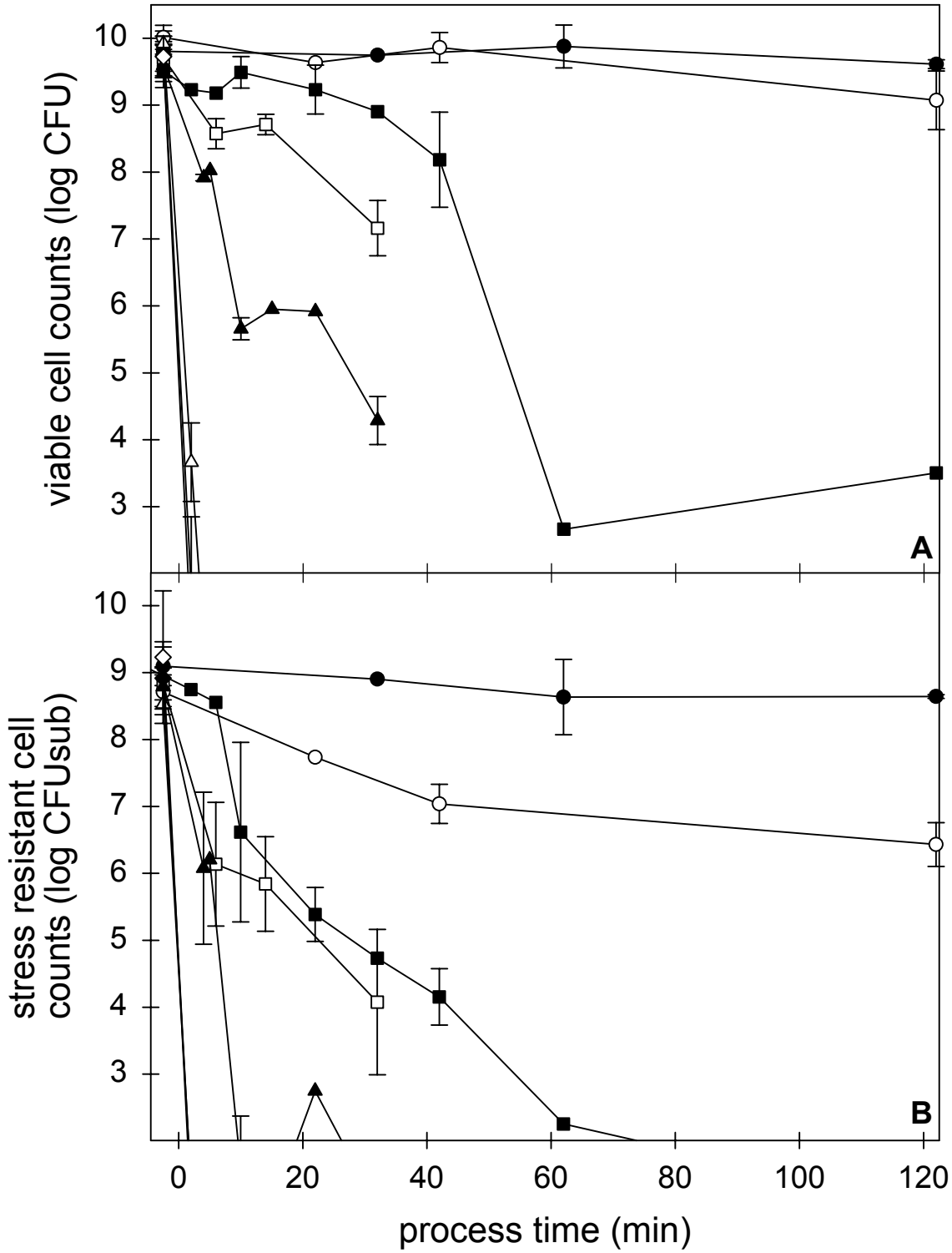


**Figure 12**: Viable cell counts (CFU, A) and stress resistant cell counts (CFUsub, B) of *L. lactis* after a treatment in milk buffer at various temperatures: 40°C (●), 45°C (○), 50°C (■), 55°C (□), 60°C (▲), 65°C (Δ), 70°C (♦) and 75°C (◊). The detection limit for CFU and CFUsub was 100 CFU $ml^{-1}$.

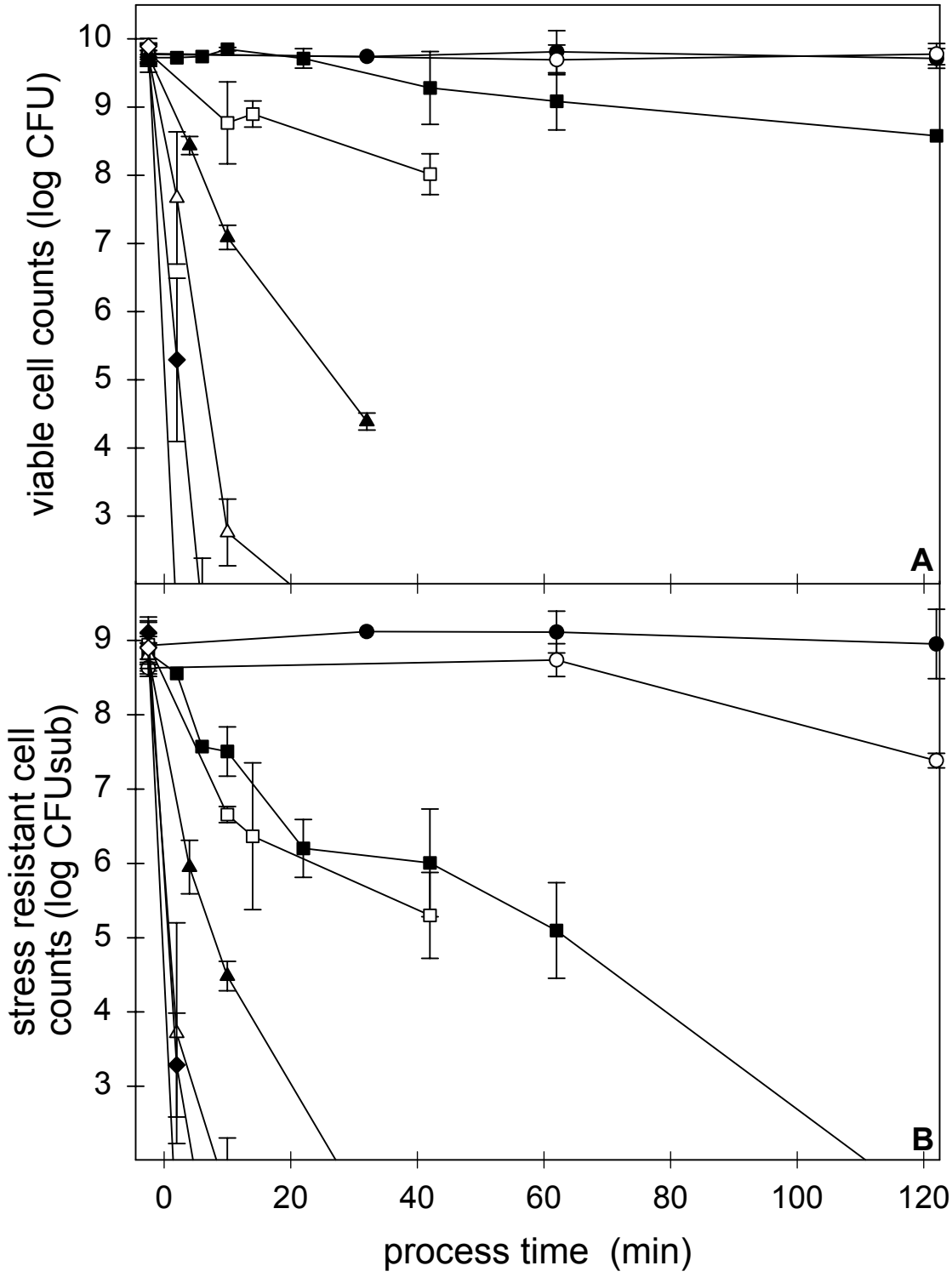


**Figure 13**: Viable cell counts (CFU, A) and stress resistant cell counts (CFUsub, B) of *L. lactis* after a treatment in milk buffer 1.5M sucrose at various temperatures: 40°C (●), 45°C (○), 50°C (■), 55°C (□), 60°C (▲), 65°C (Δ), 70°C (♦) and 75°C (◊). The detection limit for CFU and CFUsub was 100 CFU $ml^{-1}$.

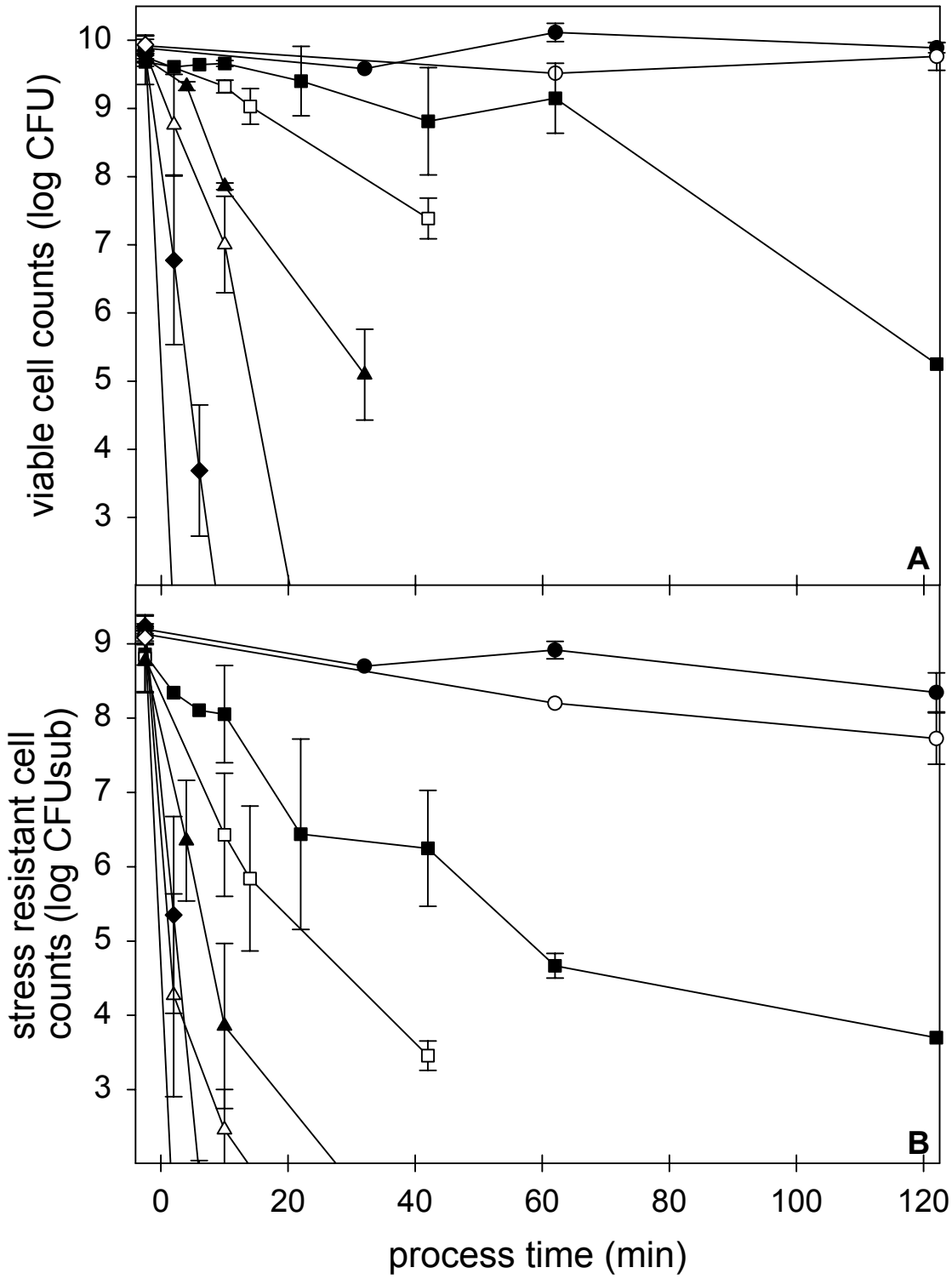


**Figure 14**: Viable cell counts (CFU, A) and stress resistant cell counts (CFUsub, B) of *L. lactis* after a treatment in milk buffer 4M NaCl at various temperatures: 40°C (●), 45°C (○), 50°C (■), 55°C (□), 60°C (▲), 65°C (Δ), 70°C (♦) and 75°C (◊). The detection limit for CFU and CFUsub was 100 CFU $ml^{-1}$.

## 3.2. Detection of the Temperature-Dependent Inactivation of *L. lactis* by FT-IR Spectroscopy

Conformational changes of proteins and internal vibrational modes of lipid acyl chains of the membrane of *L. lactis* due to elevated temperatures were measured in this work using an in-situ technique Fourier transformed infrared (FT-IR) spectroscopy. In this part of the work, data was generated starting with a temperature level of 6°C and ending in $D_2O$ using temperatures of up to 65°C and in $D_2O$-sucrose of up to 75°C. These temperatures were used, because by the application of this temperature for 2 min on *L. lactis,* the complete population was inactivated (compare chapter 3.1).

### 3.2.1. The Analysis of the Vibrational Symmetric $CH_2$

Figure 15 represents data describing the temperature induced shift of the symmetric $CH_2$ absorbance peak maxima found at wave numbers near 2852 $cm^{-1}$ in the presence of $D_2O$ or $D_2O$-sucrose.

If sucrose was added to $D_2O$, the peak was displaced to lower wave numbers. Therefore, a difference in the frequency response was observed between $D_2O$ and $D_2O$-sucrose. The osmolyte induced difference of one wave number (cold temperatures) and of 2.5 wave numbers (warm temperatures) was detected by (Linders et al. 1997, Mille et al. 2002) and was validated with our data.

The temperature dependency of this data was calculated using a sigmoidal function with four parameters. The temperature induced shift of the peak maxima to higher wave numbers was explained in that way, that the chains are “melting” and a high conformational disorder is reached at high temperatures in the liquid crystalline phase (Ulmer et al. 2002b). The temperature $T_m$ was approximately 18.7°C (melting temperature) for data measured in $D_20$ and approximately 18.0°C for data measured in $D_20$-sucrose. Concluding, no relevant influence of sucrose was found on the behaviour of $T_m$ (Linders et al. 1997).

Contrarely, in case of $D_2O$, the phase change was detected between 7°C (gel phase) and 35°C (liquid cristalline phase). If sucrose was added to $D_2O$, the phase change was found between 8°C and 30°C. A difference in the behaviour of about 6°C was detected, if both buffer systems were compared (compare Figure 15).

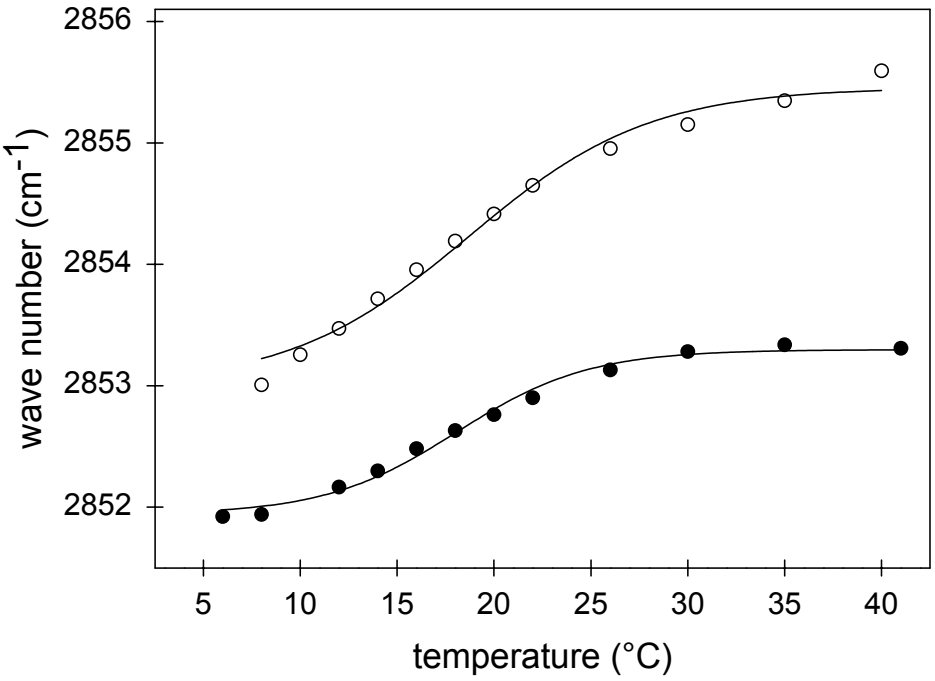


**Figure 15**: Vibrational frequencies for the $CH_2$ symmetric stretch of membrane lipids of *L. lactis* cells in $D_2O$ (○) and $D_2O$-1.5 M sucrose (●) as a function of temperature. The solid line represents the fit using a sigmoidal function with 4 parameters to describe the temperature shift of the membrane from the gel to the liquid cristallin phase.

### 3.2.2. The Analysis of the Amide A Band + HOD Stretch

The analysed peak of the amide A and the vibrational changes of HOD-stretching and its temperature induced shift in dependence on $D_2O$ and $D_2O$-sucrose could be seen in Figure 16. The peak maxima were found in a range between 3300 $cm^{-1}$ and 3400 $cm^{-1}$. By adding sucrose to $D_2O$, the peak maxima was shifted again to lower wave numbers.

Due to the fact, that the analysis took place in a liquid environment, the HOD-stretching band behaviour is dominant. Therefore, no prediction about amide A behaviour was possible. Otherwise, the calculated slope of both directs indicate nearly the same value. Therefore, the analysis of this peak was found to be an useful indicatur for the surrounding temperature of the system (compare Figure 16).

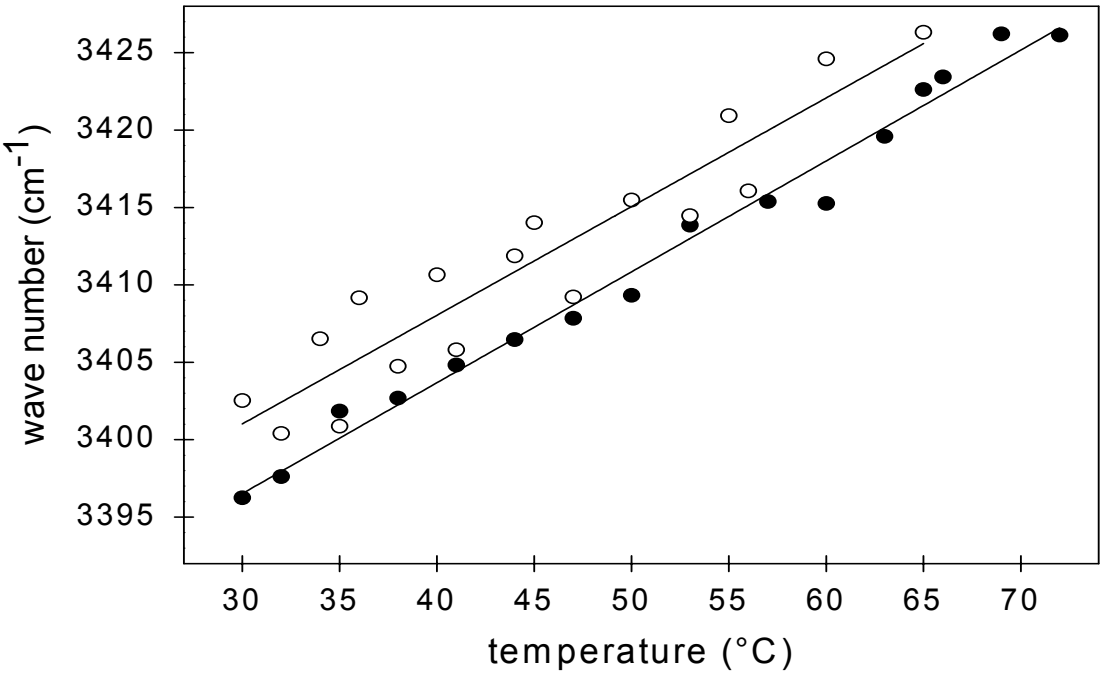


**Figure 16**: Vibrational frequencies for the HOD-stretch and the amide A of *L. lactis* cells in $D_2O$ (○) and $D_2O$-1.5M sucrose (●) as a function of temperature. The solid line represents the linear fit of the temperature shift of the peak maximum.

### 3.2.3. The Analysis of the Amide II'- and the Amide II Band

In case of amide II (~1550 $cm^{-1}$, nondeuterated) and its corresponding amide II' (~1455 $cm^{-1}$, deuterated), a sensitive indicator of hydrogen-deuterium-(D/H) exchange in proteins was found. To highlight the temperature upcoming D/H exchange, the difference spectra was generated by substracting the spectrum at 30°C from the spectra obtained at elevated temperature. The results are shown in Figure 17.

Looking at Figure 17, the characteristic infrared peak changed significantly under elevated temperatures. Therefore, the nondeuterated fraction of the amide II region at nearly 1550 $cm^{-1}$ decreased by increasing temperature. In return, its corresponding amide II' region at nearly 1455 $cm^{-1}$ increased by increasing temperature. In conclusion, nondeuterated areas become accessible to deuterium and were exchanged by the surrounding $D_2O$. Therefore, the D/H exchange is increasing with increasing temperature (compare Figure 17; Linders et al., 1997; Smeller et al., 2000; Smeller et al., 2002). This de- and increase was observed for both analysed media. The exchange started immediately after the temperature was elevated. The influence of sucrose is shown in Figure 18 and Figure 19.

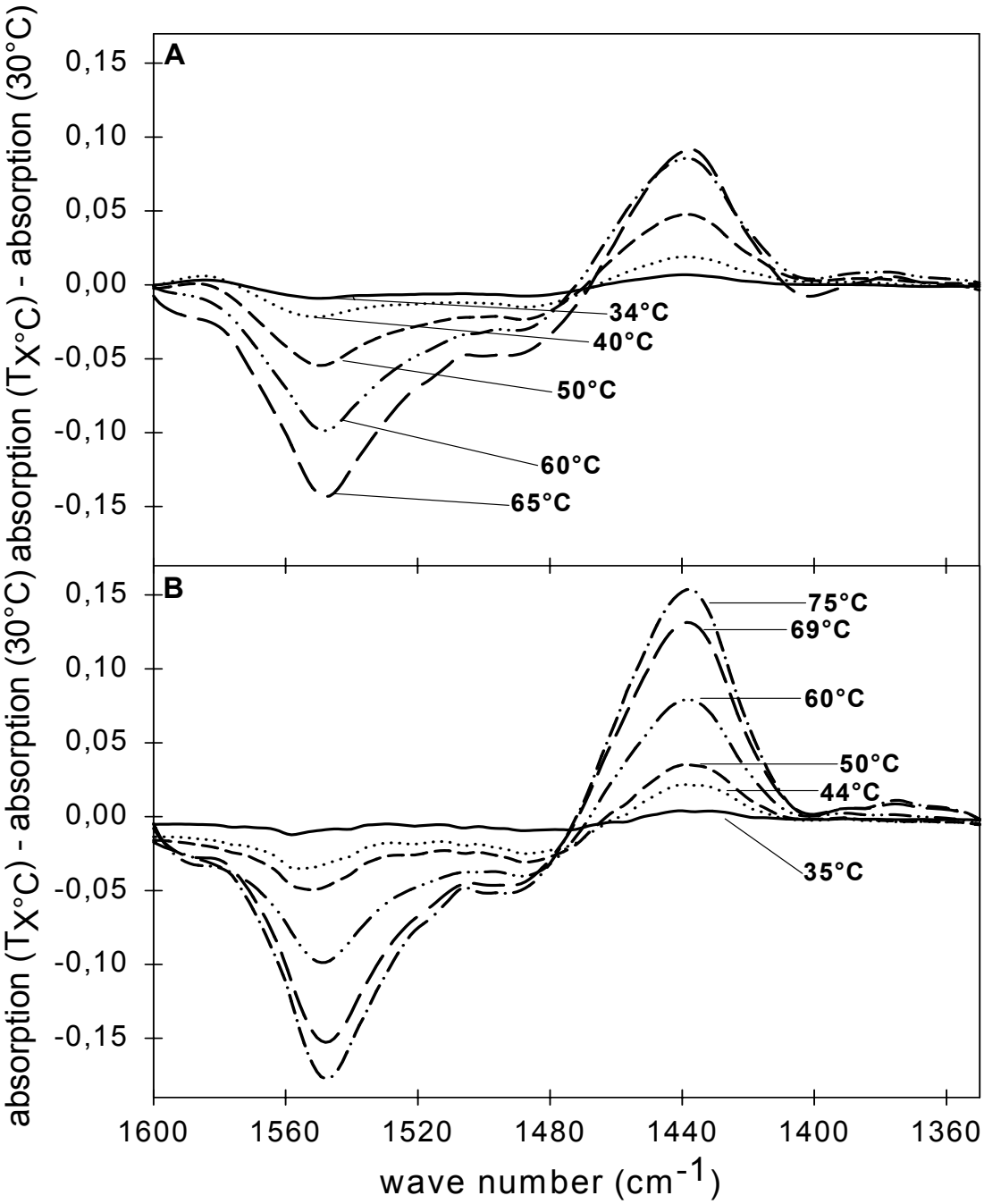


**Figure 17**: Difference FT-IR spectra of amide II and amide II' region (1360 $cm^{-1}$ - 1600 $cm^{-1}$) generated by subtraction of the spectrum at 30°C from the spectra at elevated temperatures. A: data generated in $D_2O$. B: data generated in $D_2O$-sucrose.

Figure 18 represents the ratio of the calculated area between the x-axis and the spectra ranging from 1510 $cm^{-1}$ to 1590 $cm^{-1}$. In this part of the spectra, the area is decreasing due to the increasing H/D-exchange. The calculated areas have been normalised between 0 and 1 by

using data calculated for 30°C. In contrast, the increase of the area between the x-axis and the spectra ranging from 1410 $cm^{-1}$ to 1490 $cm^{-1}$ may also be used to describe the D/H exchange.

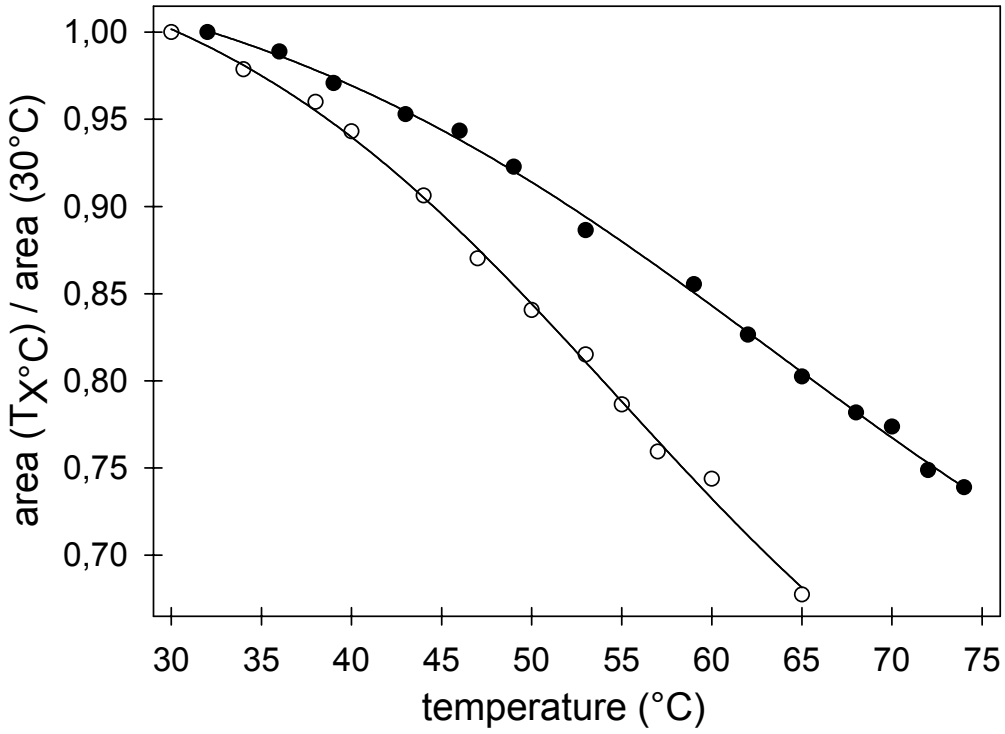


**Figure 18**: Temperature effect on the area ratio generated by dividing the calculated area of 30°C from the area at elevated temperatures. The ratio was calculated between the x-axis and the spectra ranging from 1510 $cm^{-1}$ to 1590 $cm^{-1}$ for data generated in $D_2O$ (○) and $D_2O$ sucrose (●).

The relative decrease of the area showed an accelerated exchange in case of $D_2O$ compared to $D_2O$-sucrose. This difference could be seen easily if the results obtained at 65°C were regarded. In $D_2O$, a decrease of about 33% is visible whereas only a reduction of about 20% took place in the presence of $D_2O$-sucrose at this temperature. Another idea to analyse the generated data was to calculate the intensity ratio of the peak maxima. The results, which were presented in Figure 19 let conclude the same. Here again, the D/H exchange was accelerated in $D_2O$. The measured and calculated data figured out a complete exchange at 65°C in $D_2O$. Contrarely, this was observed in $D_2O$-sucrose at a temperature level of 72°C. Here again, the complete exchange was prolongated due to the add on of sucrose to $D_2O$.

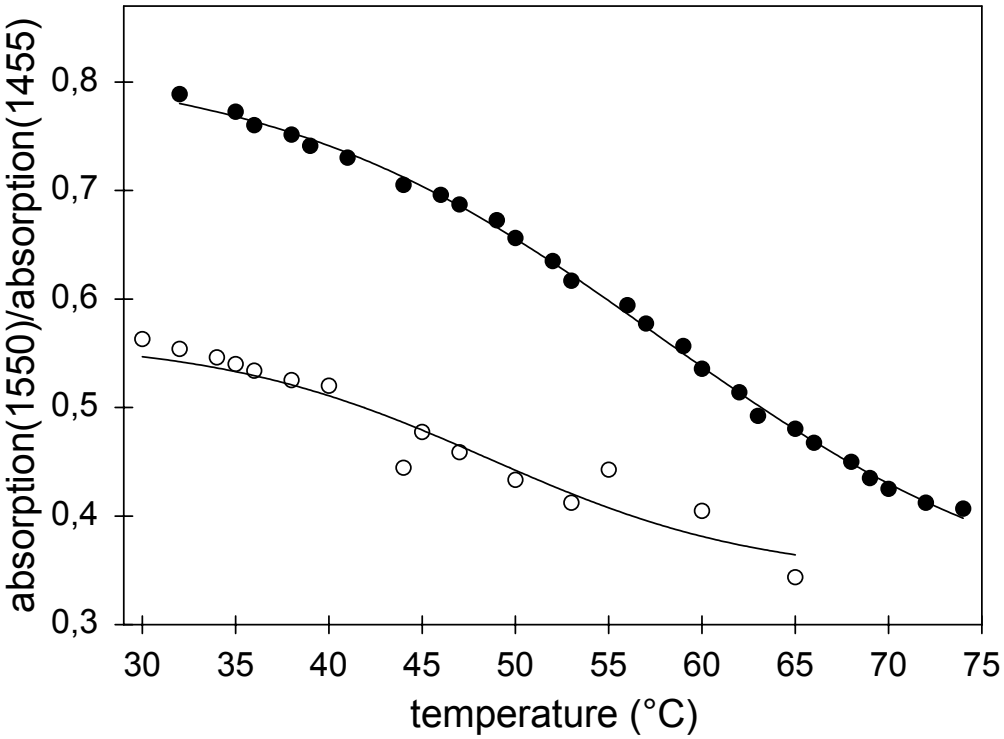


**Figure 19**: Temperature effect on the band intensity ratio 1550 $cm^{-1}$/1455 $cm^{-1}$ for data generated in $D_2O$ (○) and $D_2O$ sucrose (●).

### 3.2.4. The Analysis of the Amide I' Band

The amide I' band is detected between 1600 $cm^{-1}$ - 1700 $cm^{-1}$. In this range, it is possible to extract important informations about the secondary structure of the proteins. The detected amide I' region shows a broad and asymmetric band with the maximum around 1645 $cm^{-1}$ (compare Figure 6 and Figure 22). This is responsible to the overlapping of a number of individual amide I' components.

First, to detect temperature related changes in the spectra, the difference FT-IR spectra were calculated (Figure 20). Here again, the difference spectra for both media were generated by substracting the spectrum measured at 30°C from the spectra obtained at elevated temperature. The first indicator for the hampered conformational changes in the presence of sucrose was, that the spectral changes started in $D_2O$ at a temperature level at 45°C and in $D_2O$-sucrose at 50°C.

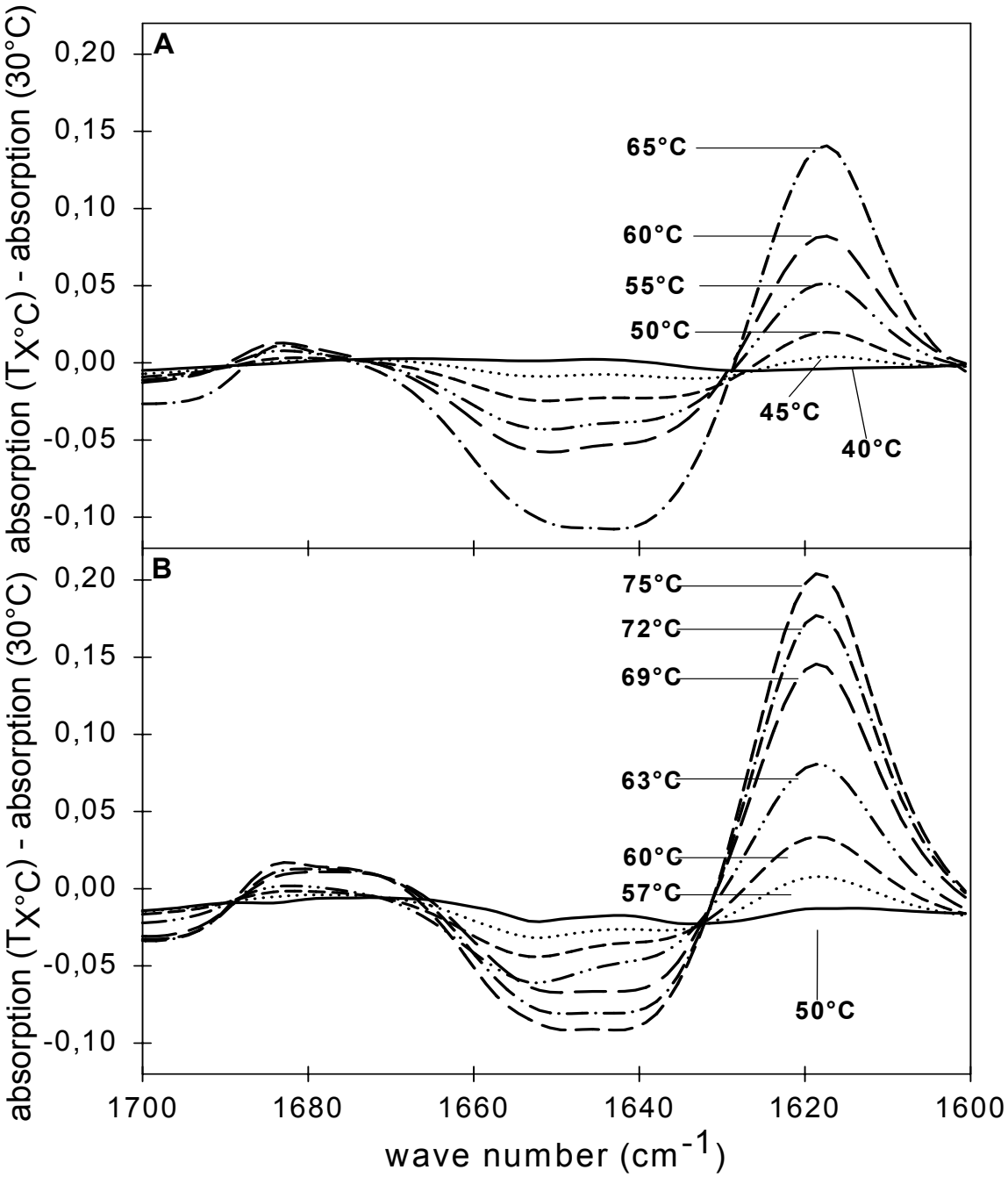


**Figure 20**: Difference FT-IR spectra of the amide I' region (1600 $cm^{-1}$ - 1700 $cm^{-1}$), generated by subtraction of the spectrum at 30°C from the spectra at elevated temperatures. A: measurement data generated in $D_2O$. B: measurement data generated in $D_2O$-sucrose.

The accelerated change of the spectra in the presence of $D_2O$ could be detected clearly in Figure 21. Therefore, the maximal- and minimal-absorbance-value at a wave number of ~1620 $cm^{-1}$ and ~1645 $cm^{-1}$ were plotted against the temperature. The described data were obtained from the difference FT-IR spectra (compare Figure 20).

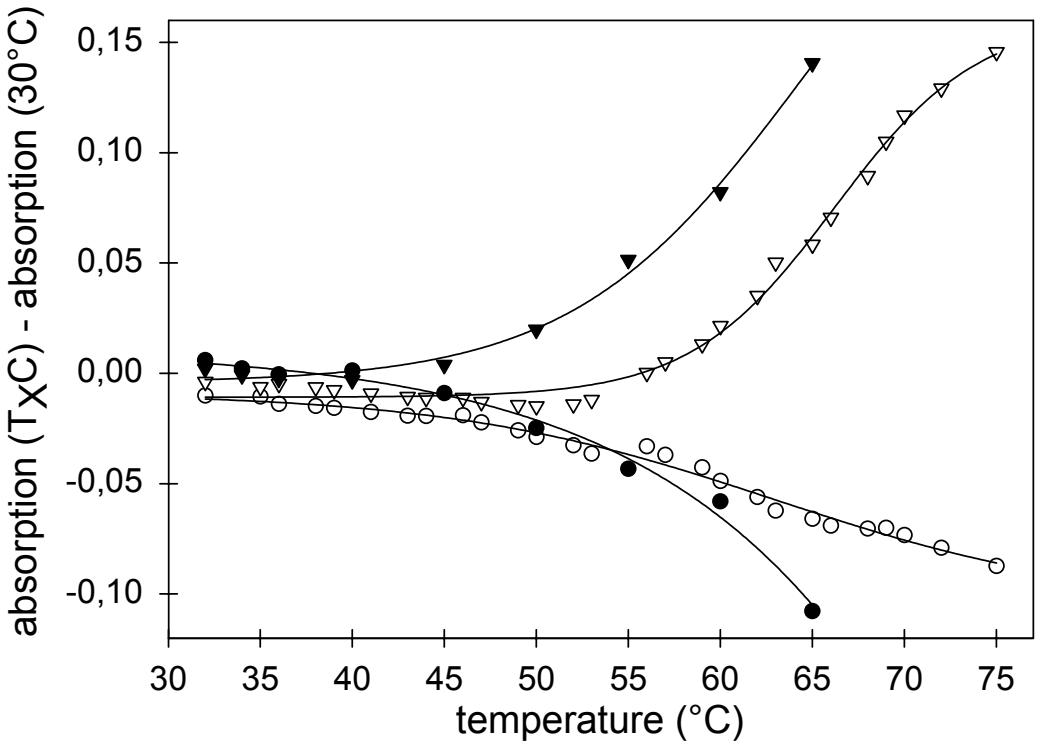


**Figure 21**: Temperature related absorption maxima (▼, ~ 1620 $cm^{-1}$) or minima (●,~ 1645 $cm^{-1}$) obtained by the calculation of the difference FT-IR spectra (compare Figure 20). The filled symbols represent data generated in $D_2O$, the empty symbols represent data generated in $D_2O$-sucrose.

In conclusion, a significant deceleration was obtained in the presence of sucrose, e.g. the difference between both buffer systems at 65°C at ~1620 $cm^{-1}$ is about 0.1. A difference in data of 0.05 was achieved using data obtained at a wave number of ~1645 $cm^{-1}$ at 65°C for both buffer systems.

Furthermore, Figure 20 reflected the formation of three peaks. The peak which was found at ~1620 $cm^{-1}$ was assigned to β-sheet structure (Luo et al., 1994; Goossens et al., 1996). Due to the fact that the peak is increasing with elevated temperature, an increasing fraction of β-sheet of the incorporated proteins is assumed. This increase is associated with increasing disorder of the secondary structure. Furthermore, the peak at ~1645 $cm^{-1}$ is associated to α-helix or other polypeptid chains without known secondary structure (Takeda et al., 1995a and b; Gilmanshin et al., 2002; Barth und Zscherp, 2002; imb Jena, w.d.). The temperature related changes were detected as process induced decrease of the detected structural elements within this range of wave numbers. The third peak, detected at ~1680 $cm^{-1}$ was related to β-sheet structure or β-

turns. Here again, this peak is related to an increasing structural disorder (Barth und Zscherp, 2002; imb Jena, w.d.).

However, clear statements about the conformational changes of protein secondary structures are impossible due to the fact, that this design inhibits a clear allocation of structural elements due to the overlapping effects of all analysed proteins. Otherwise, the frequency characteristic of different secondary structure elements may be achieved by the use of the second-derivative-analysis. Second derivative spectra were generated by using a 9-data point (9 $cm^{-1}$) function, which is implemented in OPUS. An overview of all secondary structure characteristics is given in Table 4. Furthermore, a comparison between data of the amide I' region and their second derivative spectra recorded at 32°C and 74°C is prepared in Figure 22.

**Table 4**: Overview of all found secondary structure characteristics.

| **characteristic** | **wave number ($cm^{-1}$)** | **range of values ($cm^{-1}$)** |
|---|---|---|
| α-helix | ~1652 | 1649-1653 |
| ß-sheet | ~1681 | 1680-1683 |
| ß-sheet | ~1636 | - |
| ß-sheet | ~1618 | - |
| Turn | ~1687 $cm^{-1}$ | - |
| random coil | ~1658 | - |
| unordered | ~1642 | - |

The second derivative analysis permits the direct separation of the amide I' band into its components. In this study, conformational changes, which occur over the temperature increase, were related to the formation of turn- and increasing ß-sheet-structure at ~1683 $cm^{-1}$ (compare Figure 22). Further unordered structures become visible at 1658 $cm^{-1}$ and 1642 $cm^{-1}$ which were related to random coil and unordered structure. Furthermore, the amount of α-helix is decreasing when the peaks obtained by the second derivative analysis were compared. Clear changes are visible in the range of 1618 $cm^{-1}$, where the increase of ß-sheet-structure is

detectable. In conclusion, the analysis indicates an increase of structural disorder in the complete fraction of the proteins incorporated in *L. lactis*. This increase of unorder is coupled with a decrease of ordered structural components.

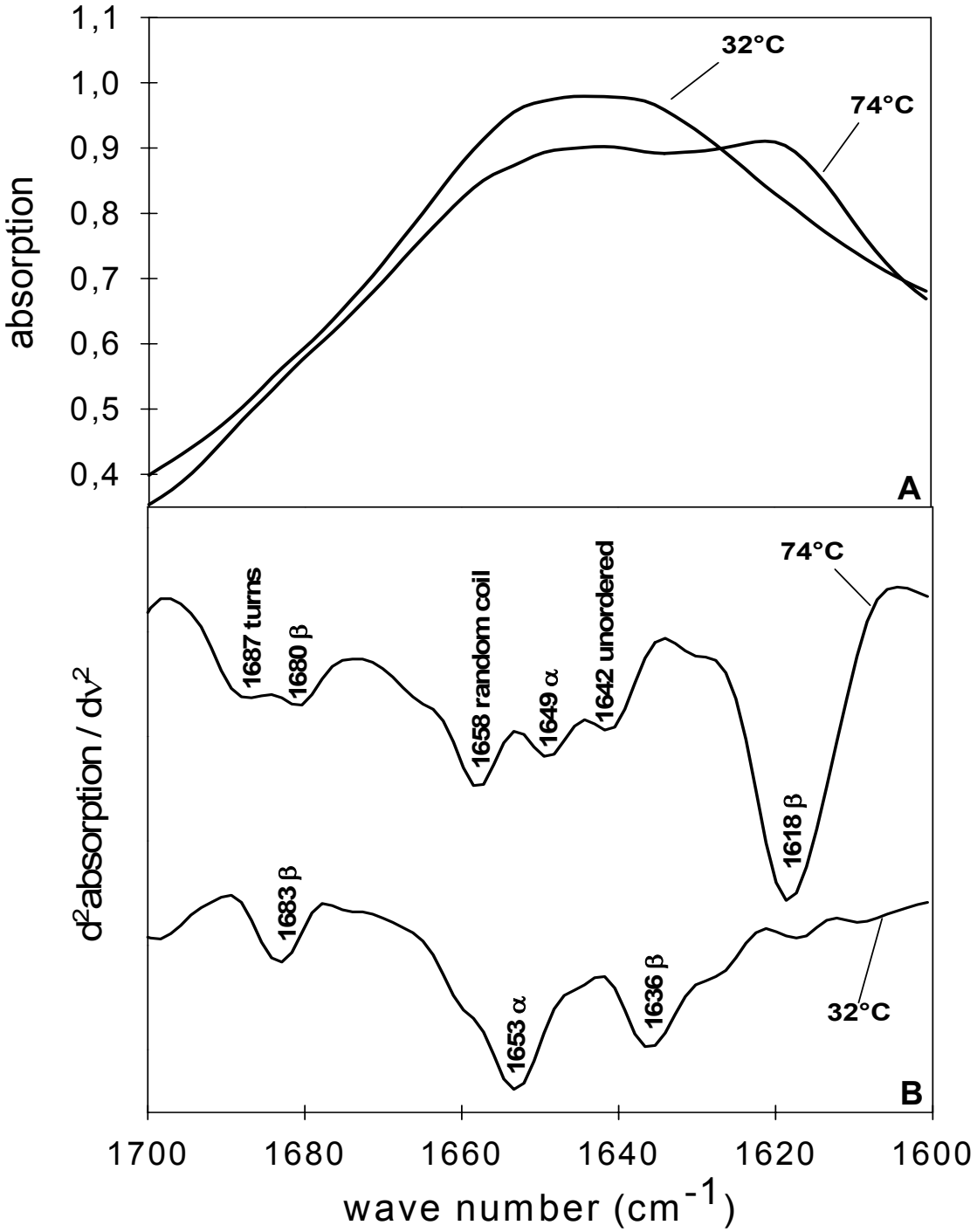


**Figure 22**: amide I' band of the infrared spectra of temperature induced inactivated or vital population (A) and its second derivative (B) recorded in $D_2O$-sucrose using a temperature of 32°C and 74°C.

## 3.3. Modelling of Thermal Inactivation and FT-IR Data of *L. lactis*

To obtain insights into the process induced inactivation of *L. lactis*, data collected by FT-IR should now be compared to data recorded by the detection of viable cell counts (CFU) and stress resistant cell counts (CFUsub) in the presence of milk buffer and milk buffer sucrose. Therefore, the data sets shown in Figure 12 and Figure 13 have to be modelled to obtain suitable parameters which may be used to correlate this data with the FT-IR data. The temperature-co-solvent induced inactivation was modelled by the use of the Logistic equation (compare equation (7), and chapter 3.7.2 and 4.5.2). An overview of the obtained results is given in Figure 23 for the physiological states viable and stress resistant cell counts and the obtained parameters are combined in Table 5.

**Table 5**: Parameter estimates of viable cell counts of *L. lactis* for the Logistic function.

| | Milk buffer | | | | | | Milk buffer sucrose | | | | | |
|---|---|---|---|---|---|---|---|---|---|---|---|---|
| | CFU | | | CFUsub | | | CFU | | | CFUsub | | |
| T (K) | $M_{Max}$ | m (s) | $t_0$ (s) | $M_{Max}$ | m ($s^{-1}$) | $t_0$ (s) | $M_{Max}$ | m ($s^{-1}$) | $t_0$ (s) | $M_{Max}$ | m ($s^{-1}$) | $t_0$ (s) |
| 313 | 0,05 | 805,0 | 3321,9 | 0,04 | 847,5 | 1997,6 | 0,03 | 846,8 | 3332,9 | 0,05 | 2232,0 | 4995,3 |
| 318 | 0,13 | 805,0 | 3321,1 | 0,31 | 843,3 | 1985,6 | 0,04 | 846,0 | 3330,6 | 0,20 | 2192,1 | 4636,0 |
| 323 | 0,68 | 804,7 | 3304,6 | 0,94 | 797,8 | 1879,5 | 0,07 | 838,3 | 3300,9 | 0,97 | 1958,0 | 3475,9 |
| 328 | 0,94 | 790,9 | 2996,7 | 0,97 | 495,3 | 1258,8 | 0,21 | 763,6 | 2967,6 | 1,00 | 1146,5 | 1629,1 |
| 333 | 0,96 | 394,9 | 1050,5 | 0,97 | 100,1 | 344,9 | 0,59 | 394,9 | 1323,3 | 1,00 | 319,2 | 514,4 |
| 338 | 0,96 | 45,0 | 127,3 | 0,97 | 18,7 | 94,9 | 0,89 | 75,6 | 214,9 | 1,00 | 74,5 | 176,0 |
| 343 | 0,96 | 15,4 | 63,3 | 0,97 | 10,8 | 63,8 | 0,96 | 21,1 | 72,8 | 1,00 | 32,5 | 97,0 |
| 348 | 0,96 | 15,0 | 60,2 | 0,97 | 10,1 | 60,4 | 0,98 | 15,6 | 61,0 | 1,00 | 26,1 | 79,7 |

A $R^2 \geq 0.95$ (compare Figure 23) was obtained for all four analysed data sets. However, a few outliers are visible which were related to the same problems described below. In spite of them, the model seems to be correct due to the fact, that almost all the data are within the range of error and were predicted correctly.

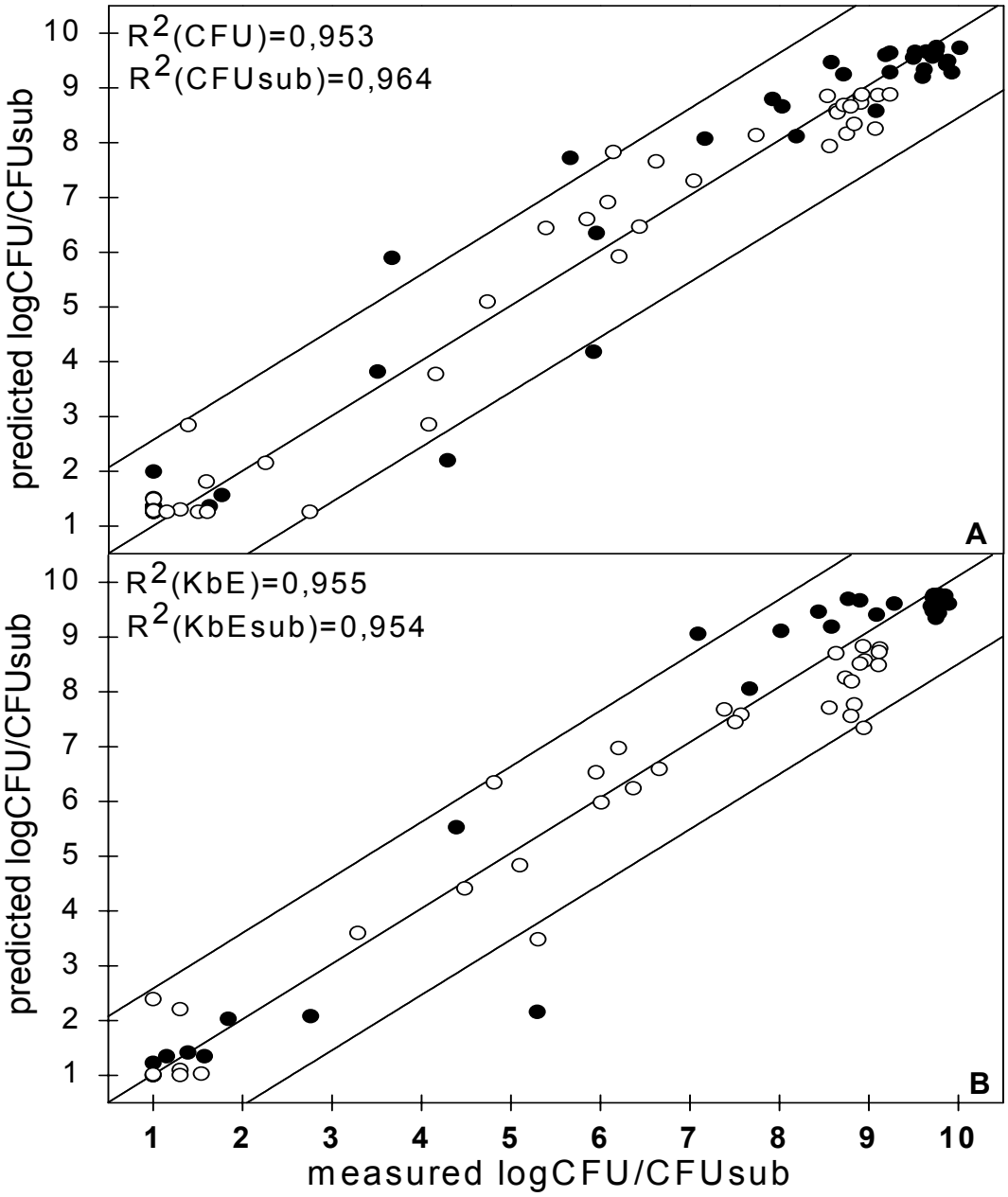


**Figure 23**: Comparison of measured and predicted data for CFU (●) and CFUsub (○) for model formulation. Shaded areas indicate the deviation explained by overall experimental errors. A: data generated in $D_2O$. B: data generated in $D_2O$ sucrose.

The obtained protective effect of sucrose is demonstrated in Figure 24. Therefore, $M_{Max}$ and the ratio of cells measured in milk buffer and milk buffer sucrose is shown.

In case of CFU, the effect of sucrose is visible in a temperature range between 43°C and 65°C. The model detected a Δ-6-log difference between both data sets measured for viable cell counts (compare Figure 24A) which is consistent with the experimental data. Furthermore, the measured Δ-1-log differences for stress resistant cell counts was also

calculated. This agreement between the measured and the predicted data also indicates the correctness of the model. Further on, the protective effect of sucrose using thermal treatment was verified for *L. lactis* (Coroller et al., 2001; Mattick et al., 2001).

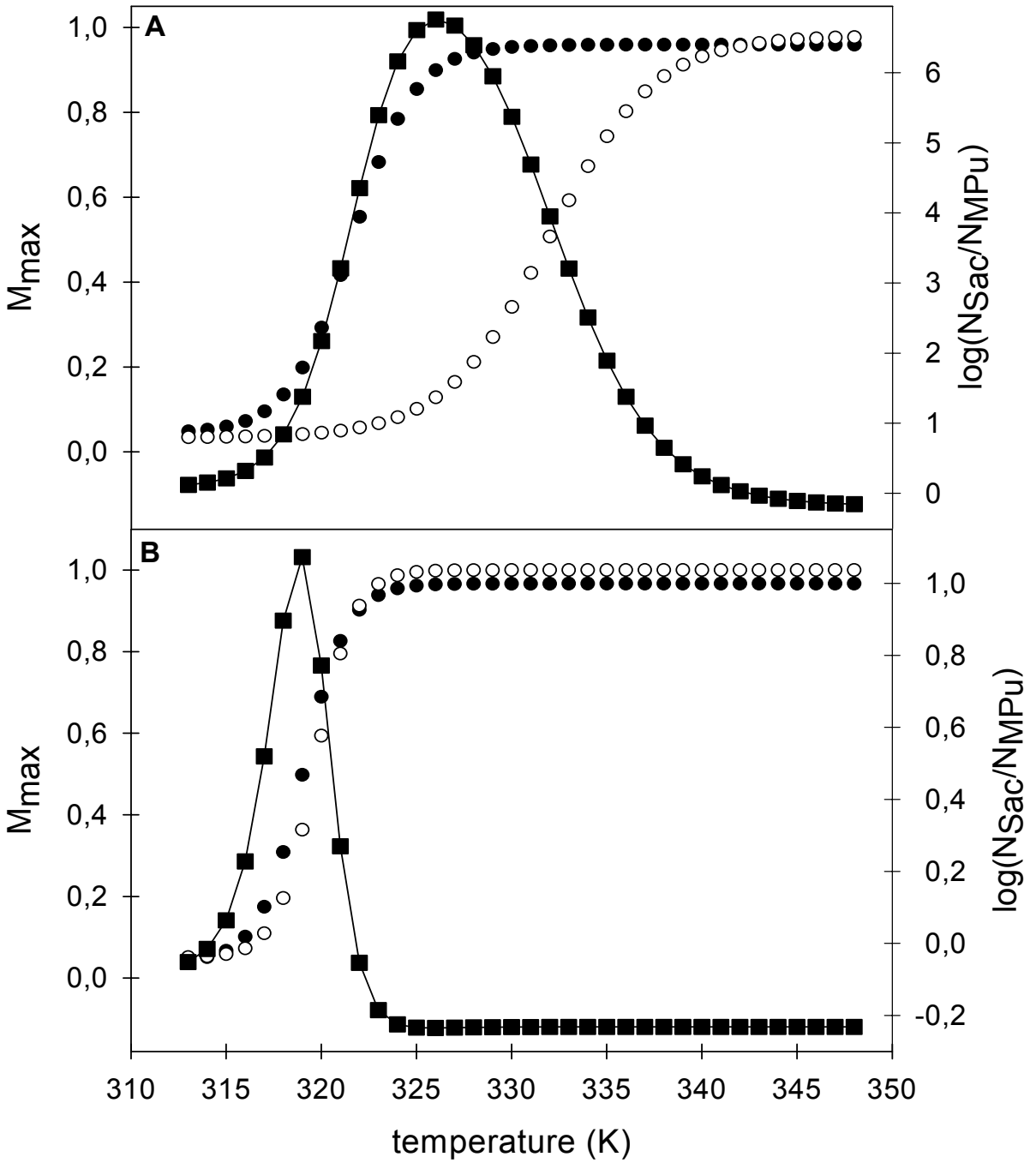


**Figure 24**: Temperature dependent change of $M_{Max}$ (left y-axis) calculated for data generated in milk buffer (○) or milk buffer sucrose (●) for viable (A) and stress resistant cell counts (B). Furthermore, the ratio of cells measured in milk buffer and milk buffer sucrose is shown (■, right y-axis).

Furthermore, $M_{Max}$ seemed to be a suitable indicator to compare process induced inactivation data with those obtained by the FT-IR study. Reasons are, that $M_{Max}$ represents the amount of the population which was irreversibly inactivated by the process. Therefore, this parameter should then be correlated to the D/H exchange and the structural changes detected by amide I' of the cumulative examination of all proteins of *L. lactis*. Thus, the increasing deuterated fraction of amide II' (1455 $cm^{-1}$, Figure 17) as well as the increase of the fraction related to β-sheet (1620 $cm^{-1}$, Figure 20) were used (compare Figure 25). This data were normalised to a range between 0 and 1 using the data measured for either 65°C in $D_2O$ or 75°C in $D_2O$-sucrose (see Figure 25).

The protective effect of sucrose was visible if the parameters m and $T_0$ were analysed. A difference of ~8.5°C in $T_0$ was calculated if data of ß-sheet (or amide II', ~5.5°C) $D_2O$ are compared to data of $D_2O$-sucrose. A difference in $T_0$ of ~10°C is visible in case of viable cell counts (CFU) and a difference of ~3°C in case of stress resistant cell counts (logCFU). Furthermore, the calculated slope (m) is almost higher for $D_2O$-sucrose than for $D_2O$ (compare Figure 25). Concluding, sublethal injury of *L. lactis* took place before the irreversible inactivation of the population was detected. Reasons were the irreversible loss of membrane bound proteins whereupon *L. lactis* lost its ability to stabilise its membrane potential. Therefore, NaCl obtained the possibility to permeate into the microorganism which finally resulted in cell death (compare Figure 25).

Furthermore, a phase-delayed inactivation of *L. lactis* was detected compared to data describing the conformationl changes of the secondary structure of proteins (amide I', compare Figure 25). This could be seen easily using the parameter m which has nearly the same value for data of $M_{Max}$-sucrose and sucrose-ß-sheet. Otherwise, $T_0$ describes a positive difference of ~7°C between sucrose-ß-sheet and $M_{Max}$-sucrose. This difference is independent of the height of the calculated value. Therefore, the complete structural changes detected by amide I' were achieved after cell death. This phenomen is also described by the calculated point of inflection of amide I' (represented by $T_0$). If it was reached, the complete population of *L. lactis* had almost been inactivated in both buffer systems.

The data describing the D/H-exchange represented the most sensitive indicator for conformational changes in proteins due to the fact, that first changes occurred using a temperature of 34°C. If this temperature was used, no inactivation of *L. lactis* was detected by the measurement of both physiological states. Otherwise, sublethal injury of *L. lactis* was

detected using 45°C. If this temperature was reached, an increase of 20% fo the D/H exchange was detected. Therefore, it may be assumed, that these 20% may describe the loss of enzymatical activity resulting in sublethal injury of the bacteria. For this purpose, the D/H exchange may represent an indicator for sublethal injury.

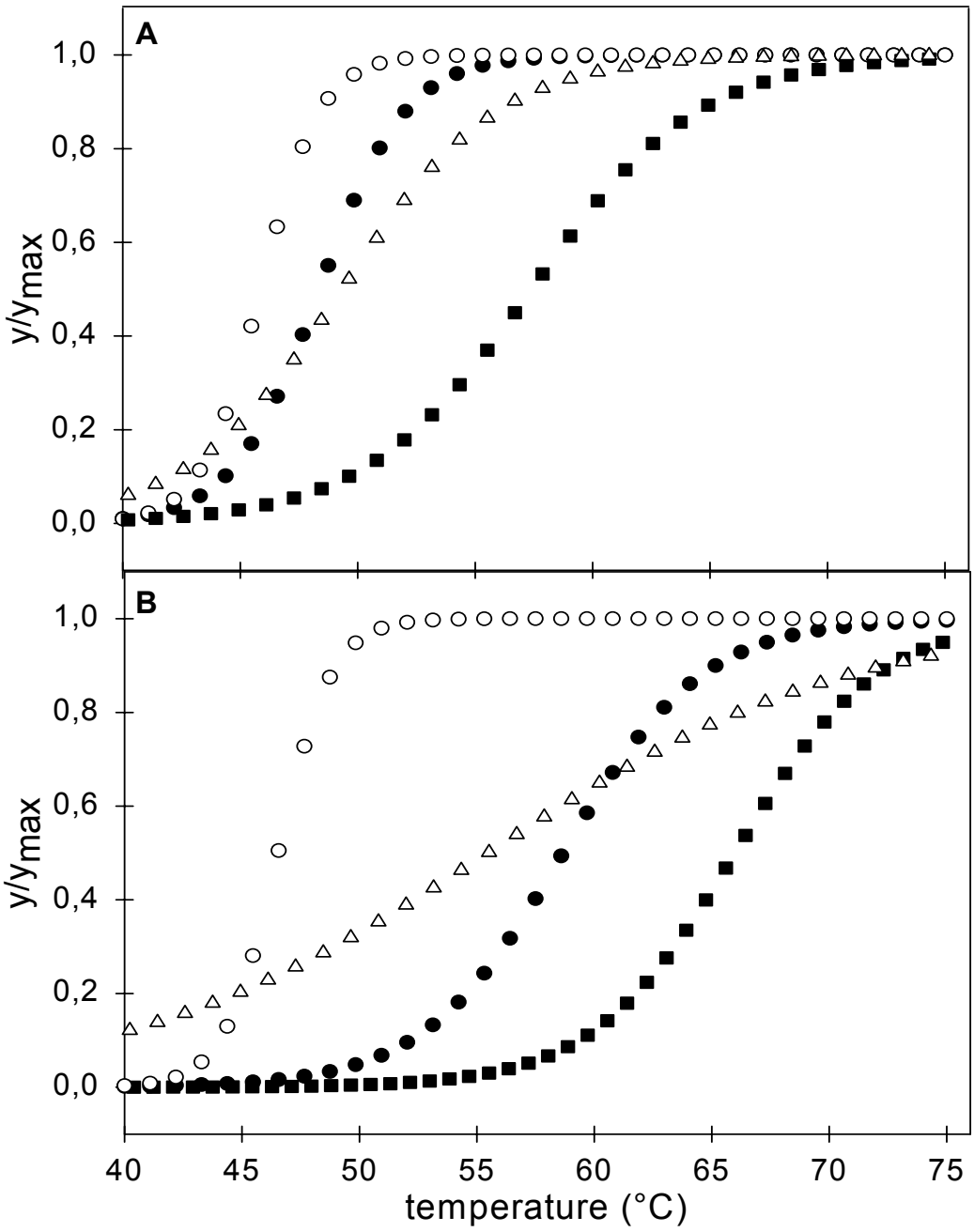


**Figure 25**: Comparison of $M_{Max}$ calculated for viable (●) and stress resistant (○) cell counts using transformed data which was obtained by difference FT-IR spectra for the associated peaks of amide II' (~1445 $cm^{-1}$, Δ) and β-sheet (~1620 $cm^{-1}$, ■). A: data generated in $D_2O$. B: data generated in $D_2O$-sucrose.

## 3.4. Effects of Combined HP/Temperature Treatments on *L. lactis*

The effect of pressure alone or in combination with low pH and co-solvents on *L. lactis* were described previously (Molina-Höppner, 2002; Kilimann et al., 2005a). In this work, the combined effects of pressure, temperature and baroprotective additives were considered. Experiments were performed in milk buffer and milk buffer 1.5M sucrose (sucrose) or 4M NaCl (NaCl). To determine lethal and sublethal inujury, inactivation of *L. lactis* at 200 MPa was characterised through five parameters, i.e. viable cell counts (CFU), stress resistant cell counts (CFUsub), metabolic activity (MA), membrane integrity (MI), and the activity of the MDR-transport enzyme LmrP (LmrP). Based on the results of the PCA analysis (see below), experiments at 300 and 500 MPa were characterised with respect to CFU, CFUsub and MA only.

Figure 26 illustrates the effect of pressure application at 200 MPa in milk buffer at different temperatures. In agreement with previous observations, the survivor curves characterised by viable cell counts (Figure 26A) exhibited a sigmoid shape with pronounced tailing. At temperatures of 30°C or lower, a fraction of 0.1 ‰ of the population invariably resisted even prolonged pressure treatments. In contrast, treatments at 40°C or higher reduced the viable cell counts below the detection limit. The other measurands were also strongly affected by the temperature of the pressure treatment and *L. lactis* was most resistant to pressure in the temperature range of 20 to 30°C. The effect of temperature on viable cell counts and stress resistant cell counts as well as for the metabolic activity was more pronounced as compared to membrane integrity and LmrP activity. Whereas the membrane integrity was not affected by most of the pressure treatments, LmrP activity was strongly reduced by pressure independent on the temperature (Figure 26B and data not shown).

To highlight temperature effects on the viability and physiology of *L. lactis* more clearly, stress resistant cell counts (CFUsub), metabolic activity (MA), and LmrP activity (LmrP) after 40 min of pressure treatment at 200 MPa in milk buffer, milk buffer sucrose, or milk buffer NaCl are shown in Figure 27. This data selection essentially represents the information obtained from the entire kinetics of inactivation (compare Figure 26 and Figure 27). At 200 MPa, viable cell counts and membrane integrity of *L. lactis* were not affected by pressure treatments in milk buffer sucrose and milk buffer NaCl at any temperature (data not shown).

In milk buffer, a maximum of baroresistance was observed between 20 and 30°C when any of the indicators for lethal or sublethal injury were considered. A further reduction or increase of

the temperature increased the lethal and sublethal effects of pressure and treatments at 5°C had a similar effect on lethal and sublethal injury of *L. lactis* as treatments at 40°C. LmrP activity was the most sensitive indicator of cellular injury and LmrP was fully inactivated by pressure treatments independent of the temperature. Only after treatments at 20°C, 200 MPa residual LmrP activity was observed after 40 min of treatment, therefore, the LmrP activity after 8 min of treatment in milk buffer is furthermore depicted in Figure 27C. The residual LmrP activity was maximal after pressure treatments at 20°C.

In milk buffer sucrose, *L. lactis* was fully protected against pressure inactivation at temperatures of 40°C or below (Figure 27A, B and C). Only treatments at 45 and 50°C appreciably reduced the stress resistant cell counts, metabolic activity, and LmrP activity (Figure 27A, B, and C). Pressure treatments at temperatures of 20 – 30°C were not performed because even treatments at 40 and 15°C failed to adversely affect *L. lactis*. In short, 1.5 M sucrose protected *L. lactis* towards pressure inactivation independent of the temperature.

In milk buffer NaCl, the effect of the temperature on pressure-induced lethal and sublethal injury differed strongly from the effects in milk buffer or milk buffer sucrose. At temperatures of 15°C or below, NaCl did not protect *L. lactis* against pressure induced injury compared to treatments in milk buffer (Figure 27). The lethal and sublethal effects of pressure were reduced at increased temperatures and the maximum of baroresistance was observed at 40°C. Treatments at 50°C inflicted less injury of *L. lactis* compared to treatments at 15°C or 5°C and at 50°C the baroprotective effect of NaCl was greater than the effect of sucrose.

To determine whether the marked differences of baroprotection of NaCl and sucrose are also effective at higher pressure levels, the kinetics of inactivation of *L. lactis* were studied at 5, 30 or 50°C and 200, 300 or 500 MPa in milk buffer, milk buffer sucrose, and milk buffer NaCl. The viable cell counts, stress resistant cell counts, and the metabolic activity of *L. lactis* after the various treatments were determined. The metabolic activity of *L. lactis* after 8 min of treatment is shown in Figure 28. In milk buffer and milk buffer sucrose (Figure 28A and Figure 28B), the strongest inactivation effects were observed at highest examined temperature, 50°C, and the organism was most pressure resistant at 30°C. Analysis of the viable cell counts and the stress resistant cell counts supported the interpretation that the optimum of baroresistance of *L. lactis* in milk buffer and milk buffer sucrose is about 30°C independent on the pressure level (data not shown). Figure 28C illustrates the protective effect of NaCl on the metabolic activity of *L. lactis* at 200 - 500 MPa. A strong protective effect was

apparent for the highest examined temperature (50°C) whereas essentially no protection towards pressure-induced inactivation of metabolic activity was observed at 5°C (compare Figure 28A and Figure 28C). This finding confirms that NaCl protects *L. lactis* only at high temperatures.

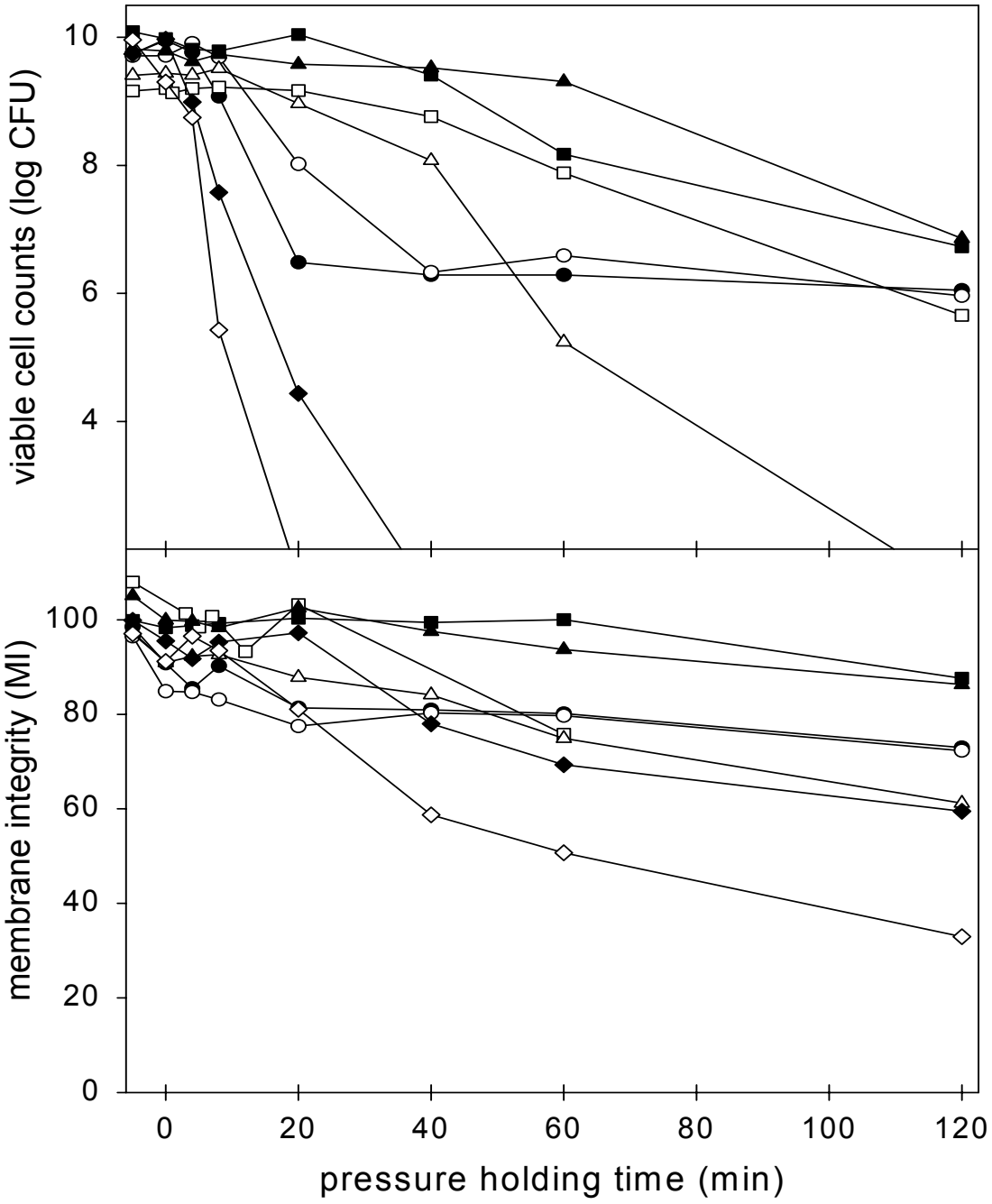


**Figure 26**: Viable cell counts (CFU, A) and membrane integrity (MI, B) of *L. lactis* after treatment in milk buffer with 200 MPa at various temperatures: 5°C(●), 10°C (○), 15°C (■), 20°C (□), 30°C (▲), 40°C (Δ), 45°C (♦) and 50°C (◊). The detection limit for CFU was 100 CFU $ml^{-1}$.

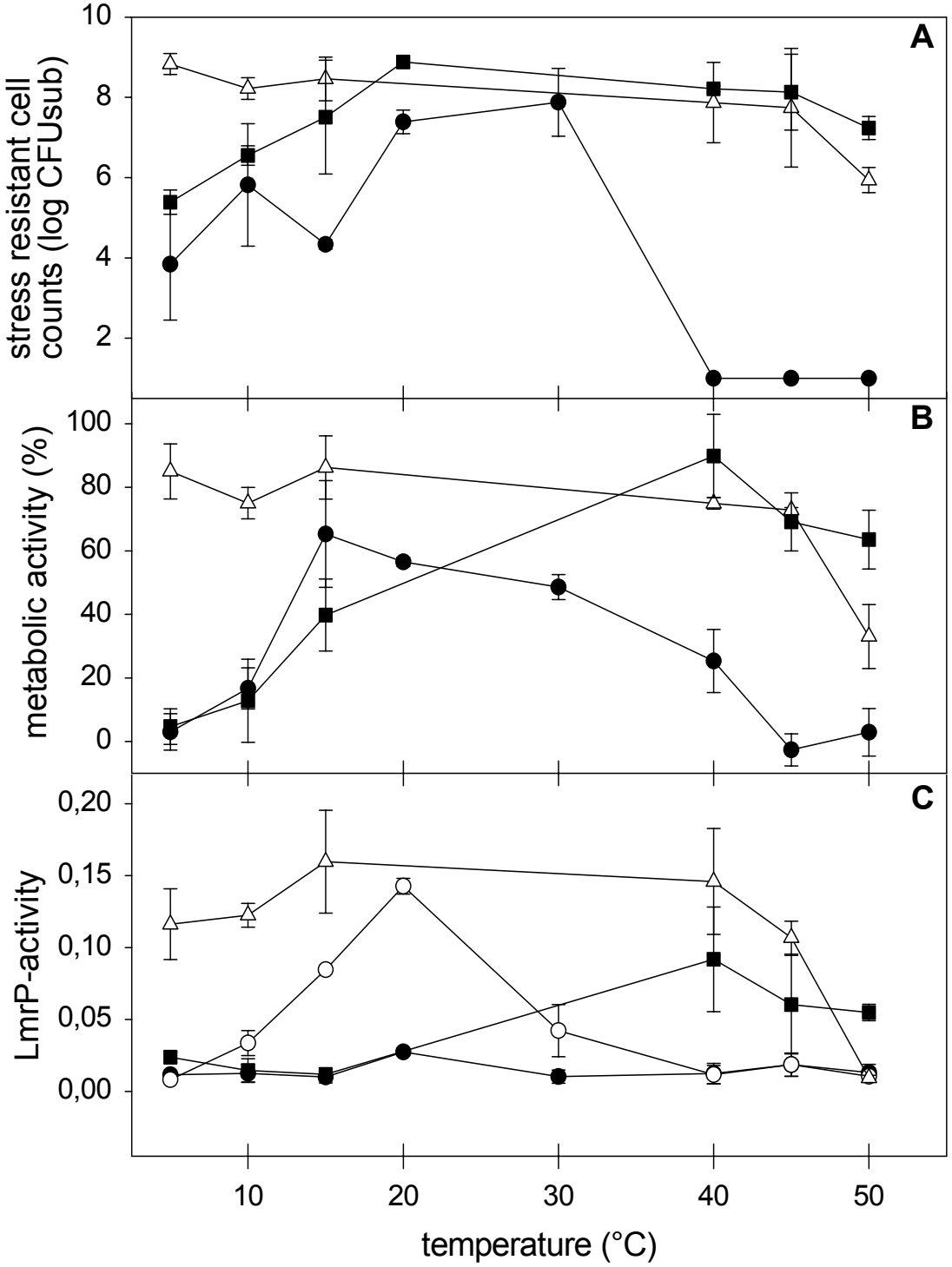


**Figure 27**: Stress resistant cell counts (CFUsub, A), metabolic activity (MA, B) and LmrP-activity (LmrP, C) of *L. lactis* after pressure treatment at 200 MPa at various temperatures. Figures A and B and C represent data for measurands after 40 min pressure application time in milk buffer (●), milk buffer with 1.5M sucrose (Δ) and milk buffer with 4M NaCl (■). Figure 27C represents data for LmrP measured at 8 min (○) and 40 min (●) in milk buffer. The detection limit for CFUsub was 100 CFU $ml^{-1}$. Data are means ± standard deviation of at least two independent experiments.

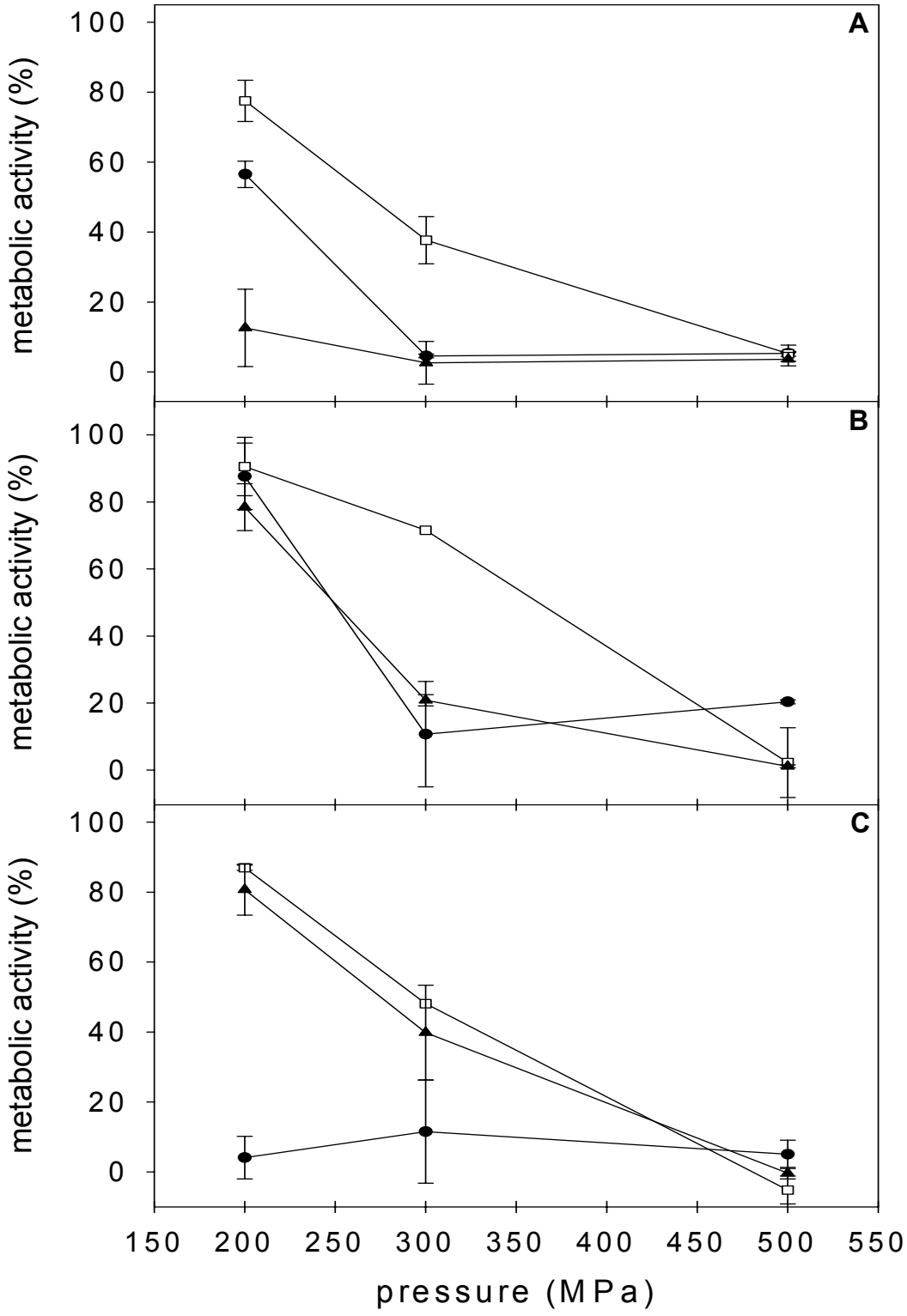


**Figure 28**: Metabolic activity (MA) of *L. lactis* after treatments with 200 - 500 MPa for 8 min at 5°C (●), 30°C (□), and 50°C (▲) in milk buffer (Panel A), milk buffer with 1.5M sucrose (Panel B) and milk buffer with 4M NaCl (Panel C). Data at 200 MPa, 30°C using milk buffer with 1.5M sucrose and milk buffer with 4M NaCl were interpolated using experimental data obtained at 15 and 40°C (compare Figure 27). Data are means ± standard deviation of at least two independent experiments.

## 3.5. Differential Inactivation of Glucose- and Glutamate Dependent Acid Resistance of *Escherichia coli* by High Pressure Treatments

The treatment of foods with pressure of 800 MPa at ambient temperature fails to achieve a 5D reduction of the most pressure resistant strains of *E. coli* and economic constraints currently prevent the use of higher pressure levels. Combination treatments have been proposed to enable the elimination of *E. coli* based on the sublethal injury inflicted by the pressure treatment. However, the acid tolerance of *E. coli* is strongly dependent on acid inducible stress proteins and the availability of amino acids in the substrate. The acid tolerance of *E. coli* is increased by the $\sigma^S$-regulated alteration of the cytoplasmic membrane (Chang and Cronan, 1999) the overexpression of proteins that prevent DNA-damage (Choi et al., 2000), as well as the induction of enzymes that extrude protons from the cytoplasm to maintain a high intracellular pH (Diez-Gonzalez and Karaibrahimoglu, 2004). The maintenance of a high internal pH is a prerequisite for the survival of microorganisms during acid challenge because it provides a favourable environment for cytoplasmic enzymes and macromolecules, and because the transmembrane pH gradient provides metabolic energy. An overview on the enzymes involved in pH-homeostasis during acid challenge of *E. coli* is given in Figure 29.

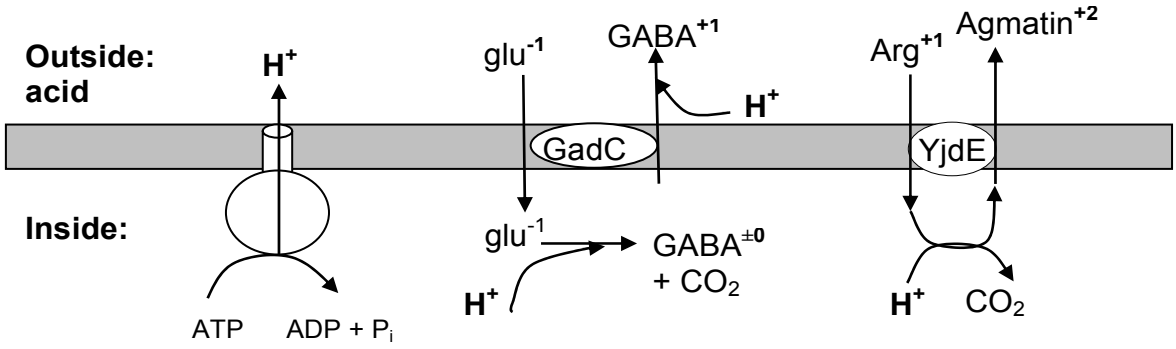


**Figure 29**: Schematic overview on enzymes involved in proton extrusion during acid challenge of *E. coli* (Richard and Foster, 2003; Diez-Gonzalez and Karaibrahimoglu, 2004). The charge of the metabolites, and protons consumed in metabolic conversions are highlighted where appropriate. (i) The $F_0F_1$-ATP-ase extrudes protons at the expense of ATP. (ii) Glutamate is internalised by the glutamate-γ-aminobutyrate (GABA) antiporter GadC, the glutamate decarboxylase GadA converts glu to GABA with concomitant consumption of one proton. Upon export, GABA is protonated when the external pH is below 4.28 thus increasing the external pH. (iii) Arginine transport, decarboxylation to agmatine, and agmatin export occurs in a manner comparable to the glu / GABA conversion.

Here, the effect of glucose, glutamate, and arginine on the survival of *E. coli* during pressure treatment, and during post-pressure acid challenge were analysed. To obtain insight on the mechanisms of protection provided by acid survival pathways, the consumption of arginine and glutamate as well as their effect on the intracellular pH of *E. coli* during pressure treatment and post-pressure acid challenge were determined in addition to the viable cell counts. The intracellular pH was determined by using the pH-dependent fluorescence of the green fluorescent protein, GFP (Olsen et al., 2002).

### 3.5.1. Effects of Arginine and Glutamate on the Viability of *E. coli* After Pressure Treatments, and the $pH_{in}$ During Pressure Treatment

The effects of pressure ranging form 200 to 400 MPa on the survival of *E. coli* suspended in MES-buffer or MES-buffer arg/glu was determined (Figure 30). At 400 and 300 MPa, cell counts were reduced by more than 6 log after 2 and 20 min of pressure treatment, respectively, and the survivor curves exhibited a pronounced tailing. At 200 MPa, viable cell counts were reduced by 4 log only after 120 min of treatment. The presence of 10 mM arginine and glutamate did not affect the survival of *E. coli* at any pressure level.

To determine the effect of pressure on the $pH_{in}$ of *E. coli* in the presence or absence of arginine and glutamate, the $pH_{in}$ was determined in situ based on the GFP-fluorescence. The $pH_{in}$ was measured by manually alternating the excitation monochromator between the pH-independent and dependent wavelengths of 410 and 485 nm, respectively, before and after compression to 200 MPa. In MES-buffer, *E. coli* maintained a transmembrane $\Delta pH$ of about 1.5 pH units before compression, and the $pH_{in}$ was slightly increased when arginine and glutamate were available. Independent of the availability of amino acids, compression to 200 MPa dissipated the transmembrane $\Delta pH$ and the internal pH was pH $5.3 \pm 0.2$, equal to the external pH of pH 5.4.

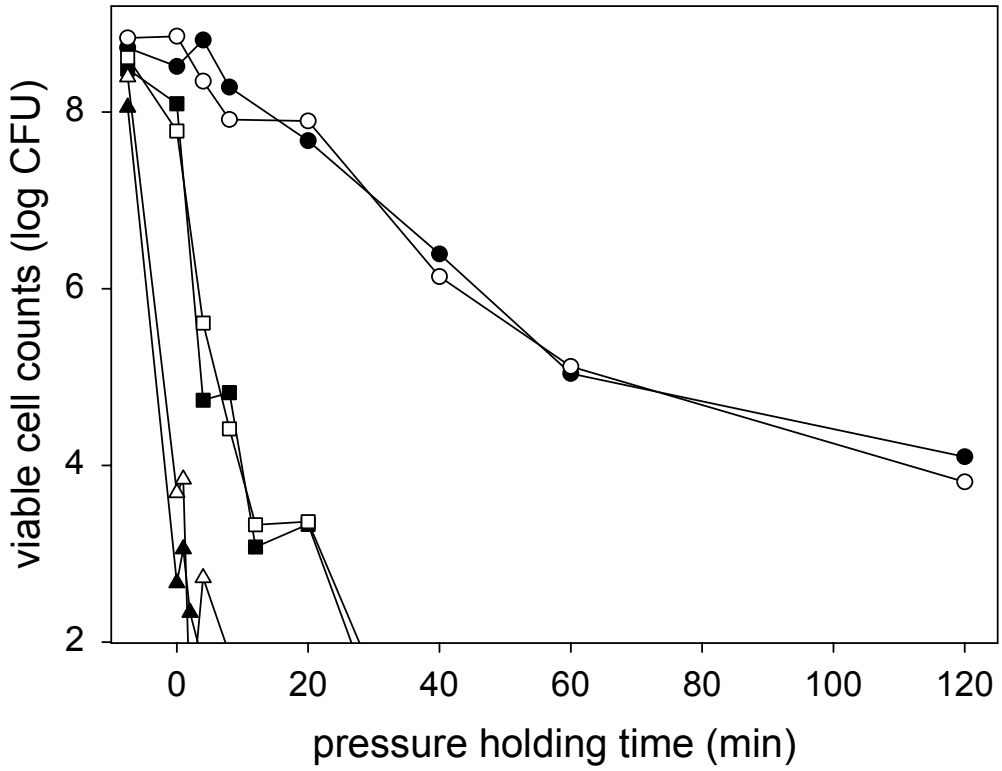


**Figure 30**: Viable cell counts of *E. coli* TMW 2.497 after pressure treatment at 200 MPa (●), 300 MPa (■) and 400 MPa (▲). Open symbols represent data measured in MES-buffer with 10 mM arginine and 10 mM glutamate, solid symbols represent data measured in MES-buffer. The data are means of experiments carried out at least in quadruplicate and the experimental error was 0.5 log or less.

### 3.5.2. **Effect of Arginine and Glutamate on the $pH_{in}$ of *E. coli* after Pressure Treatment**

To determine the capability of *E. coli* to restore a transmembrane ΔpH after pressure application, the $pH_{in}$ of pressure treated cells was determined. Treatments were carried out at 200 and 300 MPa and in the presence or absence of arg/glu, and the results are shown in Figure 31. Glucose was invariably present in all of the buffers used. Following treatments with 200 MPa in presence of arg/glu for up to 20 min, *E. coli* maintained the ability to re-establish a ΔpH within 30 min after decompression. In absence of amino acids, *E. coli* lost the capability to maintain ΔpH after 4 min of pressure application although no substantial decrease of cell viability was detected (compare to Figure 31).

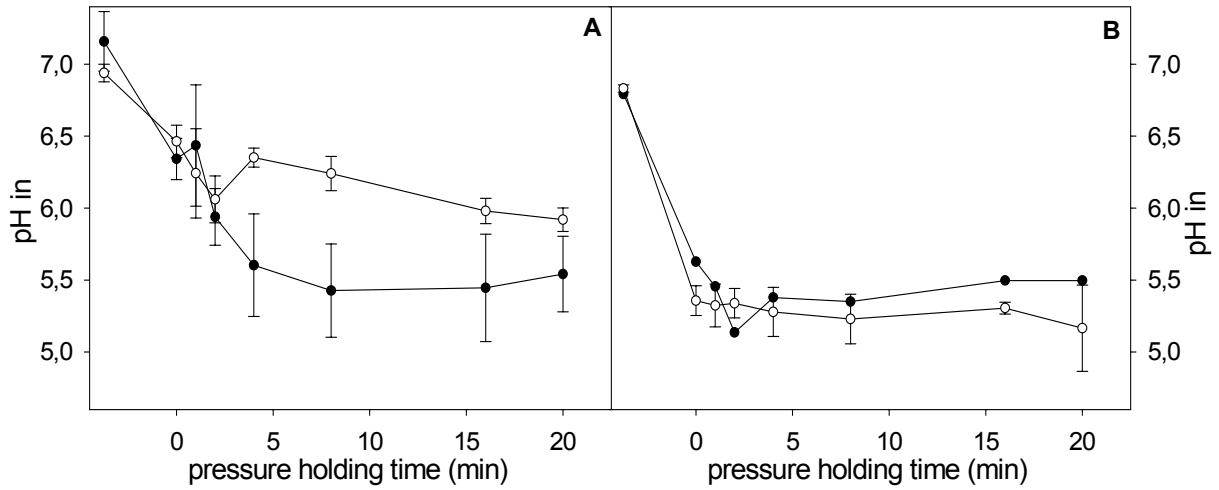


**Figure 31**: Intracellular pH of *E. coli* TMW 2.497 after pressure treatments between 0 and 20 min pressure in the presence of 10 mM each of glutamate and arginine (○) or in the absence of amino acids (●). After decompression, each sample was incubated for 30 min at 37°C to allow reenergisation of the cells. Panel A: pressure treatments at 200 MPa, Panel B: pressure treatments at 300 MPa. Shown are means ± standard deviations of triplicate independent experiments. Only a single experiment was carried out in the absence of amino acids at a pressure level of 300 MPa.

Treatments at 300 MPa eliminated the transmembrane ΔpH after pressure treatment independent of treatment time and the presence of amino acids (Figure 31B). Here, treatments for 0 and 4 min reduced the cell counts by about 0.5 and 5 log units, respectively. Thus, the glutamate- and arginine dependent systems of acid tolerance in *E. coli* did not stabilise the organism at high pressure conditions, but strengthened its ability to restore a high $pH_{in}$ after sublethal pressure treatment.

### 3.5.3. **Post-Pressure Acid Survival of *E. coli***

To determine the effect of amino acids on the post-pressure acid survival of *E. coli*, the organism was incubated at a pH 5.4 or pH 4.0 after pressure treatments. The pH 4.0 buffer was used with or without addition of arginine and glutamate. The cell counts of samples incubated at pH 5.4 for 24h following various pressure treatments were essentially identical to the cell counts of the same samples without post-pressure incubation and a reduction of cell counts by 0.5 – 1 log only was observed after incubation at pH 5.4 (Figure 32). In contrast, incubation at a pH of 4.0 was tolerated without loss of viability by untreated cells but bactericidal to *E. coli* after sublethal pressure treatment. A reduction of cell counts of up to 3

log occurred during post-pressure incubation at pH 4.0. At least one essential component of the metabolic pathways that enable *E. coli* to maintain a high intracellular pH with glucose as sole energy source was inactivated by these sublethal pressure treatments. However, if amino acids were present during post-pressure incubation at pH 4.0, the survival of *E. coli* was equivalent to those cells incubated at a pH 5.4 (Figure 32A).

It was furthermore determined whether the induction of the glutamate acid survival pathway by acid adaptation improved post-pressure acid survival (Figure 32B). *E. coli* was incubated for 100 min in MES-buffer (pH 5.4) prior to pressure treatments at 200 MPa and subsequent storage at pH 4.0 and pH 5.4. No differences in the cell counts after pressure treatment were observed between acid-adapted cells and non-adapted cells (data not shown). An acid challenge at pH 4.0 in the absence of amino acids remained bactericidal for pressure treated cells despite the acid adaptation.

Pre-pressure acid adaptation eliminated the bactericidal effect of post-pressure acid challenge at pH 4.0 when glutamate was available (Figure 32B), indicating that the induction or activation of the glutamate decarboxylase system during acid adaptation enhanced the acid tolerance of *E. coli* in the presence of glutamate. Following pressure application of 300 MPa (Figure 32C), the tolerance of *E. coli* to storage at pH 4.0 in the absence of amino acids was eliminated already after pressure treatment of 2 min. A protective effect of arginine and glutamate on the post-pressure survival at pH 4.0 was observed only after 0 to 4 min of pressure treatment. Treatments at 300 MPa for more than 8 min inactivated at least one essential component of the arginine and glutamate dependent systems for intracellular pH homeostasis.

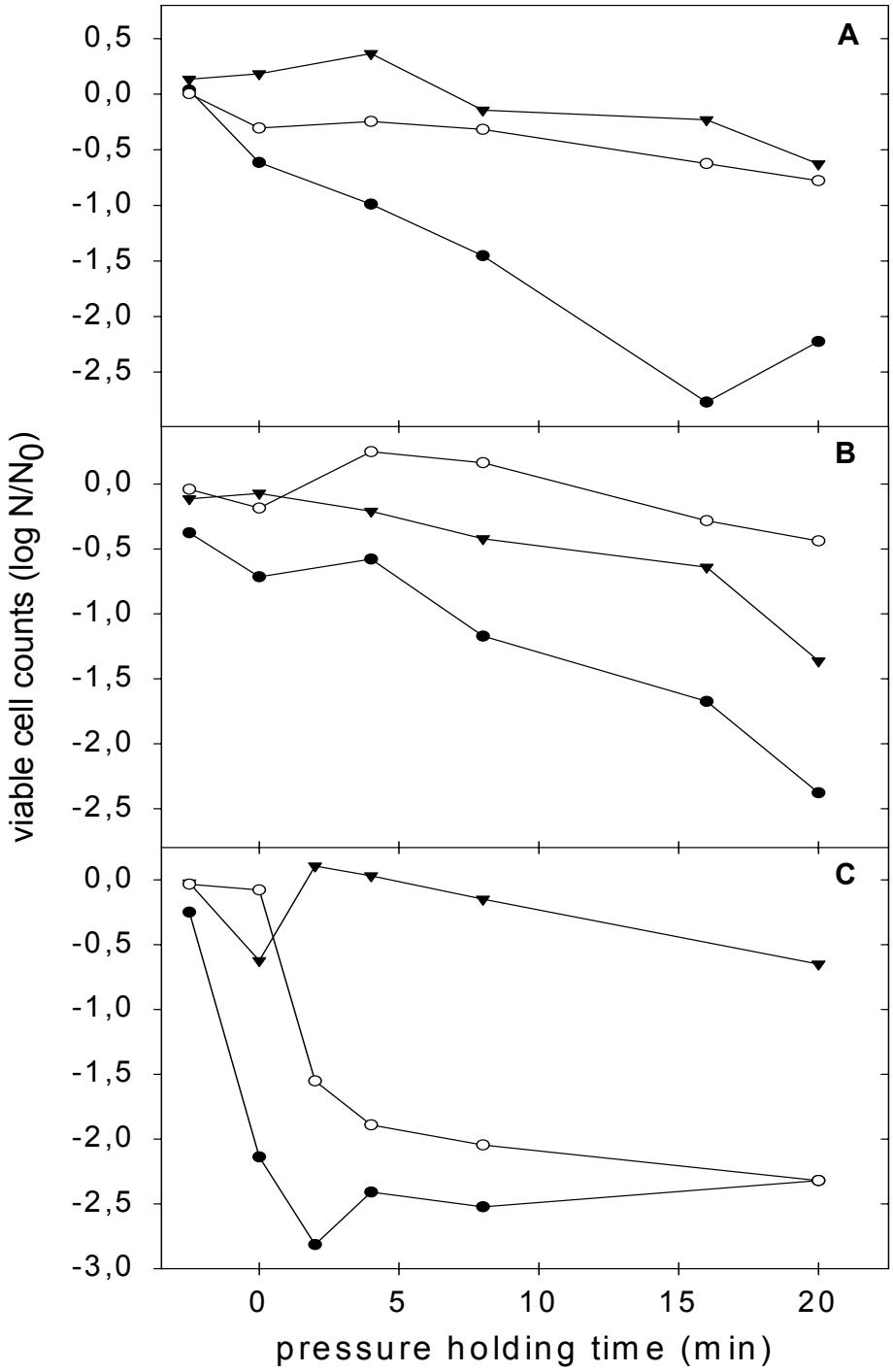


**Figure 32**: Reduction of viable cell counts of *E. coli* TMW 2.497 after pressure treatment for various pressure holding times, followed by a incubation of 24 hours at pH 5.4 (▼) or at pH 4.0 in the presence (○) or absence (●) of 10 mM each of glutamate and arginine. Panel A: Treatments of non-adapted cells at 200 MPa. Panel B: Treatments of cells adapted to a pH of 5.4 in MES buffer for 100 min immediately before pressure treatment at 200 MPa. Panel C: Treatments of non-adapted cells at 300 MPa. Depicted are the cell counts N after storage relative to the cell counts $N_0$ after pressure treatment but before storage. Data were calculated as means of duplicate independent experiments and the experimental error of the $\log(N/N_0)$ values generally was 0.6 log units or less.

To determine which of the two amino acids used – arginine or glutamate – contributed to the improved survival of *E. coli* during post-pressure acid challenge, the pH 4.0 buffer was used without additions, with 10 mM arginine, or with 10 mM glutamate (Figure 33).

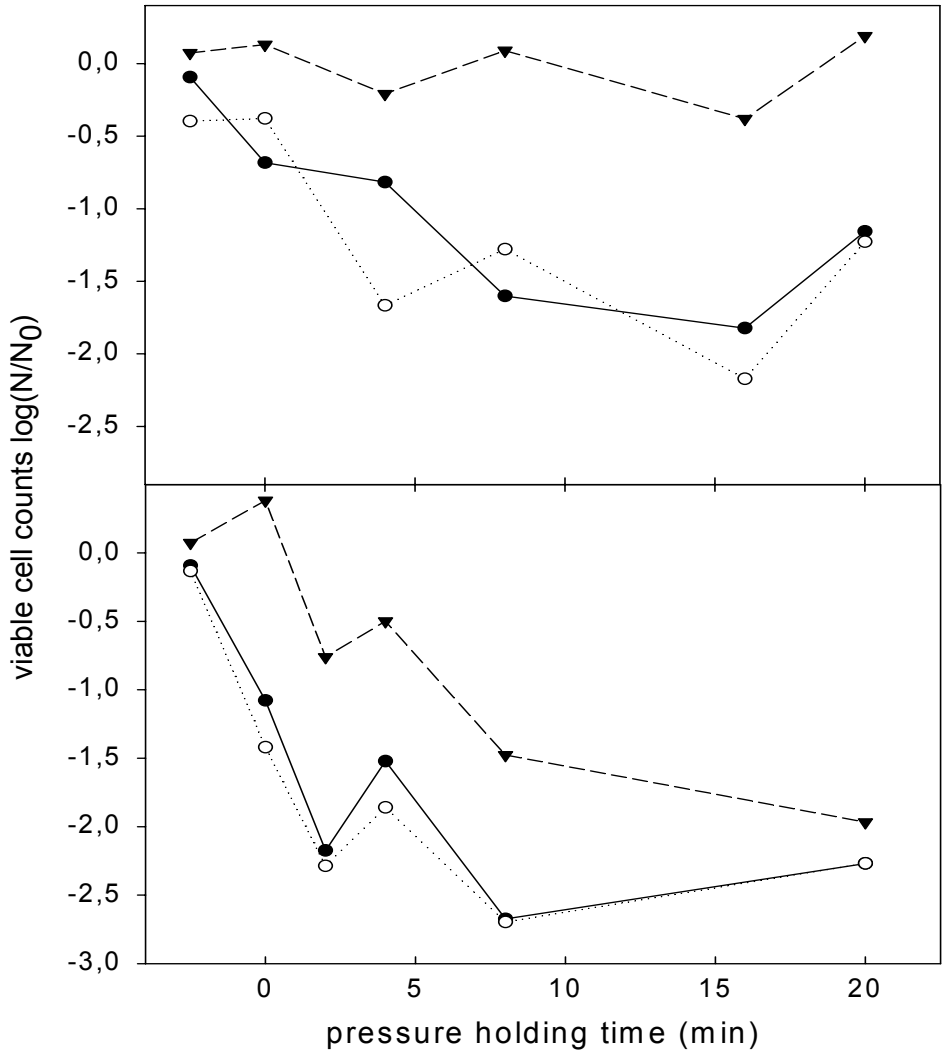


**Figure 33**: Reduction of viable cell counts of *E. coli* TMW 2.497 after pressure treatment for various pressure holding times, followed by a incubation of 24 hours at pH 4.0 in the absence of amino acids (○), in the presence of 10 mM arginine (●), or in the presence of 10 mM glutamate (▼). Panel A: Treatments at 200 MPa. Panel B: Treatments at 300 MPa. Depicted are the cell counts N after storage relative to the cell counts $N_0$ after pressure treatment but before storage. Data were calculated as means of duplicate independent experiments and the experimental error of the $\log(N/N_0)$ values generally was 0.6 log units or less.

The post-pressure survival of *E. coli* at pH 4.0 in the absence of amino acids (Figure 33) was within experimental error of those data shown in Figure 32. Addition of arginine did not improve the post-pressure acid survival compared to pH 4.0 buffer without amino acids after

treatments at 200 or 300 MPa. In contrast, the survival of *E. coli* in the presence of 10 mM glutamate only (Figure 33A and Figure 33B) was comparable to the survival in the presence of 10 mM each of arginine and glutamate (Figure 32A and Figure 32C), indicating that improved acid survival of pressure-treated *E. coli* is attributable to glutamate metabolism.

### 3.5.4. Arginine and Glutamate Turnover by *E. coli* During Post-Pressure Acid Challenge

Arginine and glutamate consumption by *E. coli* during post-pressure acid challenge was determined by HPLC (Figure 34A). Only 20% of the arginine available was consumed during post-pressure incubation, and arginine consumption was independent of pressure treatments (Figure 34A). This result confirms that arginine had little or no effect on the acid tolerance of pressure treated or untreated cells. In contrast, all of the glutamate in the incubation buffer (10 mM) was consumed by pressure treated cells after 24h of incubation, whereas untreated cells consumed only 40% of the available glutamate.

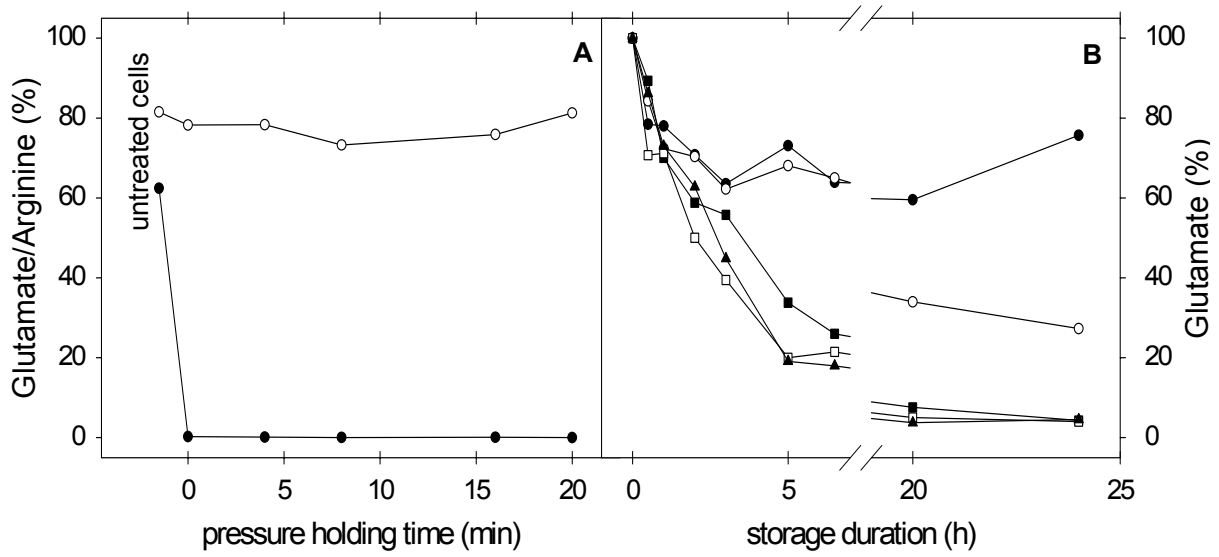


**Figure 34** Arginine and glutamate consumption of *E. coli* TMW 2.497 during storage for 24h in buffer after treatments with 200 MPa. Arginine and glutamate concentrations are depicted as a percentage of the initial concentration in buffer, 10 mM each. Panel A: Arginine and glutamate consumption during 24h of storage of untreated cells and cells treated for 0 – 20 min at 200 MPa. The glutamate (●) and arginine (○) concentrations were determined by HPLC. Panel B: Kinetics of glutamate consumption by untreated cells (●) or cells treated for 0 (○), 4 (■), 8 (▲) or 20 (□) min at 200 MPa during storage. Glutamate levels in buffer were determined enzymatically. Data shown in Panel A and B are means of two independent experiments and the experimental error was 15% or less.

A second experiment was carried out to determine the kinetics of glutamate turnover during post-pressure acid challenge (Figure 34B). In agreement with data shown in Figure 34A, untreated cells consumed about 20% - 40% of the glutamate in the buffer, whereas pressure treated cells used 80 – 100% of the available glutamate within 24h. Prolonged pressure treatments induced a more rapid glutamate turnover and cells treated for more than 8 minutes at 200 MPa consumed 80% and 100% of the available glutamate after 6 and 24h of acid challenge, respectively. Taken together, the results indicate that glutamate but not arginine plays an important role for the acid survival following sublethal pressure treatments. Furthermore, pressure treatment induced the glutamate decarboxylase system to enable a more rapid proton extrusion.

## 3.6. Elimination of Redundant Physiological States of *L. lactis*

PCA allows the detection of correlations between different measurable quantities and might reveal insight in the mechanisms involved in the inactivation. It was carried out to detect correlations between the five measured quantities (CFU, CFUsub, MA, MI and LmrP) using the data set comprising all inactivation kinetics at 200 MPa and temperatures ranging from 5 to 50°C. The loading plots were used to detect correlations as shown in Figure 35. Generally, vectors of strongly correlated variables have the same direction and include a small angle. In Figure 35, quantities exhibiting correlations have been circled. The identification of these correlations has been done on the basis of all parameter combinations and correlations were detected between MA and CFU as well as between CFUsub and LmrP.

CFUsub and LmrP are located in the upper left quadrant of the coordinate system and include a small angle for the case of milk buffer (Figure 35A). In milk buffer sucrose (Figure 35B), both vectors for CFUsub and LmrP have rotated and are located in the lower left quadrant of the coordinate system. In milk bufer NaCl (Figure 35C), both quantities remain in the lower left quadrant but inverted position with respect to each others. Hence, sublethal injury as determined by plating on selective media correlated well to the inactivation of the membrane-bound MDR-transport enzyme LmrP.

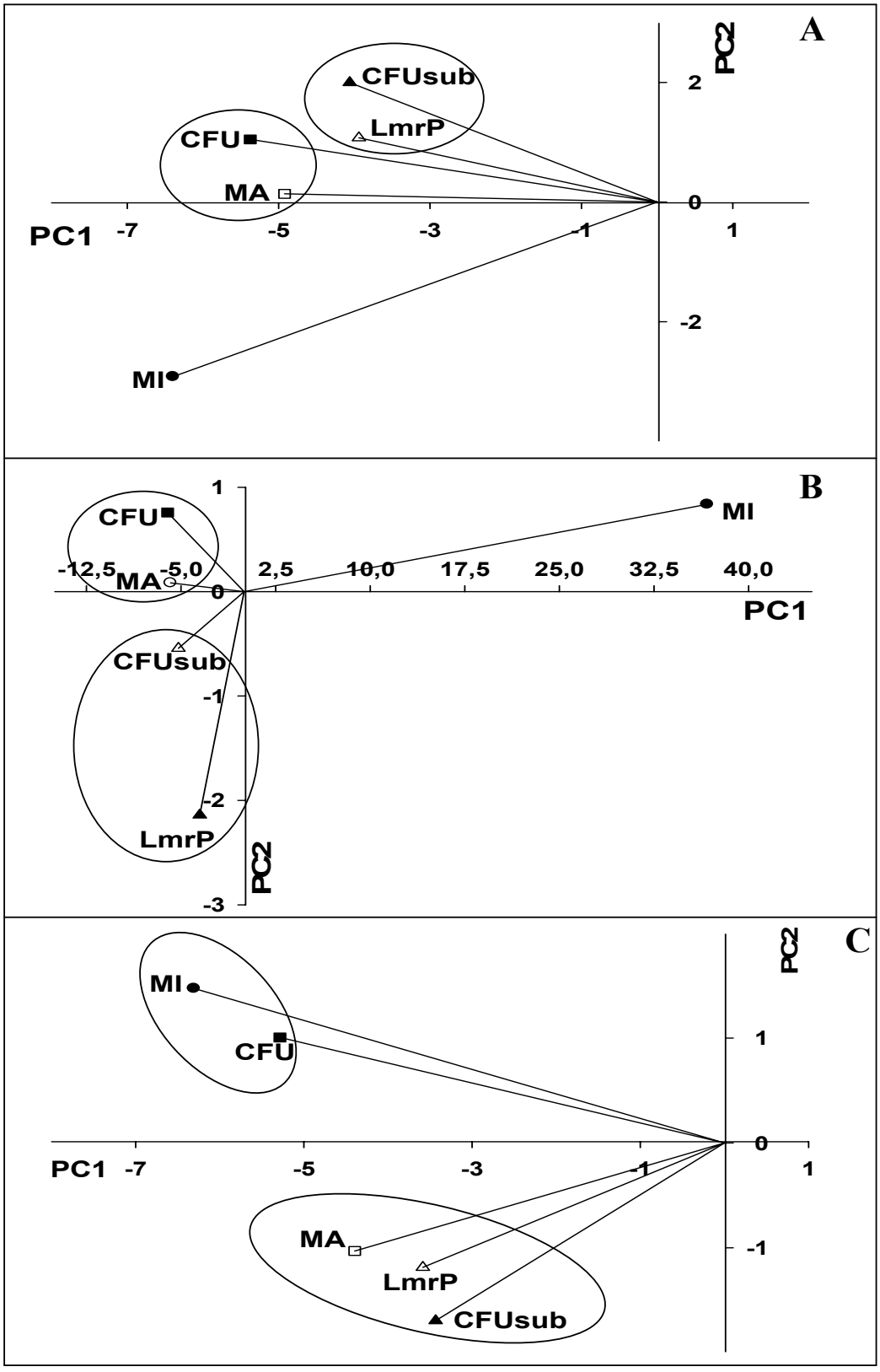


**Figure 35**: Display of the calculated loadings for all combined HP/temperature-data to the subspace of each variable on PC 1 plotted against the calculated loadings of each variable on PC 2. Figures represent data for milk buffer (Panel A), milk buffer sucrose (Panel B) and milk buffer NaCl (Panel C).

MA and CFU remain located around the negative abscissa in milk buffer, milk buffer sucrose, or milk buffer NaCl (Figure 35A-C). The inclusion angle does not vary much in the case of milk buffer and milk buffer sucrose. This points to a correlation of both variables, indicating that cells experienced during pressure treatment a concomitant loss of metabolic activity and viability. In case of milk buffer NaCl, a shift of MA towards LmrP and CFUsub can be observed. Thus, treatments in milk buffer NaCl impaired the metabolic activity of *L. lactis* after treatments that did not affect cell viability. This indicates that the mechanisms of inactivation differ when NaCl is present compared to treatments with sucrose or in milk buffer. The correlation of MI to CFU in milk buffer NaCl is explained mainly by the fact that most treatments in the presence of NaCl failed to affect MI or CFU, i.e. that most numerical values for these variables are equal to 1 after normalization.

## 3.7. Modelling of Pressure-Temperature-Co-Solvent Induced Inactivation of *L. lactis*

The prediction of pressure-induced lethal and sublethal cell damage in practical applications requires the availability of suitable mathematical models that are based on large data sets that fully encompass single and combined effects of pressure and temperature. To reduce computational capacities as well as computation time, relationships between the five physiological states of *L. lactis* have been detected. Here, the correlations detected by PCA were used in two different ways. First, autonomous output variables have been defined for the generation of a multi-layer Fuzzy Logic based model. These variables shall contain all information concerning the lethal and sublethal behaviour of the bacteria after the process. They are calculated directly by the use of the input variables. The results obtained for the autonomous output variables were used to calculate the remaining output variables, which are then almost independent on the input variables.

After that, one indicator of lethal and sublethal injury was used to generate a model using the Logistic equation. The time dependent first order differential equation of the Logistic equation has been used to describe the inactivation behaviour of *L. lactis* in a 3.3-litre-medium-sized-high-pressure vessel. Therefore, the focus was based on process induced spatiotemporal heterogeneties and their influence on the inactivation behaviour of *L. lactis.*

### 3.7.1. Fuzzy Modelling

To incorporate variables in the Fuzzy rulebase, the novel software tool Fuzzy-Studio was used. Based on the results of PCA, CFU and LmrP were used as autonomous variables in Fuzzy modelling, and MA, CFUsub and MI were calculated essentially dependent on CFU and LmrP. Thus, a simplification of a Fuzzy Logic model was achieved by the minimisation of the rulebase.

For the formulation and the validation of the model, all observed effects have to be considered in the new model structure. For model formulation, 53 combinations of environmental conditions were used (Table 2). At least 8 different pressure holding times were analysed for each kinetic. Fewer data points were analysed at parameter combinations resulting in a rapid inactivation (pressure > 300 MPa, temperature > 45°C), or at parameter combinations that did not affect viable cell counts even after 120 min of treatment. The plots of predicted vs. observed data for those parameter combinations used in model formulation are depicted in Figure 36. Shaded areas indicate the overall experimental errors of the methods.

For the majority of data points, the deviation of the model predictions from the measured values is smaller than the experimental error. Several of those deviations that are larger than experimental error were model intrinsic. The model was built to allow only a decrease in output variables with increasing treatment duration. However, in some experimental kinetics, the experimental values for the output variables increase despite of longer pressure application times.

The prediction quality of the model was validated on the basis of data that were not used for the formulation of the model. The parity plots for model validation are shown in Figure 37A, 37B and 37C for CFU and CFUsub, MA and MI, and LmrP, respectively.

Virtually all predicted values for the validation data set were within experimental error of the measured values. This improved quality of fit of the validation data set compared to the data set used for formulation can be explained by the fact that the former was compiled in a consecutive series of experiments within 6 months whereas the data for model formulation was collected over a period of 4 years by several persons.

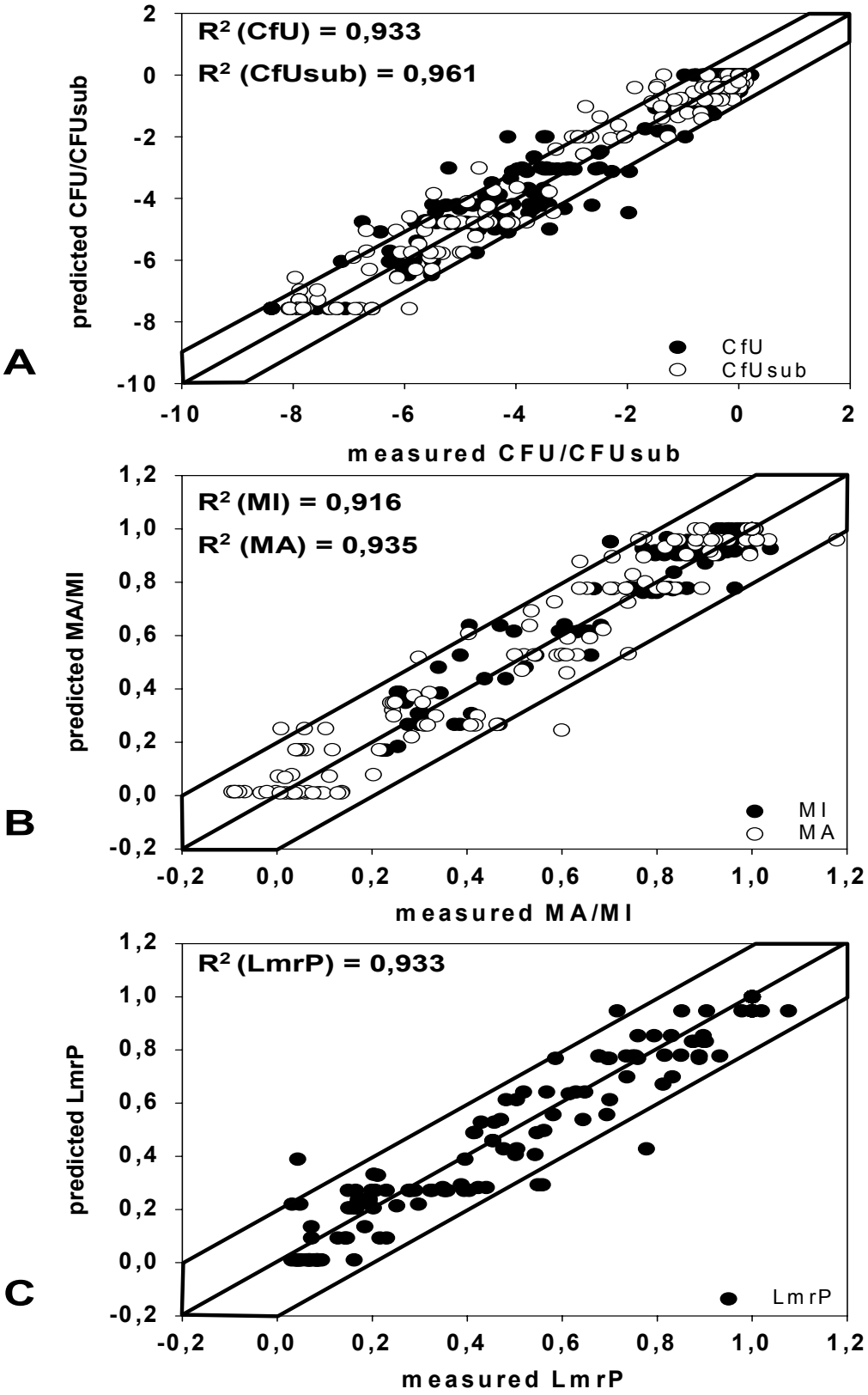


**Figure 36**: Comparison of measured and predicted data for model formulation. Shaded areas indicate the deviation explained by overall experimental errors. A: viable cell counts (CFU) and stress resistant cell counts (CFUsub). B: membrane integrity (MI) and metabolic activity (MA). C: LmrP activity.

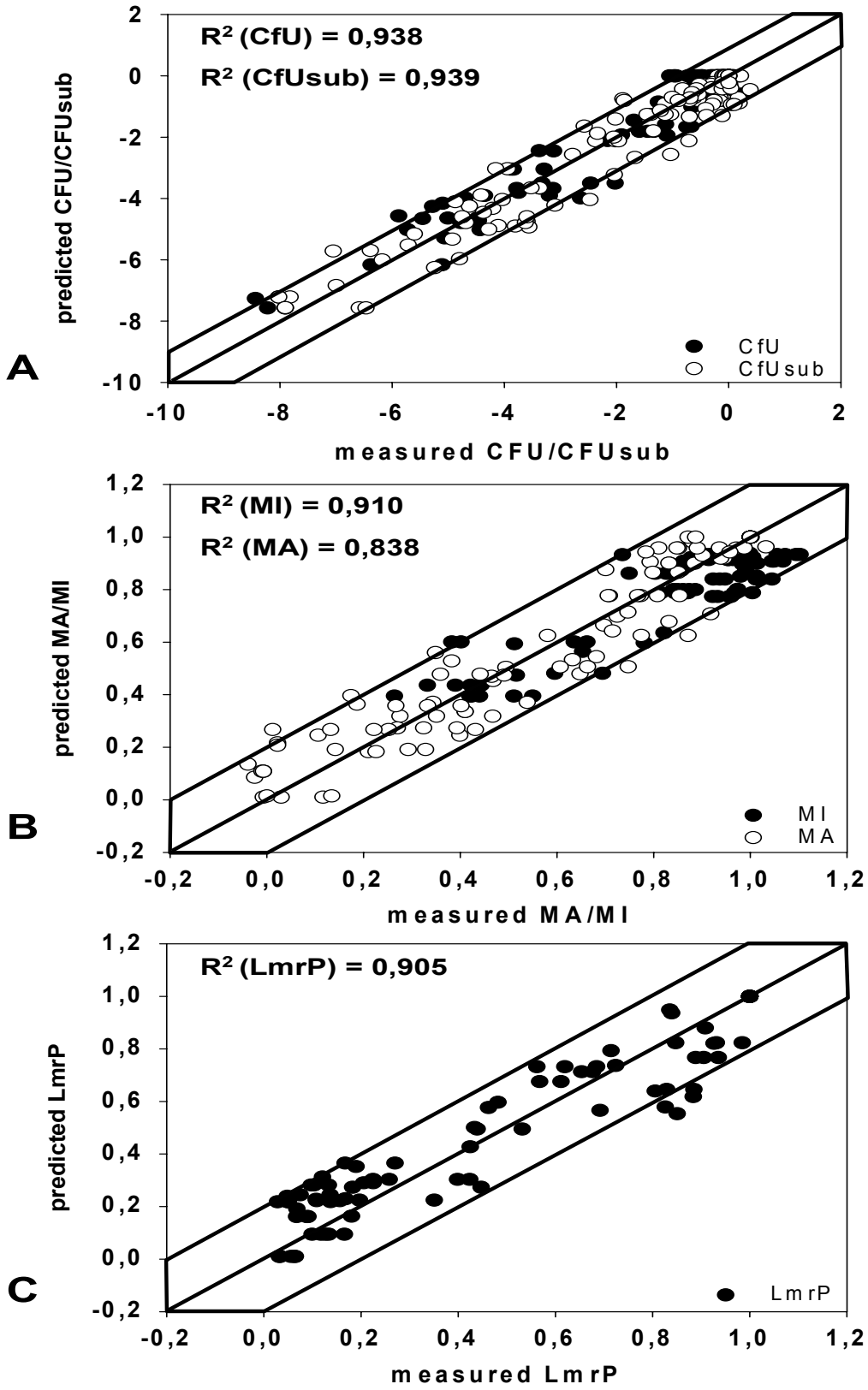


**Figure 37**: Comparison of predicted data and data measured for model validation. Shaded areas indicate the deviation explained by overall experimental errors A: viable cell counts (CFU) and stress resistant cell counts (CFUsub). B: membrane integrity (MI) and metabolic activity (MA). C: LmrP activity.

Using this Fuzzy rulebase, the inactivation of *L. lactis* dependent on the single effects of the input variables pressure level, temperature, pH, and concentrations of NaCl, sucrose and mannitol could now be described adequately by Fuzzy Logic using a set of 200 rules. Moreover, the combined effects of the following input variables are taken into account: Pressure level x NaCl concentration, pressure level x sucrose concentration, and pressure level x pH. At 200 MPa, 300 MPa and 500 MPa, all combinations of pressure level x temperature x 1.5M sucrose or 4M NaCl are taken into account. Concerning the effect of pH, CFU and CFUsub are the only available output variables (compare Table 2). Furthermore, results of PCA were verified due to the fact, that it was possible to predict nearly 90% of the depending output variables by the use of the autonomous ones.

### *3.7.2.* The Logistic Equation

Inactivation data of *L. lactis* were generated by the use of the 10 ml autoclave while the temperature was varied between 5°C and 50°C and a pressure range between 0.1 to 600 MPa was used. In such laboratory-scale high pressure autoclave, the temperature gradient inside of the autoclave is insignificant. This could be confirmed with numerical simulations. Thus, this small temperature increase is not taken into account for the findings of the parameters of the differential equations which were used to describe the effects of spatiotemporal heterogeneities on the inactivation of *L. lactis* (compare equation 8). Therefore, experiments were performed in milk buffer and milk buffer containing either 4M NaCl (NaCl) or 1.5M sucrose (sucrose). After the transformation of the data, the high pressure induced inactivation of *L. lactis* was described using the Logistic function (compare equation (7)). Therefore, the inactivation process seems to be a two step process involving the intermediate state of sublethal injury. The parameter estimates of the Logistic function for the transformed pressure death time kinetics for both states of *L. lactis* in dependence of the buffer system are shown in Table 6 and Table 7.

**Table 6**: Parameter estimates of viable cell counts of *L. lactis* for the Logistic function.

| T (K) | p (MPa) | pressure holding time (s) | milk buffer | | | sucrose | | | NaCl | | |
|---|---|---|---|---|---|---|---|---|---|---|---|
| | | | $M_{Max}$ | m ($s^{-1}$) | $t_0$ (s) | $M_{Max}$ | m ($s^{-1}$) | $t_0$ (s) | $M_{Max}$ | m ($s^{-1}$) | $t_0$ (s) |
| 278 | 200 | 0 - 7200 | 0.40 | 119.40 | 562.27 | 0.03 | 1514.00 | 11649.34 | 0.05 | 1511.90 | 14220.43 |
| 283 | | 0 – 7200 | 0.40 | 262.30 | 1342.22 | 0.03 | 1514.00 | 11641.55 | 0.05 | 1505.50 | 14220.26 |
| 288 | | 0 – 7200 | 0.40 | 499.80 | 2757.38 | 0.03 | 1514.00 | 11622.01 | 0.05 | 1494.20 | 14219.62 |
| 293 | | 0 – 7200 | 0.40 | 792.60 | 4497.51 | 0.03 | 1513.90 | 11573.15 | 0.05 | 1474.40 | 14217.09 |
| 303 | | 0 – 7200 | 0.41 | 1096.20 | 5540.66 | 0.03 | 1511.90 | 11158.51 | 0.05 | 1381.70 | 14168.22 |
| 313 | | 0 – 7200 | 0.94 | 674.70 | 2428.82 | 0.06 | 1456.90 | 9101.80 | 0.06 | 1148.60 | 13452.60 |
| 318 | | 0 – 7200 | 0.95 | 394.30 | 1136.38 | 0.10 | 1254.20 | 6848.01 | 0.08 | 961.90 | 11615.89 |
| 323 | | 0 – 7200 | 0.95 | 193.90 | 471.69 | 0.18 | 726.60 | 4248.72 | 0.15 | 745.70 | 7577.98 |
| 293 | 250 | 0 - 5400 | 0.50 | 190.50 | 993.26 | 0.03 | 1513.90 | 7457.83 | 0.06 | 1333.10 | 6765.38 |
| 278 | 300 | 0 - 3600 | 0.53 | 20.00 | 140.00 | 0.03 | 1514.00 | 5753.60 | 0.08 | 1255.20 | 3675.36 |
| 293 | | 0 – 3600 | 0.53 | 44.70 | 332.61 | 0.03 | 1513.80 | 5694.86 | 0.08 | 1224.10 | 3674.54 |
| 303 | | 0 – 3600 | 0.54 | 257.60 | 961.67 | 0.03 | 1509.00 | 5412.42 | 0.08 | 1147.40 | 3662.50 |
| 323 | | 0 – 3600 | 0.95 | 20.00 | 140.00 | 0.22 | 430.90 | 1914.04 | 0.18 | 620.80 | 2024.89 |
| 293 | 400 | 0 – 3600 | 0.54 | 21.20 | 174.04 | 0.03 | 1513.20 | 4333.73 | 0.14 | 1075.30 | 1860.80 |
| 278 | 500 | 0 - 3600 | 0.54 | 20.00 | 140.00 | 0.03 | 1514.00 | 4098.35 | 0.27 | 1011.80 | 1549.01 |
| 303 | | 0 – 3600 | 0.55 | 32.80 | 209.55 | 0.11 | 1483.90 | 1420.39 | 0.42 | 925.30 | 1546.70 |
| 323 | | 0 – 3600 | 0.95 | 20.00 | 140.00 | 0.46 | 107.10 | 279.19 | 0.85 | 502.40 | 1050.00 |
| 293 | 600 | 0 - 3600 | 0.54 | 20.10 | 148.71 | 0.10 | 1512.90 | 2340.81 | 0.56 | 934.30 | 1495.20 |

Therefore, $M_{Max}$ reflects the fraction of maximal possible inactivation, m denotes the growth rate constant, and $t_0$ is the time to reach 50% of $M_{Max}$. To obtain the pressure-temperature characteristics of lethal and sublethal injury of *L. lactis*, the estimated coefficients have to be calculated in dependence of the above mentioned inputs pressure, temperature and additive.

**Table 7**: Parameter estimates of stress resistant cell counts of *L. lactis* for the Logistic function.

| T (K) | p (MPa) | pressure holding time (s) | milk buffer | | | sucrose | | | sodium chloride | | |
|---|---|---|---|---|---|---|---|---|---|---|---|
| | | | $M_{Max}$ | m ($s^{-1}$) | $t_0$ (s) | $M_{Max}$ | M ($s^{-1}$) | $t_0$ (s) | $M_{Max}$ | m ($s^{-1}$) | $t_0$ (s) |
| 278 | 200 | 0 - 7200 | 0.588 | 103 | 387.93 | 0.16 | 1373.8 | 4007.04 | 0.505 | 906.3 | 1265.93 |
| 283 | | 0 – 7200 | 0.588 | 230.5 | 941.72 | 0.16 | 1373.6 | 4007.04 | 0.366 | 901.4 | 1250.48 |
| 288 | | 0 – 7200 | 0.588 | 440.3 | 2027.81 | 0.161 | 1373.1 | 4007.03 | 0.23 | 893.3 | 1227.9 |
| 293 | | 0 – 7200 | 0.588 | 681.3 | 3376.98 | 0.162 | 1371.7 | 4006.97 | 0.114 | 880 | 1195.24 |
| 303 | | 0 – 7200 | 0.595 | 820.3 | 3814.87 | 0.174 | 1357.4 | 4004.83 | 0.114 | 824.6 | 1086.18 |
| 313 | | 0 – 7200 | 0.992 | 393.1 | 1313.08 | 0.25 | 1258.4 | 3937.9 | 0.089 | 700.3 | 903.37 |
| 318 | | 0 – 7200 | 1.00 | 198.1 | 551.85 | 0.362 | 1097.3 | 3647.05 | 0.197 | 604.9 | 788.3 |
| 323 | | 0 – 7200 | 1.00 | 87 | 245.29 | 0.53 | 813.2 | 2689.39 | 0.329 | 493.2 | 667.31 |
| 293 | 250 | 0 - 5400 | 0.693 | 60 | 626.38 | 0.163 | 1176.3 | 3620.29 | 0.275 | 808.8 | 1195.24 |
| 278 | 300 | 0 - 3600 | 0.714 | 20 | 140 | 0.161 | 973.6 | 3000 | 0.813 | 811.2 | 1559.4 |
| 293 | | 0 – 3600 | 0.714 | 37.4 | 337.39 | 0.167 | 973.1 | 2999.86 | 0.343 | 780.4 | 1469.67 |
| 303 | | 0 – 3600 | 0.719 | 223.3 | 573.32 | 0.197 | 968.4 | 2996.8 | 0.047 | 717.3 | 1331.24 |
| 323 | | 0 – 3600 | 1.00 | 20 | 140 | 0.63 | 585 | 1918.68 | 0.343 | 386.7 | 801.71 |
| 293 | 400 | 0 – 3600 | 0.718 | 27.3 | 192.81 | 0.205 | 598.3 | 1457.92 | 0.466 | 627.9 | 1721.46 |
| 278 | 500 | 0 - 3600 | 0.718 | 20 | 140 | 0.191 | 330.5 | 595.26 | 0.976 | 749.7 | 1846.41 |
| 303 | | 0 – 3600 | 0.912 | 56.3 | 198.36 | 0.404 | 329.4 | 579.15 | 0.9 | 389.6 | 1306.34 |
| 323 | | 0 – 3600 | 1.00 | 20 | 140 | 0.73 | 209.5 | 395.07 | 0.942 | 97.9 | 592.85 |
| 293 | 600 | 0 - 3600 | 0.719 | 21.3 | 161.73 | 0.331 | 174 | 347.27 | 0.946 | 583.1 | 1604.48 |

In case of milk buffer, the temperature dependency of $M_{Max}$ was calculated using a sigmoidal function with four parameters to describe tailing phenomena if temperatures below 30°C were used (compare Figure 44 and Table 6 and Table 7). A pressure resistant fraction of *L. lactis*

was measured independent on the temperature. In case of a temperature below 20°C, $M_{Max}$ was reached faster if the process temperature was colder. In case of temperatures above 40°C, no tailing was detected and the population was completely inactivated using a pressure level of 200 MPa. Further on, the parameters m and $t_0$ described in milk buffer a symmetric Gauss distribution which has been used as the temperature connection of those parameters (Table 6, Table 7). Therefore, the temperature optimum was detected for viable cell counts at 302 K and for stress resistant cell counts at 300 K. To calculate the influence of pressure, all predicted parameters of those functions were described by exponential function (data not shown).

In case of sucrose, no temperature optimum was detected. This could be proved by all parameters describing viable cell counts. On the one hand, no substantial reduction could be measured using temperatures below 303 K at all analysed pressure levels. On the other hand, no substantial change of the parameters is also obvious. In case of stress resistant cells, the inactivation starts at a temperature of 303 K and a pressure level of 500 MPa. Furthermore, temperatures of 318 K or higher induced sublethal injury after a short pressurisation using a pressure level of 200 MPa or higher (Table 6, Table 7). Due to the strong baroprotection of sucrose, only sigmoidal functions with 4 parameters have been used to calculate the temperature as well as the pressure effects on the inactivation of *L. lactis* (data not shown).

In case of NaCl, minor baroprotection of *L. lactis* was detected compared to sucrose. This could be seen easily in case of 500 MPa/323 K or 600 MPa/293 K (Table 6, Table 7). For the physiological state of viable cell counts, the pressure-temperature dependencies of all all three estimates have also been calculated by the use of sigmoidal functions with 4 parameters. In terms of stress resistant cell counts, *L. lactis* was sublethal injured at temperatures below 293 K. In this temperature range, no protection was detected compared to sucrose (Figure 27). Therefore, the operating characteristic curve of the Gauss distribution has been used to describe $M_{Max}$ in the range of 278 K to 323 K. The pressure-temperature dependency of m and $t_0$ have then been detected by the use of sigmoidal functions with four parameters (compare Table 6, Table 7, and data not shown).

With those parameters, very good agreements between measured and predicted lethal and sublethal injury were obtained. Overall, a $R^2$=0.92 for stress resistant and a $R^2$=0.93 for viable cell counts were obtained analysing the data set obtained in the 10 ml autoclave (Figure 38). In case of CFU, most of the outliers belong to data measured in milk buffer. Further on, data

for CFUsub approved this and showed also outliers in the case of NaCl. Just a few outliers were visible for data measured in sucrose.

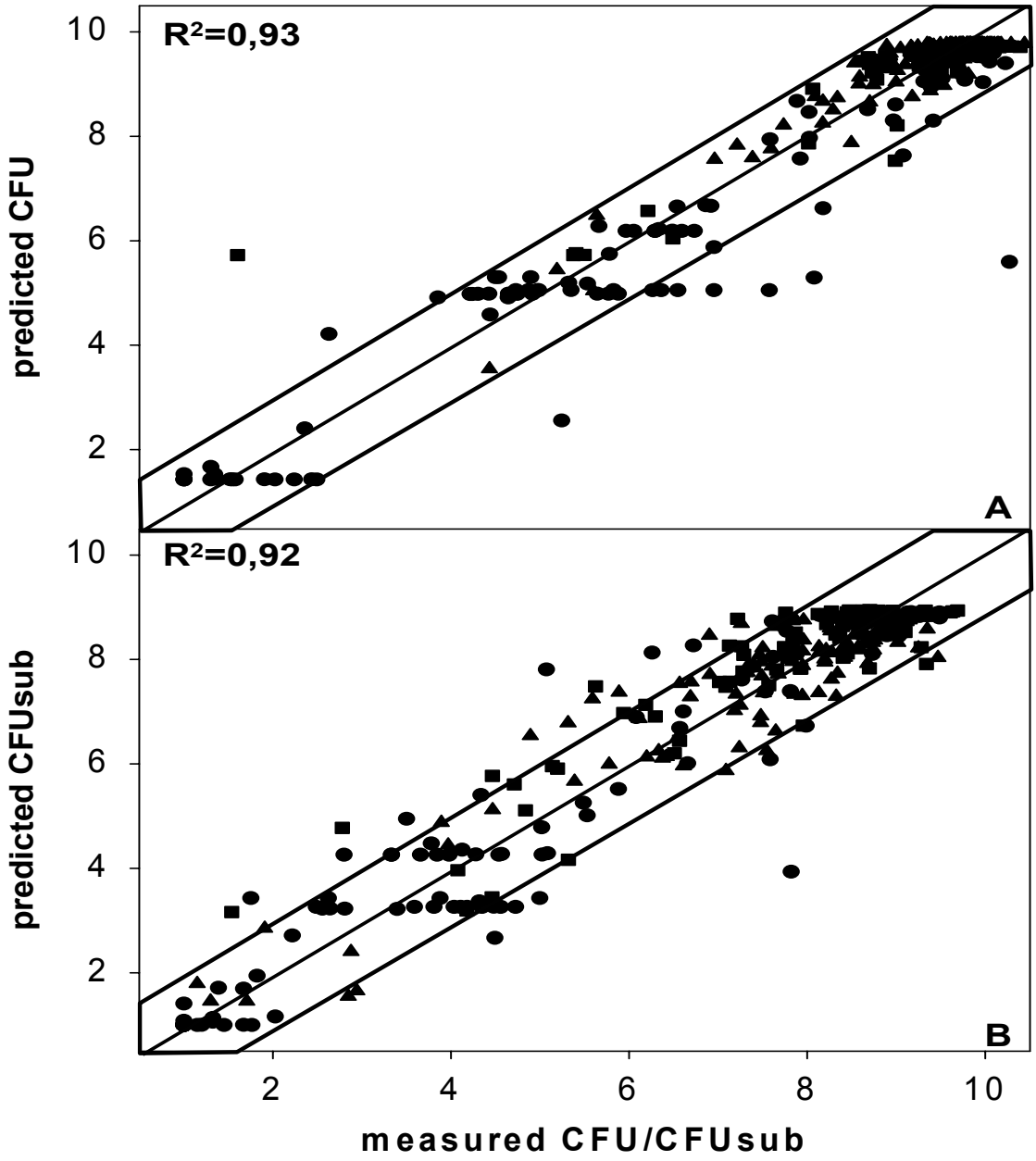


**Figure 38**: Comparison of predicted and measured data for model establishment. Framed areas indicate the deviation explained by overall experimental error. A: viable cell counts (CFU). B: stress resistant cell counts (CFUsub). Symbols represent data for the measurands in milk buffer (●), milk buffer sucrose (■), and milk buffer NaCl (▲).

### *3.7.3.* The Influence of Spatiotemporal Process Heterogeneities on the Inactivation of *L. lactis*

This part of the thesis describes experimentally and numerically the influence of non-uniformity on the inactivation of *L. lactis* in a medium size high pressure autoclave. Cells were packed in single 0.2 ml standard PCR-tubes (Brand, 78 13 00). PCR-tubes have been used to assure optimal heat transfer between the probes and the pressure fluid due to their material properties. This enabled the assumption that the temperature inside of the probes equaled that of the surrounding fluid. Furthermore, the calculated parameters of the Logistic function were used for the numerical prediction of the inactivation behaviour of *L. lactis* by the differential equation belonging to the Logistic equation (compare chapter 2.6.4). Subsequently, this model was combined with the High Pressure Computer Fluid Dynamics (HD-CFD) technique in order to investigate the effect of spatiotemporal heterogeneity due to the process which may exist in a medium size high pressure autoclave on the inactivation behaviour of the bacteria. To inform about the temperature characteristics of the process, Figure 39 reflects the spatial and transient temperature and flow distribution inside the 3.3-l autoclave during a 12 min high pressure treatment at the starting temperature of 28°C (Kitsubun, 2005).

After pressurisation, a temperature difference of about 6 K is visible which will be reduced the longer the process took place. After a pressure holding time of 12 min, the temperature difference between the top and the bottom of the autoclave is about 3 K (compare Figure 39 from left to right).

The main reason for the thermally induced process heterogeneity during high pressure treatment is the free convection due to the cooling process during the pressure holding phase (Kitsubun, 2005). The colder steel wall removes heat from the warmer fluid in the autoclave. This leads to a downward-directed boundary layer flow at the steel wall and the upward movement of warmer fluid in the middle of the autoclave, resulting in higher fluid temperature at the top and lower fluid temperature at the bottom of the autoclave. The temperature gradient become less significant with increasing pressure holding time. If the pressure holding phase is significantly long, the temperature gradient become less prominent as the fluid is cooled down to the given temperature of the tempering bath. However, this phenomenon has already been discussed and validated in previous contributions thoroughly (Hartmann, 2002; Hartmann et al., 2004; Kowalczyk et al., 2004).

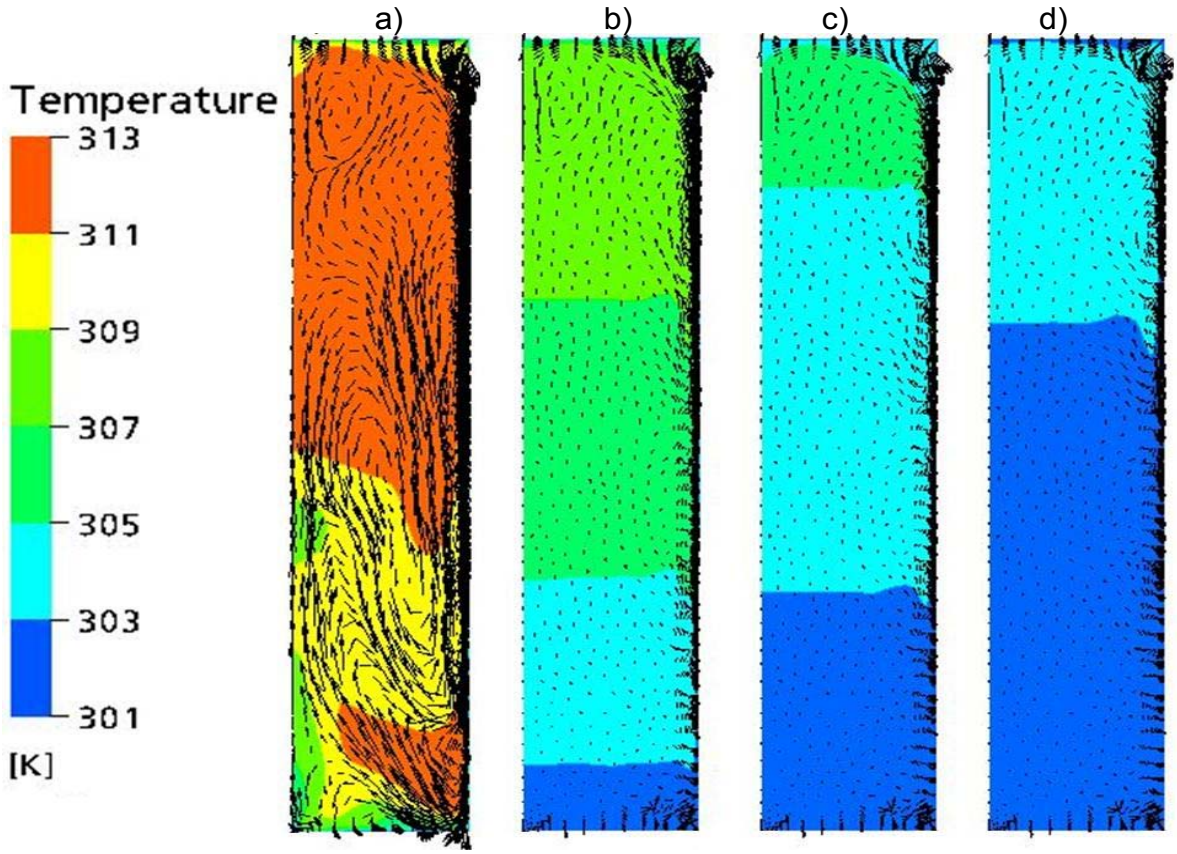


**Figure 39**: Temperature distribution and flow field inside the 3.3-l high pressure autoclave tempered at 301 K using a pressure of 500 MPa. The figure shows the distributions right after the compression (a), 4 min (b), 8 min (c) and 12 min (d) of pressure holding.

**Table 8**: Reduction of both physiological states of *L. lactis* after a treatment in milk buffer at 500 MPa using different temperatures. Data were calculated (Sim.) as means of duplicate independent experiments (Exp.) and the experimental error of the $\log(N/N_0)$ values generally was 0.6 log units or less. Bold numerics represent data, where a discrepancy exists greater than one log between the measured and simulated data.

| | | **CFU Top** | | **CFU Bottom** | | **CFUsub Top** | | **CFUsub Bottom** | |
|---|---|---|---|---|---|---|---|---|---|
| | | | | | **log ($N/N_0$)** | | | | |
| **T (K)** | **t (min)** | **Sim.** | **Exp.** | **Sim.** | **Exp.** | **Sim.** | **Exp.** | **Sim.** | **Exp.** |
| 301 | 8 | -6.5 | -6.1 | -4.9 | -5.1 | -7.9 | -8.2 | -7.9 | -7.6 |
| | 12 | -6.5 | -6.2 | **-4.9** | **-6.0** | -7.9 | -8. 2 | -7.9 | -8.2 |
| 304 | 4 | -7.7 | -6.9 | -6.6 | -5.9 | -7.9 | -7.8 | -7.9 | -7.5 |
| | 8 | -7.7 | -6.7 | -6.6 | -5.7 | -7.9 | -7.8 | -7.9 | -7.4 |
| | 12 | -7.7 | -6.4 | -6.6 | -6.2 | -7.9 | -7.8 | -7.9 | -7.8 |

In general, results achieved in the 3.3-litre-pressure-autoclave at two different locations comprised spatiotemporal heterogenities on the temperature- and inactivation-distribution of *L. lactis* due to the process. An overview of all data concerning the measurements and simulations in milk buffer is given in Table 8. Bold numerics represent data, where a discrepancy of greater than one log between the measured and simulated data exist.

In general, a very good agreement between the simulations and the measurands is visible. In case of milk buffer, just one outlier was detected using 301 K. Furthermore, a difference of 1-log could be validated by the simulation as well as the measurands detected in milk buffer.

An example is given in Figure 40. It illustrates the reduction of viable (Figure 40A) and stress resistant cell counts (Figure 40B) measured at the different locations at 500 MPa taking into account the temperature non-uniformity shown in Figure 39. At this temperature a Δ-1-log difference of CFU could be observed between the top and the bottom of the autoclave respectively. In terms of CFUsub, the whole population is inactivated after short pressure application. The agreement between predicted and validated data were excellent. Nearly in the same way, an overall reduction of CFUsub was observed throughout the whole autoclave using a starting temperature of 304 K and milk buffer (Table 8). CFU was detected in both probes whereas a difference of 1-log-unit could be measured and calculated between both tubes (Table 8). In accordance to the results above, no CFUsub was detected using this temperature.

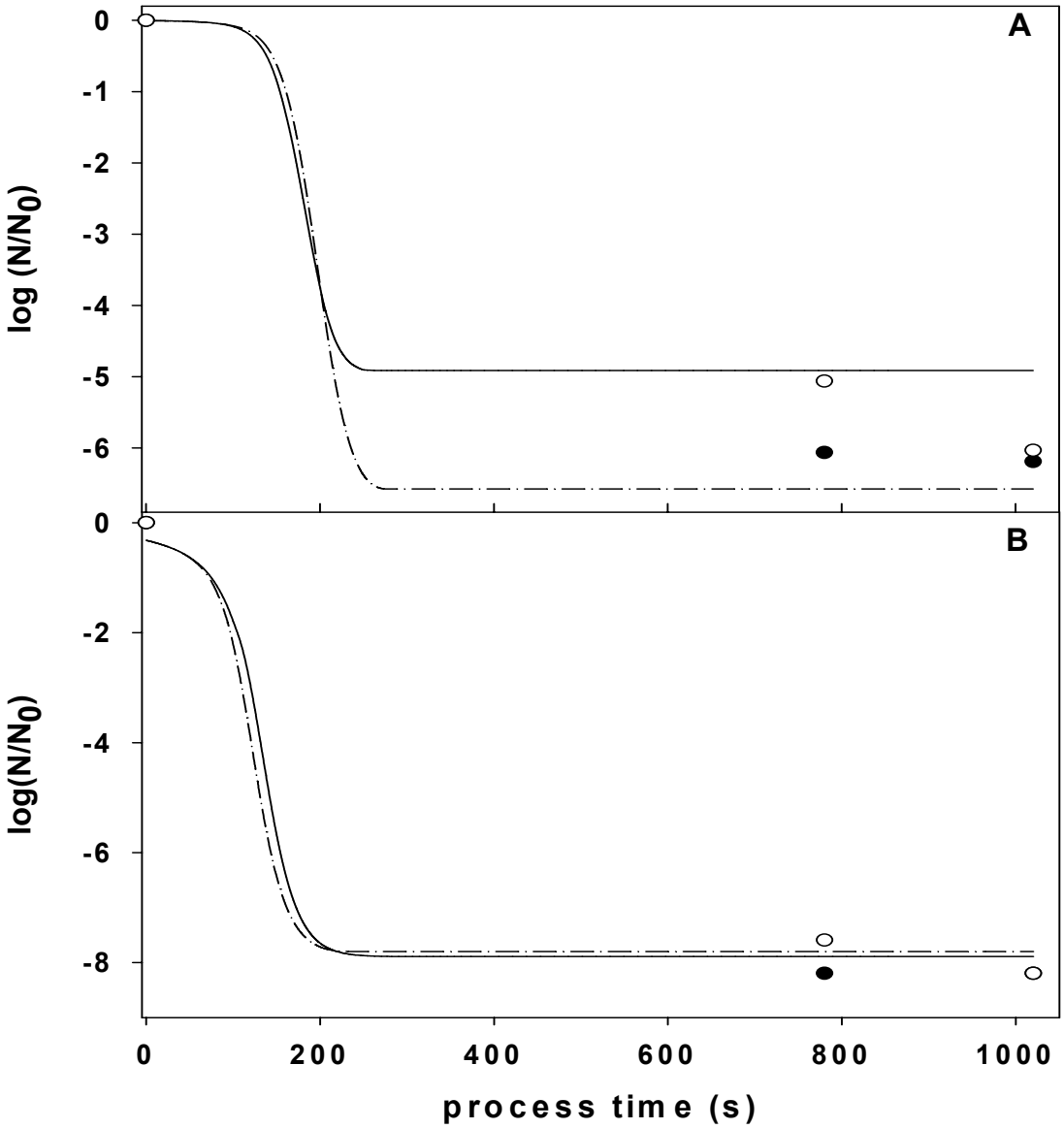


**Figure 40**: log(N/N$_0$) of *L. lactis* after 8 and 12 min using milk buffer as pressure medium. The start temperature was set to 301 K. A: viable cell counts. B: stress resistant cell counts. The dotted and solid curves represent the calculated reduction of the upper and the lower probes respectively. The measured data are shown as (●) for the upper and (○) for the lower probe.

Moreover, widely used additives such as NaCl and sucrose increased the pressure resistance of microorganisms significantly as discussed above. For instance, by adding 1.5 M sucrose to milk buffer, no reduction of CFU and CFUsub is detected using temperatures below 293 K. In terms of 4 M NaCl, a complete protection of the population is proved of up to 400 MPa for CFU.

An overview of all data measured in the presence of sucrose is given in Table 9. Significant differences between the predicted and measured data were just obtained in one case (Table 9). Also, a difference of nearly one-log was measured and detected for both states.

**Table 9**: Reduction of both physiological states of *L. lactis* after a treatment in milk buffer sucrose at 500 MPa using different temperatures. Data were calculated (Sim.) as means of duplicate independent experiments (Exp.) and the experimental error of the $\log(N/N_0)$ values generally was 0.6 log units or less. Bold numerics represent data, where a discrepancy exists greater than one log between the measured and simulated data.

| | | **CFU Top** | | **CFU Bottom** | | **CFUsub Top** | | **CFUsub Bottom** | |
|---|---|---|---|---|---|---|---|---|---|
| | | | | | | **log ($N/N_0$)** | | | |
| **T (K)** | **t (min)** | **Sim.** | **Exp.** | **Sim.** | **Exp.** | **Sim.** | **Exp.** | **Sim.** | **Exp.** |
| 311 | 8 | -1.7 | -1.8 | -1.3 | -0.9 | -4.0 | -4.2 | -3.6 | -3.4 |
| | 12 | -1.7 | -1.5 | -1.3 | -0.8 | -4.0 | -4.5 | -3.6 | -4.1 |
| 316 | 4 | **-4.0** | **-2,5** | -3,1 | -2,1 | -4,9 | -4,1 | -4,2 | -3,7 |
| | 8 | -4.0 | -3.6 | -3.1 | -3.3 | -4.9 | -5.4 | -4.2 | -5.0 |
| | 12 | -4.0 | -4.1 | -3.1 | -3.4 | -5.2 | -5.6 | -4.7 | -5.1 |
| 321 | 4 | -5.8 | -4.9 | -5.2 | -4.3 | -6.0 | -5.6 | -5.0 | -5.3 |
| | 8 | -5.8 | -5.6 | -5.2 | -5.4 | -6.0 | -6.5 | -5.2 | -6.1 |

Figure 41 shows the results of CFU and CFUsub achieved at 500 MPa after 8 min and 12 min of pressure holding time as the autoclave was tempered at 311 K. Comparing these data with those of milk buffer, the strong protection is demonstrated by Figure 41. Despite of the higher temperature, just a two-log-reduction of CFU and a 4-log-reduction of CFUsub was measured after 12 min at the top of the autoclave. Furthermore, a difference between the two probes of nearly 1-log was detected. Here again, due to the temperature distribution in the vessel, a more effective inactivation of *L. lactis* was measured and calculated in the upper region of the autoclave. This conclusion supported Table 9 and is also validated by the numerical simulations.

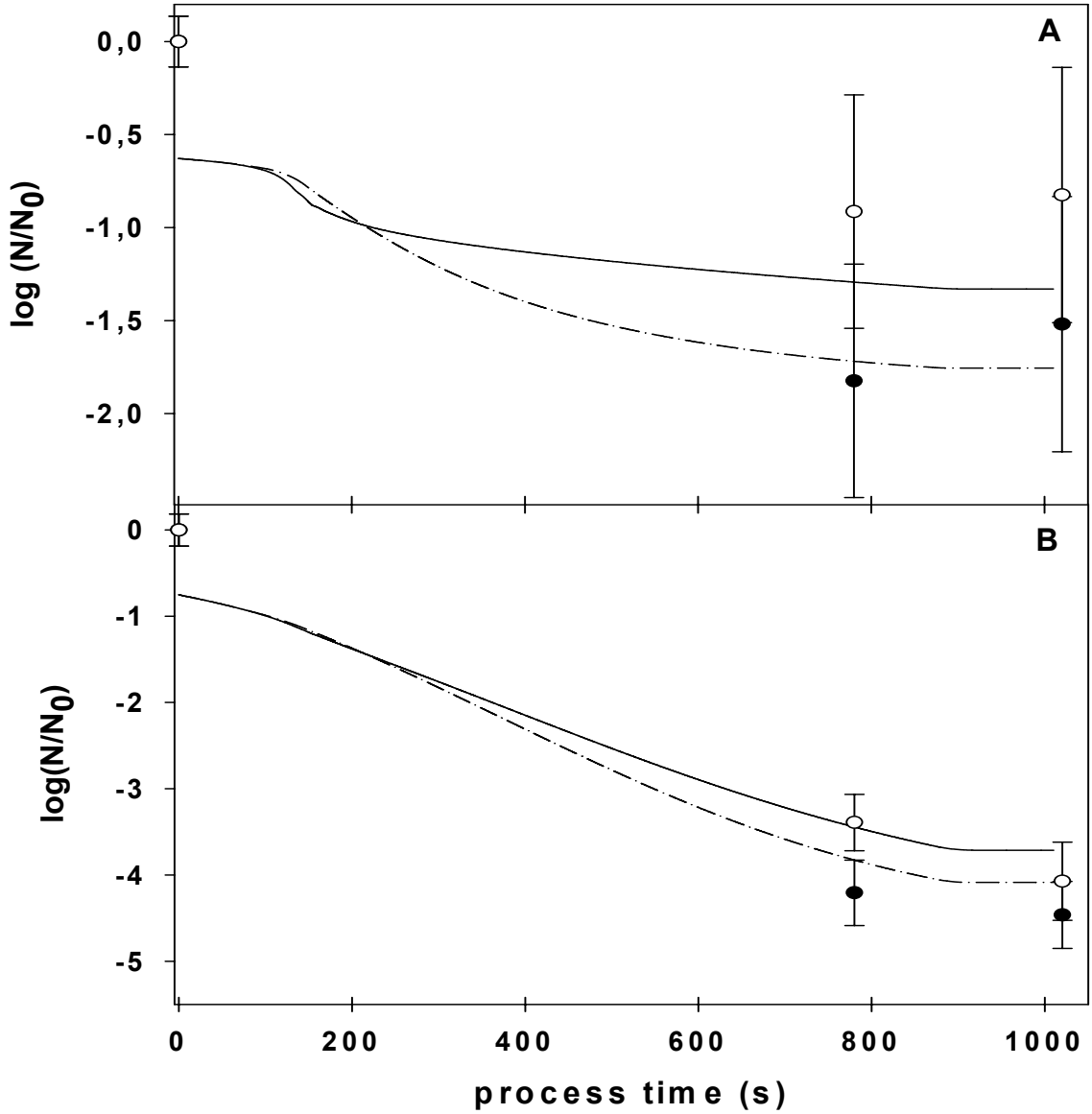


**Figure 41**: log($N/N_0$) of *L. lactis* after 8 and 12 min using milk buffer 1.5 M sucrose. The start temperature was set to 311 K. A: viable cell counts. B: stress resistant cell counts. The dotted and solid curves represent the calculated cell count reduction of the upper and the lower probes respectively. The measured data are shown as (●) for the upper and (○) for the lower probe.

In case of NaCl, all data concerning the simulations and experiments were united in Table 10. Furthermore, an example for this buffer is given in Figure 42. There, the reduction of viable and stress resistant bacteria is shown after 8 and 12 min of pressure holding at 500 MPa as the autoclave was tempered at 316 K. In case of NaCl, nearly no effect of spatiotemporal heterogeneties were measured. Therefore, the model failed to predict the inactivation correctly

twice at the top and once at the bottom of the autoclave in case of CFUsub. A maximal reduction of viable cell counts of approx. 4-log was observed and the inactivation seems to be linear in the chosen range of values. Further on, a 5-6 log reduction of CFUsub could be detected.

**Table 10**: Reduction of both physiological states of *L. lactis* after a treatment in milk buffer NaCl at 500 MPa using different temperatures. Data were calculated (Sim.) as means of duplicate independent experiments (Exp.) and the experimental error of the $\log(N/N_0)$ values generally was 0.6 log units or less. Bold numerics represent data, where a discrepancy exists greater than one log between the measured and simulated data.

| | | **CFU Top** | | **CFU Bottom** | | **CFUsub Top** | | **CFUsub Bottom** | |
|---|---|---|---|---|---|---|---|---|---|
| | | | | | | **$\log(N/N_0)$** | | | |
| **T (K)** | **t (min)** | **Sim.** | **Exp.** | **Sim.** | **Exp.** | **Sim.** | **Exp.** | **Sim.** | **Exp.** |
| 311 | 8 | -2.1 | -2.6 | -1.9 | -1.9 | -5.2 | -4.2 | -3.6 | -3.4 |
| | 12 | -2.3 | -2.6 | -2.1 | -2.1 | -5.5 | -5.4 | -4.2 | -4.9 |
| 316 | 8 | -3.9 | -2.8 | -2.6 | -2.4 | **-6.4** | **-4.8** | -5.0 | -4.5 |
| | 12 | -4.6 | -4.1 | -3.3 | -3.6 | -7.0 | -6.8 | -6.6 | -6.3 |
| 321 | 4 | -2.3 | -1.5 | -1.7 | -0.9 | **-5.2** | **-3.7** | -3.5 | -3.9 |
| | 8 | -3.3 | -3.4 | -2.4 | -2.7 | -5.9 | -6.1 | **-4.5** | **-6.2** |

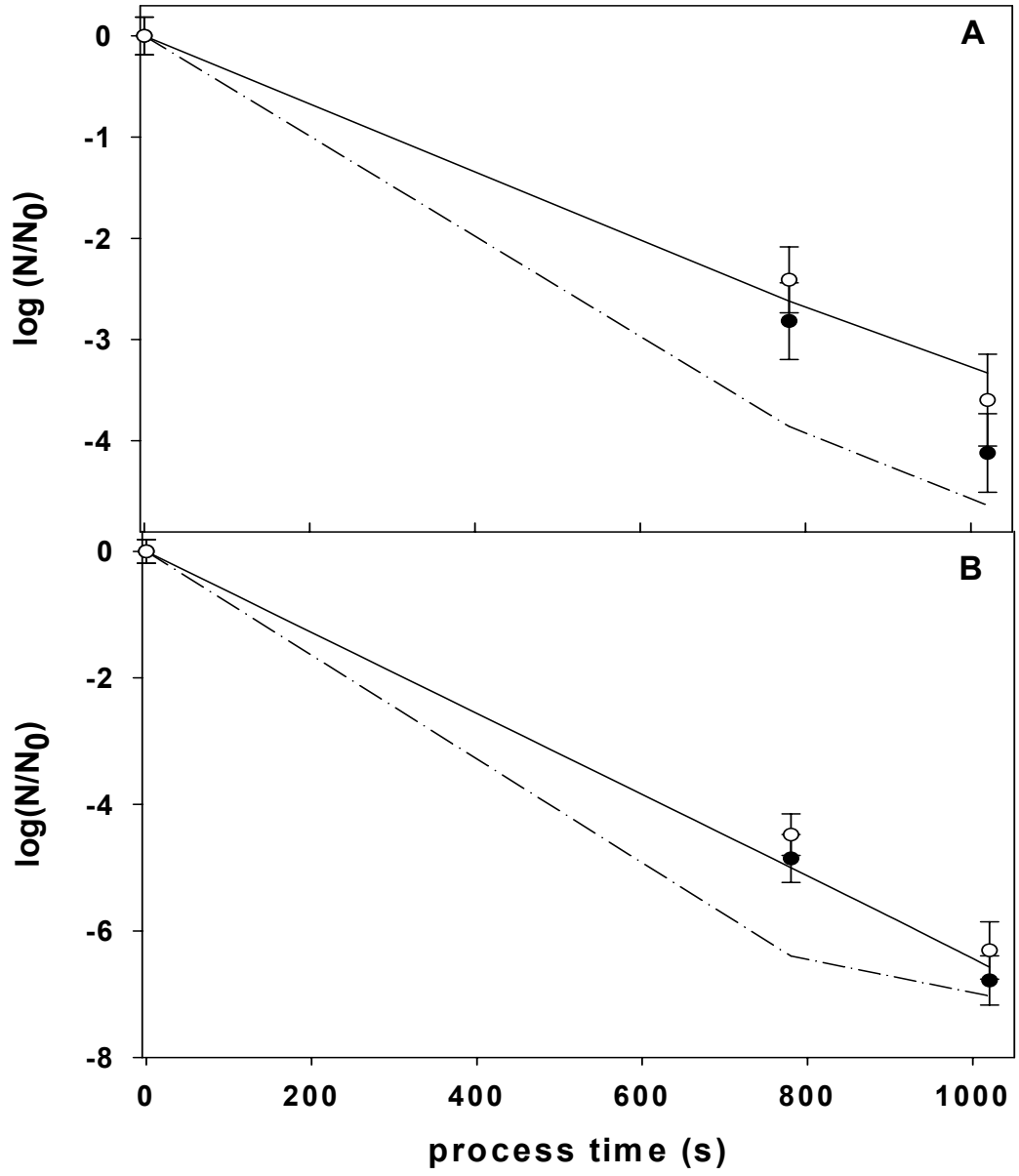


**Figure 42**: log($N/N_0$) of *L. lactis* after 8 and 12 min using milk buffer 4.0 M NaCl. The start temperature was set to 316 K. A: viable cell counts. B: stress resistant cell counts. The dotted and solid curves represent the calculated cell count reduction of the upper and the lower probes respectively. The measured data are shown as (●) for the upper and (○) for the lower probe.

The overall agreement between all measured and predicted data is found in Figure 43. For CFU, a $R^2$=0,95 and a $R^2$=0,96 for CFUsub was achieved for all parameter combinations. In milk buffer, the predicted results of CFUsub were in very good agreement with the measured ones (Figure 43B). Contrarely, two outliers were detected in terms of CFU (Figure 43A). On the other side, if the results in milk buffer sucrose were regarded, just one outlier for both

physiological states is visible in case of CFU. Comparing these results with those obtained in the presence of NaCl, a very good agreement between the predicted and measured data for CFU was obtained by the numerical simulation. Contrarely, the results of CFUsub showed three obvious outliers.

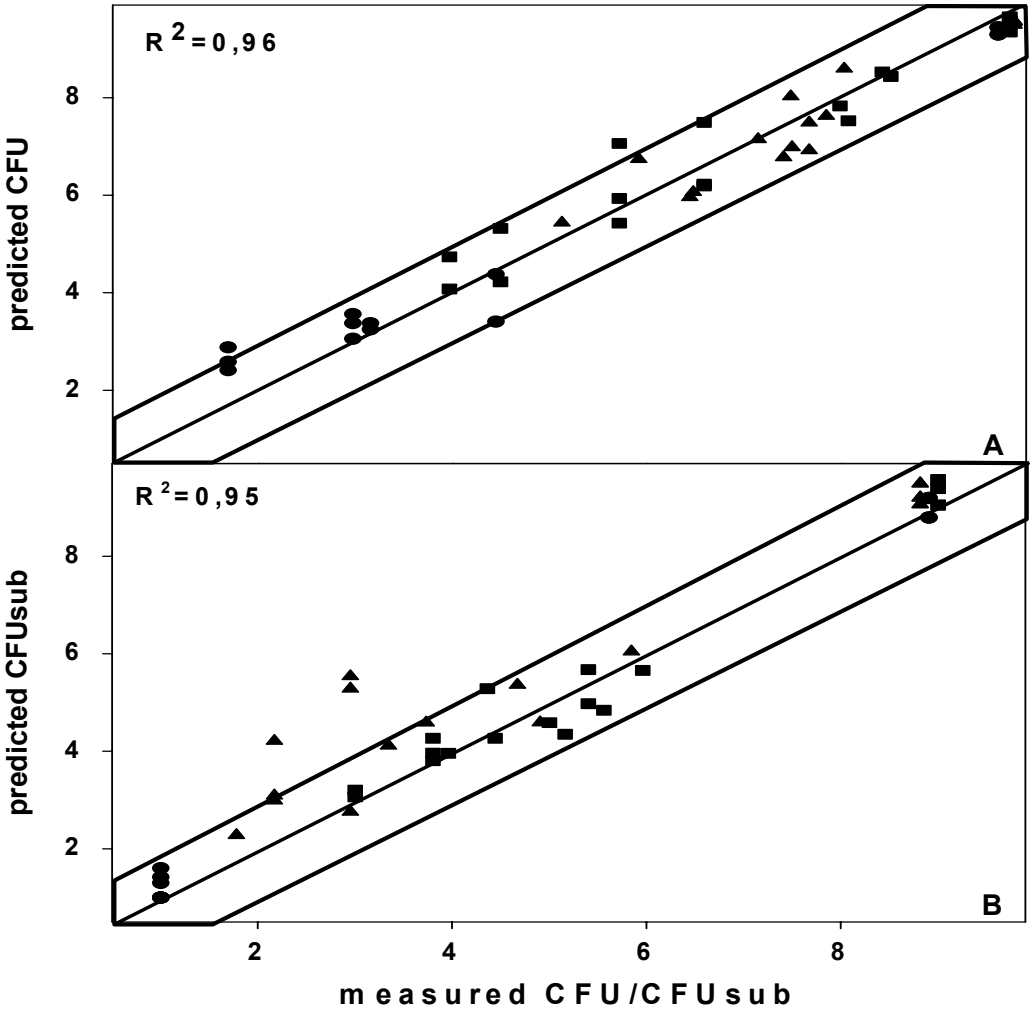


**Figure 43**: Comparison of predicted data and data measured for model validation after model establishment. Framed areas indicate the deviation explained by the overall experimental error of the methods for determination of CFU and CFUsub. Symbols represent data for the measurands in milk buffer (●), milk buffer sucrose (■), and milk buffer NaCl (▲). A: viable cell counts (CFU). B: stress resistant cell counts (CFUsub).

In conclusion, the results achieved in the 3.3-litre-pressure-autoclave comprised spatiotemporal heterogenities on the temperature-distribution as well as on the inactivation of *L. lactis*. A maximum of Δ-1-log between the upper and the lower probes was obtained by both, the experiments and the numerical simulations.

# 4. Discussion

This work provides a detailed analysis of temperature and temperature-pressure-induced inactivation of *Lactococcus lactis* ssp. *cremoris* MG 1363 or pressure-pH inactivation of *Escherichi coli* TMW 2.497. The focus of this work was set on the physiological description of *L. lactis* in milk buffer and different variations of this buffer using a temperature- or combined pressure-temperature-process. Therefore, a temperature level was analysed using either 40°C to 75°C using just temperature or 5°C to 50°C in case of combined pressure treatment. In terms of pressure-temperature treatments, a pressure level of up to 600 MPa was used. To describe the inactivation in detail and to obtain insights into the mechanisms involved in bacterial survival, lethal and sublethal measurement techniques were used. Further on, resistance mechanisms in *E. coli* as well as the detection of conformational changes of proteins in *L. lactis* allowed to achieve the aim of this thesis.

Further on, the recorded inactivation data for *L. lactis* were enhanced with an additional data set. The united one was then utilised to generate mathematical models and to extract additional knowledge by the use of chemometric tools, algorithmic tools and Fuzzy Logic. Concerning *Escherichia coli*, *rpoS* induced protection mechanisms have been analysed to detect correlations between cell death and the behaviour of the intracellular pH during and after the treatment.

## 4.1. Temperature-Co-Solvent Dependant Inactivation of *L. lactis*

The inactivation of enzymes is caused by process induced conformational transitions in the protein-molecule. In terms of increasing temperature, cooperative intramolecular motions occur until a critical temperature is reached. At that time, noncovalent forces that maintain the native structure of the protein can not longer prevail against the temperature induced change in entropy and volume (Ahern and Klibanow, 1985; Somero, 1995). In consequence, the protein looses most of its ordered secondary and tertiary structures and gets denatured.

The thermal stability of a protein can be changed intrinsincally by the alteration of amino acids or extrinsically by the addition of suitable stabilising effectors, e.g. peptides or osmolytes (Sola-Penna and Meyer-Fernades, 1994; Saad-Nehme et al., 1997). A general mechanism proposed to explain the stabilising effect is the exclusion of the solute from the protein hydration shell.

Organisms and cellular systems are required to adapt to stress conditions such as high temperature or high pressure, often responding by accumulating organic solutes such as sugars (Crowe et al., 1984; Van Opstal et al., 2003; Molina-Höppner et al., 2004). This accumulation is associated with the effectiveness of these osmolytes in minimising protein denaturation and membrane damage under stress conditions. The ability of carbohydrates to stabilise proteins has been attributed to the preferential hydration of proteins in carbohydrate solutions. An increase in the concentration of carbohydrates engages more water molecules in solubilisation of protein and protein and solute begin to compete for the available water. This leads to a reduction in the protein solvation layer, which results in a decreased aparent molar volume of the protein. Therefore, soluble proteins become more compact and less susceptible to destabilising forces (Timasheff, 1993).

The analysis of process induced conformational changes of the protein behaviour of *L. lactis* were analysed in this work by the use of FT-IR spectroscopy. Therefore, the conformational changes of the proteins as well as the D/H exchange of the *L. lactis* population were analysed using $D_2O$ as well as $D_2O$-sucrose (1.5M). The analysis of the results of the amide A and HOD-stretch promised an internal sensor to detect the surrounding temperature of the system due to the fact, that the amide A band was almost covert by the HOD-stretching band . By the analysis of the amide II' and the amide II structure, an accelerated exchange of hydrogen-deuterium (D/H) was detected if data recorded in $D_2O$ were compared to those obtained in $D_2O$-sucrose. The same phenomen was achieved by the comparison of both data sets achieved for thermal induced structural changes of proteins by the amide I' analysis. Furthermore, by the analysis of amide I', an increase of unordered characteristics were obtained by the calculation and the analysis of the second derivative spectra. If the temperature was elevated, random coil, turn-, β-sheet and unordered structures increase whereas the ordered fraction described by the α-helix decreased. In conclusion, a protective effect of sucrose was clearly determined by the analysis of amide II, amide II', and amide I' and demonstrated the above mentioned theory.

Furthermore, the addition of sodium chloride in molar concentrations prevents temperature or pressure induced bacterial inactivation (Blackburn et al., 1997; Mattick et al., 2000; Molina-Höppner et al., 2004). In general, the $a_w$ is lowered in the presence of sodium chloride. Therefore, the decrease of the $a_w$ is proportional to the increase of NaCl. The addition of 4M

NaCl resulted in a decrease of the $a_w$ of milk buffer from 0.996 to 0.8954. In case of 1.5M sucrose, the $a_w$ is lowered just from 0.996 to 0.9663 (Molina-Höppner, 2002).

The results shown and discussed above confirmed the theory, that the used co-solvents protect the bacteria in case of increased temperature. 1.5M sucrose as well as 4M NaCl showed differences of up to 6-log cycles, if the inactivation data is compared with data obtained in milk buffer. Furthermore, NaCl protects *L. lactis* more efficient against temperature inactivation than sucrose (compare chapter 3.1). These results confirm the findings discussed above. The addition of sucrose as well as the addition of NaCl prolongate bacterial survival due to elevated temperature. Nevertheless, a temperature of about 65°C or higher result in a complete inactivation of the population of the bacteria. In case of sucrose, the achieved FT-IR data give information about the decelerated inactivation of both physiological states of *L. lactis* after the thermal treatment. A slowed exchange of D/H as well as thermal induced structural changes of proteins by the amide I' analysis was detected for the protein behaviour in *L. lactis* in the presence of sucrose.

The obtained data were compared to data describing the inactivation of *L. lactis*. Therefore, $M_{Max}$ (percentage of irreversibly inactivated population) was correlated to the D/H exchange whereas the structural changes detected by amid I' could not reassigned to cell death. First, the protective effect of sucrose was determined for microbial inactivation as well as for the detection of the process induced protein behaviour. Second, data describing the D/H exchange could be correlated to the sublethal injury of the bacteria.The transfer of proton exchange was found nearly in the same temperature range than the area of $M_{Max}$ conncerning to stress resistant cell counts. Third, conformational changes of the secondary structure of the proteins was found phase delayed to higher temperatures compared to viable cell counts of *L. lactis*.

In conclusion, a simple and robust method was established to detect conformational changes of proteins in microoranisms. Therefore, the cumulative behaviour of a few thousand proteins is analysed in-situ of *L. lactis*. However, data acquisition was done concerning just the temperature dependency and not the time-dependency of the conformational changes. Therefore, it seemed to be hard to detect correlations between time-dependent inactivation kinetics.

## 4.2. Pressure-Temperature-Co-Solvent Dependant Inactivation of *L. lactis*

Pressure is known to inflict sublethal injury in vegetative cells of bacteria. This effect is highly relevant in food applications because sublethally injured cells loose their resistance towards antimicrobial agents or adverse environmental conditions. For example, *Escherichia coli* is sensitised to nisin or lysozyme because structure and function of the outer membrane is deteriorated by pressure treatments. Moreover, *E. coli* is rendered acid tolerant through sublethal pressure application (Pagan et al., 2001) and the hop resistance of beer spoiling *Lactobacillus plantarum* is suppressed by pressure (Ulmer et al., 2002b). Generally, sublethal injury is thought to be mediated by the inactivation of membrane bound enymes. Wouters et al. (1998) have shown that the $F_0F_1$-ATPase is inactivated in *L. plantarum* after sublethal pressure treatments. Likewise, in *L. lactis* and *L. plantarum* are inactivated enzymes involved in pH homeostasis after sublethal pressure treatments (Molina-Höppner, 2002) as well as the membrane bound MDR-transport enzymes LmrP and HorA, respectively (Ulmer et al., 2002b ; Molina-Höppner et al., 2004). In this work, the use of PCA revealed a strong correlation between LmrP inactivation and stress resistant cell counts. This analysis was carried out with a large data set comprising the kinetics of inactivation of *L. lactis* at 200 MPa in milk buffer, milk buffer with 4M NaCl or 1.5M sucrose at 8 different temperatures between 5°C and 50°C. The correlation between sublethal injury and LmrP inactivation was obvious after treatments in milk buffer, milk buffer with sucrose, and milk buffer with NaCl. LmrP is a pmf-driven transport enzyme, therefore, loss of LmrP activity may result either from LmrP inactivation, or from inactivation of enzymes involved in pH homeostasis. In any case, the loss of LmrP activity after pressure treatment is caused by the inactivation of integral membrane proteins. The results substantially support the hypothesis that integral membrane proteins are among the most pressure sensitive targets in bacterial cells.

Generally, pressure application induces a phase transition to the gel phase in bacterial membranes (Ulmer et al., 2002b; Molina-Höppner et al., 2004). This phase transition reversibly inactivates membrane proteins (Kato et al., 2002). Whereas monomeric proteins in aqueous solution generally do not experience irreversible inactivation after pressure treatments below 300 MPa, integral membrane proteins are irreversibly inactivated already by pressure treatment with 100 MPa. Remarkably, the activity of a $Na^+K^+$-ATP-ase in membrane vesicles was restored after pressure treatment with 250 MPa by incubation for one hour at

ambient conditions (Kato et al., 2002). Therefore, sublethally injured cells may recover under optimal conditions after pressure treatment even in the absence of *de novo* protein synthesis.

Bacteria exhibit a maximal resistance against pressure at ambient temperature or a few degrees below their growth temperature. In agreement with previous studies (Sonoike et al., 1992; ter Steeg et al., 1999), *L. lactis* exhibited maximum resistance to pressure when treated in milk buffer at a temperature that was approximately 2-3°C below the growth temperature. This temperature of maximum resistance was determined with all of the indicators of lethal or sublethal injury. Remarkably, a temperature upshift to 40°C virtually eliminated the tailing that was apparent at ambient or low temperature. This effect was not reported by previous studies on the temperature effects on pressure inactivation of bacteria because the kinetics of inactivation were not sufficiently resolved (Sonoike et al., 1992). A pronounced tailing in bacterial pressure inactivation kinetics was frequently reported and the level of the pressure resistant fraction of the population was found to be independent of the medium pH, the ethanol concentration, and sucrose levels (Gänzle et al., 2001; Casadei et al., 2002; Molina-Höppner, 2002). Because the presence of pressure-resistant fractions within populations of target organisms may hamper the application of pressure processes in food production, the possibility of eliminating strong tails in survivor curves by a mildly elevated temperature represents a significant improvement of this work.

1.5M sucrose protected *L. lactis* at any temperature using a pressure level of 200 MPa. If a pressure level of 500 MPa and a temperature greater than 45°C was used, a decrease of viability was observed. No significant reduction was achieved by the use of 600 MPa and temperatures below 30°C. In case of CFUsub, the reduction started at temperatures above 40°C at a pressure level of 200 MPa. The higher the pressure was, a reduction of CFUsub was shifted towards colder temperatures. Nevertheless, temperatures below 30°C did not affect CFUsub at any pressure level.

However, viability of *L. lactis* is protected in the presence of 4M NaCl to a pressure level of up to 400 MPa. In contrast, NaCl provided protection against pressure inactivation only above 20°C in terms of CFUsub. For this physiological state, the temperature of maximum baroresistance was shifted to 40°C. This result reflects different mechanisms of baroprotection of sucrose and of NaCl. Protection by sucrose or other carbohydrates was suggested to be related to the high intra- and extracellular concentration of sucrose, which protect biomolecules against physical stressors by the mechanism of preferential exclusion. In

contrast, high levels of NaCl do not prevent temperature- or pressure inactivation of proteins or membranes. The baroprotective effect of NaCl could only be attributed to the intracellular accumulation of compatible solutes (Molina-Höppner et al., 2004). A different mechanism of baroprotection became also apparent through correlations between the various indicators of sublethal and lethal injuries as determined by PCA. The loss of metabolic activity correlated well to cell death after treatments in milk buffer or milk buffer with 1.5M sucrose. However, the loss of metabolic activity is an indicator for sublethal injury after treatments in milk buffer with 4M NaCl.

This temperature effects on pressure inactivation of bacteria reflect the elliptic or hill-shaped phase diagrams of protein denaturation in the p/T plane (Smeller, 2002). Moreover, the fluidity of the cytoplasmic membrane as affected by addition of lipids to the growth medium, by the cultivation temperature and/or by the pressurisation temperature affects bacterial survival at lethal pressure levels, and the inactivation of integral membrane proteins (Casadei et al., 2002; Molina-Höppner, 2002). Structural studies on the phase transitions of model biomembranes at various pressure/temperature conditions have shown that the membrane phase strongly affects the conformation of integral membrane proteins (Winter, 2002).

## 4.3. Pressure-pH Dependent Resistance of *E. coli*

During acid challenge, the survival of *E. coli* is dependent on its ability to maintain a high intracellular pH to prevent damage to intracellular macromolecules, and to provide favourable conditions for intracellular enzymes. Three transport systems are known to contribute to the extrusion of protons in *E. coli*. Among these, the glutamate decarboxylation pathway is the most favourable because it stabilises the internal pH without the expense of ATP, and neutralises the external medium at low pH-values (Figure 29; Cui et al., 2001; Richard and Foster, 2003). The *gadABC* operon coding for the glutamate survival pathway is overexpressed upon induction of the alternative sigma factor $\sigma^S$ in the stationary phase of growth, and during acid adaptation (Richard and Foster, 2003). *E. coli* cells that fully staged their adaptive response to acid conditions are able to survive at a pH of 2.5 or less for hours, and at a pH of 4.0 for weeks or month. In this work was determined the effect of glutamate and arginine on the survival of *E. coli* during pressure treatment, and during post-pressure acid challenge.

It was previously shown in lactic acid bacteria that pressure treatments at 200 MPa or higher reversibly dissipate the transmembrane proton- and potassium gradients concomitant with compression (Molina-Gutierrez et al., 2002; Vogel et al., 2003) and the same pattern was observed in this work with *E. coli*. Glutamate and arginine did not influence the survival of *E. coli* during pressure treatment (Figure 30) and, independent on the presence of amino acids, the intracellular pH of *E. coli* during pressure treatment was equal to the external pH. Pressure induces a phase transition of the cytoplasmic membrane from the physiological, liquid-crystalline phase to the gel phase. A phase transition to the gel phase reversibly inactivates integral membrane proteins (Silvius and McElhaney, 1980), and the glutamate- and arginine acid survival pathway are dependent on transport processes across the cytoplasmic membrane. Therefore, these metabolic pathways can be expected to be inactive at high pressure conditions.

Sublethal pressure application rapidly resulted in an irreversible loss of the ability of *E. coli* to restore a high internal pH after pressure treatment with glucose as the sole source of metabolic energy. The enzymes required for pH homeostasis in MES-buffer were inactivated after 4 and 0 min of treatment at 200 and 300 MPa, respectively, and these treatment times correspond well to the treatment intensities that were required to eliminate the tolerance of *E. coli* to incubation in pH 4.0 buffer (compare Figure 31 and Figure 32). In agreement with these observations, sublethal pressure treatments of *E. coli* enabled the elimination of this organisms during storage in various fruit juices at pH-values below 4.0 (Garcia-Graells et al., 1998; Jordan et al., 2001). Despite the pressure-induced inactivation of enzymes required to maintain a high intracellar pH, pressure-treated *E. coli* suffered little loss of viability when incubated in MES buffer, pH 5.4. This pH apparently does not question the short / mid-term survival even in the absence of a transmembrane pH gradient, in agreement with the observation of short-term survival of *E. coli* and *Shigella flexneri* at a $pH_{ex}$ of 3.3 and a $pH_{in}$ of 4.9 (Small et al., 1994).

The availability of glutamate strongly improved the survival of *E. coli* during post-pressure acid challenge. This improved acid tolerance correlated well to an improved ability of *E. coli* to restore a high intracellular pH after pressure treatment (compare Figure 31 and Figure 32). Apparently, the enzymes required for the glutamate acid survival pathways remain functional even after pressure treatments that inactivate those enzymes that are required to establish a transmembrane pH gradient with glucose as sole energy source. During 24h of acid challenge,

pressure treated cells consumed 10 mM glutamate, whereas only 4 mM glutamate were consumed by untreated cells. Pressure treated or untreated cells utilised 2 mM of arginine. It was previously reported that *E. coli* preferred the glutamate pathway more than the arginine pathway during exposure to acid (Richard and Foster, 2003; Diez-Gonzalez and Karaibrahimoglu, 2004). The utilisation of glutamate was enhanced in pressure treated cells compared to untreated cells, indicating induction or activation of the glutamate acid survival pathway. Adaptation of *E. coli* to mild acid conditions (pH 5.4) further improved the survival of *E. coli* to post-pressure acid exposure.

In conclusion, the availability of glutamate strongly improves the post-pressure acid survival of *E. coli*. Apparently, enzymes that enable *E. coli* to stabilise a high internal pH with glucose as sole substrate are more rapidly inactivated by pressure than the enzymes of the glutamate acid survival pathway. Therefore, the glutamate availability in foods must be taken into account when sublethal pressure treatment and post-pressure acid exposure are used to achieve a 5D reduction of *E. coli* in foods (Garcia-Graells et al., 1998; Jordan et al., 2001). For reasons of laboratory safety, our work has not been carried out with a pathogenic strain of *E. coli* exhibiting high resistance to pressure (Alpas et al., 1999; Alpas et al., 2000; Hauben et al., 1997; Robey et al., 2001). Moreover, transformation of *E. coli* with a multi-copy plasmid designed for high expression of GFP as a prerequisite or the determination of the intracellular pH may affect the pressure resistance of the host strain. However, a decisive role of glutamate for the post-pressure acid survival of pressure resistant, pathogenic strains of *E. coli* can be anticipated. The importance of the glutamate acid survival pathway for the survival of pathogenic strains of *E. coli* at acid conditions in food is well established (Cui et al., 2001) and $\sigma^S$-regulated genes are known to be crucial for the resistance of *E. coli* to high pressure (Gänzle and Vogel, 2001).

## 4.4. Principal Component Analysis

The experimental data concerning temperature-pressure-co-solvent induced inactivation of *L. lactis* was generated by ex-situ analysis of five physiological states after pressure decrease. To reduce redundancies in data, Principal Component Analysis (PCA) was carried out. The correlations detected here by PCA were used to improve a multi-layer Fuzzy Logic model describing the lethal and sublethal effects of pressure on *L. lactis* (compare Figure 9). The model was structured by defining the autonomous output variables viable cell counts and

LmrP activity. The remaining quantities (stress resistant cell counts, metabolic activity, and membrane integrity) were calculated mainly based on the independent output variables (Figure 9).

Specifically, the detected correlations between culture-dependent and culture-independent methods for the determination of cellular viability and physiology were proved and also validated by the Fuzzy model. These findings enable a more rapid data aquisition and additionally reduces computation time and computer capacities concerning industrial modelling. For example, the determination of viable and stress resistant cell counts provided information on the metabolic activity of the cells as well as the activity of MDR-transport enzymes involved in the resistance to bactericidal agents. Likewise, the determination of the metabolic activity with tetrazolium salts can be used as a rapid screening of lethal pressure effects at various combinations of pressure, temperature, and co-solvents.

## 4.5. Modelling of Pressure-Temperature-Co-Solvent Induced Inactivation of *L. lactis*

In this work, two different kinds of modelling tools have been used to describe the effects of pressure, temperature and co-solvents on the inactivation of *L. lactis.* First, Fuzzy Logic was used as a data based modelling tool and second, the Logistic equation was used as a differential equation modelling tool.

### 4.5.1. Fuzzy Logic Modelling

The pressure inactivation process of *Lactococcus lactis* ssp. *cremoris* MG 1363 is considered as a multi-stage inactivation process (Molina-Höppner, 2002; Kilimann et al., 2005a). In this work, the activity of the membrane bound transport enzyme LmrP was found to be a sensitive indicator of pressure induced sublethal injury and correlates well to the amount of stress resistent cell counts. The metabolic activity of *L. lactis* was inactivated concomitant with or earlier than cell death. After pressure inactivation in milk buffer, the membrane remained impermeable to propidium iodide even under conditions that reduced viable cell counts by more than 99%. A reduction of the pH value, or the addition of NaCl or sucrose in molar concentrations exerted synergistic and antagonistic effects on pressure inactivation,

respectively. These different additives exerted specific effects on individual stages of pressure inactivation of *L. lactis*.

A Fuzzy Logic model was formulated that predicts the membrane integrity, the metabolic activity, viable cell counts, stress resistant cell counts and the activity of the membrane bound transport system LmrP as a function of a pressure level ranging from 0.1 to 600 MPa, pressure holding time up to 2 hours and for 21 different variations of milk buffer (compare Table 2). The predictive power of the model was determined using experimental data that were generated after model establishment at conditions not taken into consideration for model establishment. The values predicted by the Fuzzy model are in excellent agreement with the experimental data sets used for model establishment and model validation.

This model was simplified compared to another one substantially by the obtained results of PCA. Thus, PCA was used to detect correlations between the five physiological states and these correlations were used to designate viable cell counts and LmrP activity as autonomous output variables. Other physiological states (stress resistant cell counts, metabolic activity, and membrane integrity) were calculated mainly based on the autonomous output variables. The excellent prediction quality, which was obtained for the entire data set, supports the correlations identified through PCA on a data subset. Compared to a previous Fuzzy model (Kilimann et al., 2005a), the data set used in this work was more than doubled in size to include temperature effects on pressure inactivation in the presence or absence of various additives. Nevertheless, the model could be simplified substantially by the designation of autonomous and dependent output variables and the model rulebase had to be extended only by 25% to a total of 200 rules without compromising the quality of fit.

In conclusion, a model based on Fuzzy Logic rules was established which accounts for the specific knowledge on the multi-step high-pressure inactivation of *L. lactis*, and which allows the prediction of the quantities of lethally and sublethally damaged cells after pressure treatment. The Fuzzy model accurately predicts pressure inactivation of *L. lactis* using conditions not taken into account in model generation. Because Fuzzy type models are increasingly used to control unit operations in food production, the development of models that include the prediction of microbial behaviour during food production can be envisaged in the future. Additionally, it may serve as a tool for model and measurement based analysis of correlations between the various physiological states of *L. lactis* during pressure treatment in

order to improve the understanding of the complex process of bacterial inactivation by high pressure.

### 4.5.2. The Logistic Equation and Real-Time-Simulation of Process Induced Spatiotemporal Heterogeneities and its Effect on *L. lactis*

In particular, a variety of food exist containing different concentrations of baroprotective and bactericidal co-solvents. Concerning the safety or quality of minimally processed food, process parameter detection is just necessary for neutral and most effective baroprotective co-solvents to obtain information about those parameters which will end in the demanded 5D reduction of bacteria (Anonymous, 2003). Howerver, the analysed bacteria is not a representative of contaminating ones, but the expiration date may be negatively affected if food will be insufficiently pasteurised. Therefore, the effects of bactericidal co-solvents were not taken into account due to their synergistic effect in combination with the high pressure process. All informations about the quality of the process was obtained by the detection of the inactivation behaviour in neutral milk buffer or milk buffer 1.5M sucrose (sucrose) or milk buffer 4M NaCl (NaCl, Figure 44 and data not shown).

Vegetative bacteria tend to have significant tailing at ambient tempertarture or below. Furthermore, suitable osmolytes prolongate or inhibit the inactivation of the population. Therefore, this work provided a closer analysis of the combined effects of pressure, temperature, neutral medium and two of the strongest known baroprotective additives namely sucrose and NaCl to gain insight into the inactivation process of *L. lactis* under worst possible scenario.

In milk buffer, the tailing effect of viable cell counts of *L. lactis* was visible in a temperature range between 278 K and 303 K. The decimal reduction level is not influenced by the pressure and further inactivation was achieved by increasing temperature (Figure 44). Comparing these results with those obtained in sucrose, full protection of the population was provided by this additive. The demanded 5D reduction was detected and calculated just using temperatures above 318 K and a pressure level of 600 MPa (Figure 44). In case of milk buffer supplemented with NaCl, the protective effect of this additive decreased at pressure levels of over 400 MPa and temperatures above 293 K (data not shown, Table 6, Table 7 and Molina-Höppner, 2002).

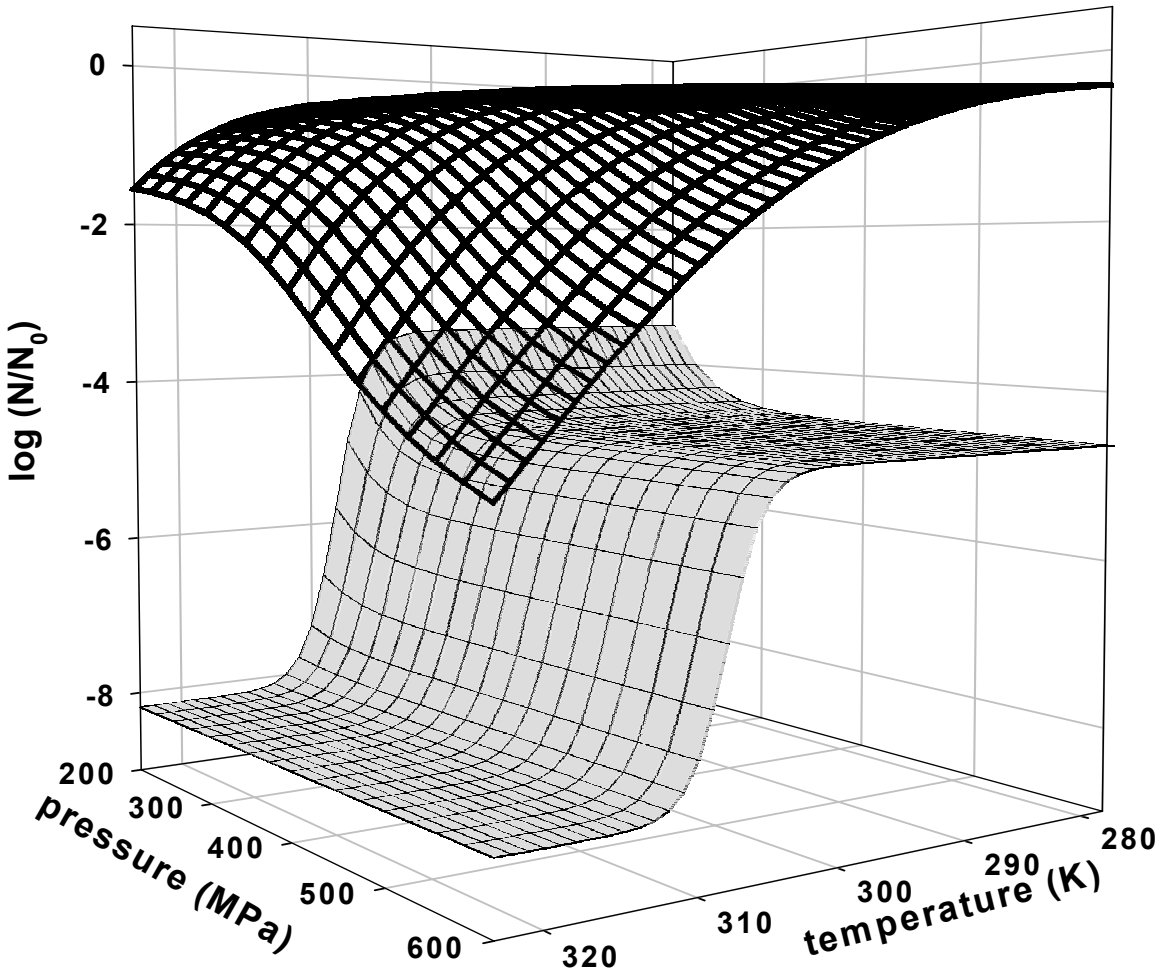


**Figure 44:** Predicted distributions of $\log(N/N_0)$ of viable cell counts (CFU) after pressure-temperature processing using sucrose (▭) or milk buffer (▭).

In general, stress resistant cell counts quantify the fraction of the population, which are not affected by the process and thus, showed a nearly one log difference to the viable cell counts of the analysed bacteria. As expected, the tailing behaviour also exists for this physiological state in milk buffer (Table 6, Table 7). For the baroprotections, unexpected behaviour of the population in the presence of NaCl occurred in the temperature range between 5 and 20°C (compare Figure 27). For sucrose, the sublethal injury effects became significant at 500 MPa and 30°C or temperatures greater than 40°C and a pressure level greater than 200 MPa (Table 6, Table 7).

In case of high pressure processing, the compression of the pressure fluid leads to a significant temperature increase. In isentropic cases the temperature increases approx. 2-3 K

per 100 MPa in pure $H_2O$. In real high pressure applications, however, the temperature increase is local and transient. Using biocrystals, the temperature distribution inside a high pressure autoclave could be visualised (Pehl et al., 2000; Pehl and Delgado, 2002; Özmutlu, 2005). Hartmann (2002), Hartmann and Delgado (2002), and Hartmann et al. (2004) developed a numerical technique that allows for simulations of thermofluiddynamics of high pressure processes. Thermal and hydrodynamic compensation time scales as well as a locally recorded temperature profiles are compared to measurements in laboratory and industrial scale and found to be in good agreement. Especially for this process uniformity and its effect on the inactivation of enzymes and microorganisms, investigations confirmed, that the activity is non-uniformly distributed throughout the HP-autoclave (Denys et al., 2000; Hartmann and Delgado, 2003). The temperature distribution in this process strongly influences the efficiency and homogeneity of the analysed process parameters. Hence, baroprotective media and too low processing temperature may locally prolongate bacterial survival.

The pressure inactivation of *Lactococcus lactis* was determined and calculated using a pressure range beetween 0.1 and 600 MPa, a temperature range of 5°C to 50°C, and as buffer systems milk buffer or milk buffer 1.5M sucrose or 4M NaCl (see above). The generation of the necessary parameters to solve the differential equation belonging to the Logistic equation were detected after the establishment of a smart transformation. This transformation converted the inactivation curves to the growth function.

After model establishment, deviations are visible in case of milk buffer and milk buffer sucrose if the parity plot of viable cell counts was analysed (Figure 38A and Figure 38B). In terms of milk buffer, huge deviations occured at a temperature of 278 K and a pressure of 200 and 300 MPa for both physiological states (CFU, CFUsub). Therefore, the assumption of symmetric distribution of the parameters m and $t_0$ seemed to be not correct. By the use of non-symmetric distributions like Weibull, this error may be eliminated. However, this modification will result in a very complex model which will end in too long calculation times and cost.

Furthermore, in case of sucrose, a further different inactivation behaviour was detected for CFU and CFUsub using 500 MPa/323 K and for CFUsub using 500 MPa/303 K. Therefore, a fast, followed by a slow inactivation of the population is visible. This means, that a fast inactivation took place after short pressurisation and after a critical process time, the existing

pressure resistant fraction was inactivated by the process. This phenomen was described in detail in Gänzle et al. (2001). To avoid this prediction failure, the proposed model of chapter 2.6.3 has to be extendend:

$$M(t) = \frac{M_s}{1 + \exp\left(-m_S\left(t_S - t_0\right)\right)} + M_R \exp(-m_R t_R), \tag{9}$$

where index S represents the coefficients of the sensitive fraction and R of the resistant fraction of the population. Due to the fact, that a simulation run needs at least 2 weeks with the simplified model, this extention was not taken into account. Furthermore, the inactivation of the baroresistant fraction took place using a process time of about 30 min or more. In industrial application, the process should be limited to about 20 min or shorter (Baars et al., 2004). For all data of viable cells predicted in milk buffer NaCl , the deviation of the model predictions from the measured values is smaller than the experimental error (Figure 38A). In case of NaCl and CFUsub, the operating characteristic curve (which described also a symmetric distribution) represented the best quality of symmetric fit. If a non-symmetric fit like Weibull would be used, it may also end in high computational cost and capacity.

In general, the results achieved in the 3.3-litre-medium-sized pressure-autoclave detected at two different locations comprised spatiotemporal heterogenities on the temperature-distribution and the inactivation of the bacteria. A maximum of Δ-1-log between the upper and the lower probes is obtained by both, the experiments and the numerical simulations. Furthermore, very good agreement between the experimental and numerical results were obtained (Figure 43). Comparing these result with data belonging to model generation, a better correlation was achieved. Therefore, reasons were found in the used temperature range: In this part of the work, no temperature below 20°C was used. Therefore, one error type was eliminated. Further on, the process time was limited to 12 min. With this setting, no process induced reduction of a resistant fraction took place.

Despite these findings, a few outliers are obvious for CFU and CFUsub. One typical errror occurs due to the proposed type of model. First, the calculated temperature distribution seems to be incorrect if the calculated temperatures measured at the bottom of the autoclave are compared with the measured ones. Therefore, the deviation exceeded the calculated standard deviation of 1.2 K obtained out of all experiments. Hartmann et al. (2004) explained that underestimation due to the asymmetry of the real geometry (inlet is 10 mm off the central

axis) which is not accounted for in the simulation as well as the presence of the fixture including the lower ring that may interfere with the local flow field. On the other side, an excellent agreement between measured and calculated temperatures was found in the upper part of the autoclave (Figure 45).

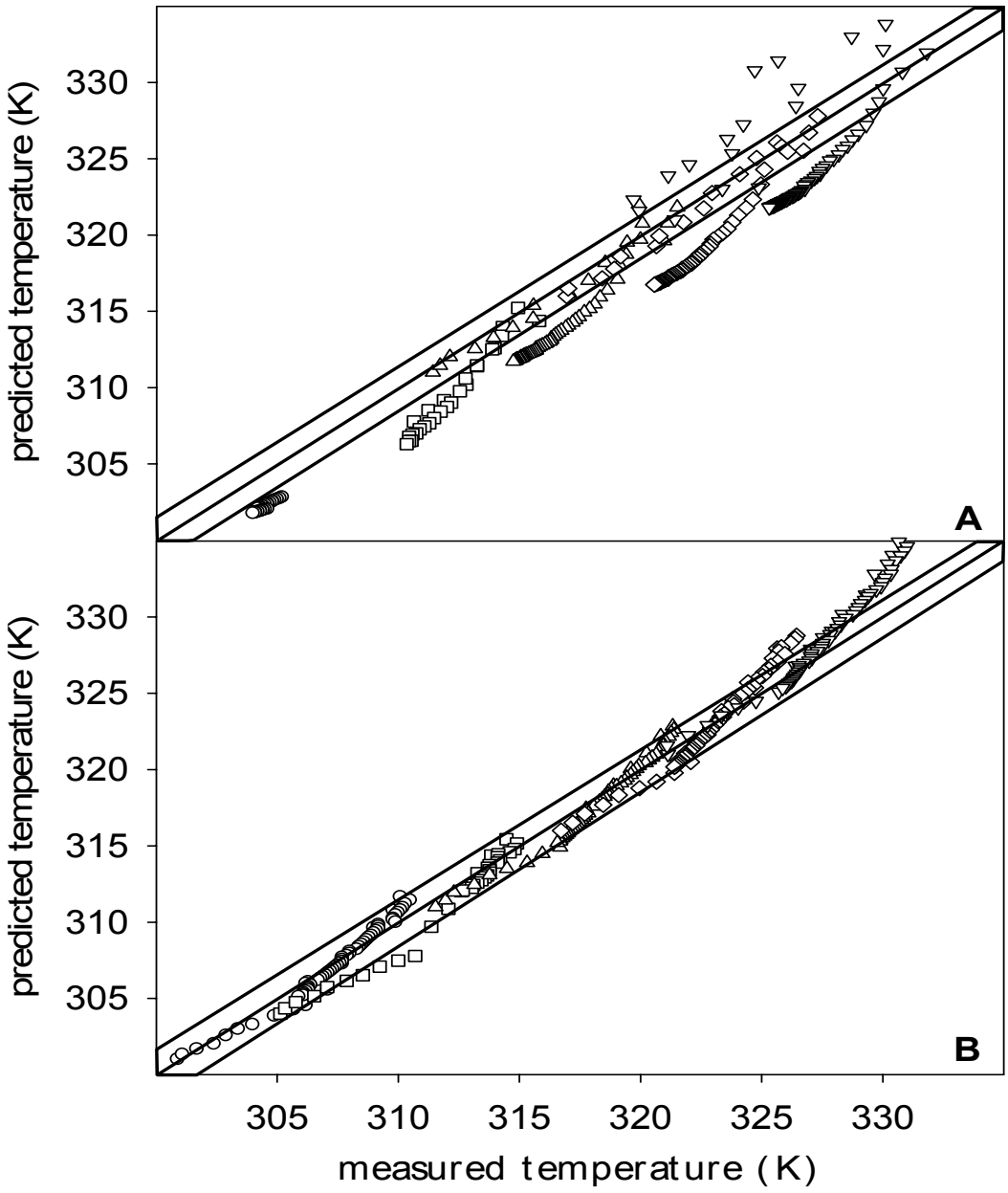


**Figure 45**: Comparison of measured and predicted temperature at the bottom (A) and the top (B) of the medium-size high-pressure vessel. Shaded areas indicate the deviation explained by overall experimental errors. 30°C (○), 33°C (□), 40°C (Δ), 45°C (◊) and 50°C(∇) initial temperature.

For the first time, the process heterogeneity of HP-induced biological conversion in an industrial sized high-pressure autoclave was confirmed in both ways, experimentally and numerically. Furthermore, the combination of this state-of-the-art modelling techniques and numerical simulations enabled highly precise prediction of the mass conversion process, i.e. inactivation process of microorganisms. The heterogeneity of the mass conversion processes was found to have a strong influence on the quality of the products. If the high pressure techniques are to be applied in the food industry, the process non-uniformity has to be reduced, so that the quality of the treated substances can be assured.

The examples shown in this work discussed the treatment of small packed systems. Using the PCR-tubes with good heat transfer properties, the temperature of the probes inside of the tubes were assumed to be equal to that of the surrounding fluid. Thus, the temperature and pressure are used as a local and transient parameter. In that case, the differential equation concerning the inactivation is solved at two different locations with a self written FORTRAN 90 program (Kitsubun, 2005).

Overall, three buffer systems were studied describing neutral or different kinds of baroprotective media. In this work, the use of bactericidal additive was not studied, because the same results parallel to those in milk buffer may then be achieved, only much faster (due to the synergistic effect to pressure). In the case with milk buffer representing neutral food matrix, the desired 5D reduction of viable cell counts was achieved throughout the whole autoclave at relatively low temperatures (30°C and 33°C).

In the two worst case scenarios with extremely high sodium chloride (4M) and sucrose (1.5M) concentrations, the demanded 5D concept was achieved for stress resistant cell counts at temperatures of 45°C and pressure holding time longer than 4 min, at least in the upper part of the autoclave. In most of the cases, viable cell count reduction of 5 log was not achieved with a temperature of 45°C. Higher temperatures contributed to the desired 5D reduction for both buffer systems. Thus, for food matrix with higher salt or sugar concentrations, high pressure processes at higher temperatures with longer pressure holding time should be considered to obtain the demanded quality of food. However, such high concentrations of sucrose and NaCl can hardly be found in industrial applications. Smaller salt and sugar concentrations mean less baroprotection and more inactivation (compare Table 11). This data was measured when a temperature of 20°C was used and should be illustrated in Table 11 (Molina-Höppner, 2002). Most of the $M_{Max}$-values are greater than 0.5 representing the

desired 5D reduction. Furthermore, shortened pressure application may be achieved with a temperature upshift to a minimum of 40°C. Furthermore, using a pressure level of 600 MPa, the process seems to be adequate for each analysed configuration using this temperature.

**Table 11**: Parameter combinations used for the detection of inactivation kinetics due to their concentration of NaCl and sucrose. Shown are data for viable cell counts detected at 20°C in laboratory-scale out of Molina-Höppner (2002).

| T (K) | pressure (MPa) | pressure holding time (s) | pressure medium | $M_{Max}$ | $t_0$ (s) | m ($s^{-1}$) |
|---|---|---|---|---|---|---|
| 293 | 400 | 0 - 3840 | 1 M NaCl | 0,57 | 314,07 | 97,71 |
| | | | 2 M NaCl | 0,55 | 389,23 | 97,71 |
| | | | 3 M NaCl | 0,25 | 486,91 | 138,84 |
| | 600 | 0 - 3960 | 1 M NaCl | 0,59 | 140,00 | 20,00 |
| | | | 2 M NaCl | 0,60 | 140,00 | 20,00 |
| | | | 3 M NaCl | 0,59 | 339,16 | 28,17 |
| | 400 | 0 - 3840 | 0,5 M sucrose | 0,42 | 289,04 | 24,76 |
| | | | 1 M sucrose | 0,05 | 4077,73 | 1500 |
| | 600 | 0 - 3960 | 0,5 M sucrose | 0,53 | 140 | 20,00 |
| | | | 1 M sucrose | 0,38 | 383,17 | 24,52 |

The findings animate the process design for industrial applications strongly due to the observed spatiotemporal heterogeneities on the temperature- and the inactivation-behaviour during the process. These phenomenon have to be seriously regarded especially in case of the production of safe and high quality food using high pressure technology.

A spatial temperature increase of approx. 2-3 K per 100 MPa was observed in water. Furthermore, the work of compression during pressure treatment will increase the temperature depending on the composition of the food. For example, in foods containing a higher amount

of fat (butter, cream, mayonnaise) the temperature increase will be even larger resulting in increased heterogeneity of the treated products (Rasanayagam et al., 2003). Comparing this with the results found in this work or with data generated out of packaged food (where the fluid movement is hampered), temperature heterogeneities have to be taken into account.

### 4.5.3. Advantage and Disadvantage of Both Tools

The prediction of pressure-induced lethal and sublethal cell damage in practical applications require the availability of suitable mathematical models that are based on large data sets that fully encompass single and combined effects of pressure and temperature. The Fuzzy model employed here enabled accurate predictions of the accelerated inactivation at both higher and lower temperatures. Thus, the model developed here has been shown to be a powerful tool for the prediction of bacterial inactivation at high pressure and high temperature conditions and to unravel mechanisms of bacterial lethal and sublethal injury. The great advantages of Fuzzy Logic are, that it copes with a large bandwidth in experimental data and it allows the elimination of obvious errors without change of the overall structure of the model. Furthermore, by the use of Fuzzy Logic, microbial phenomena were predicted easily due to the simple way of adding additional knowledge by just one linguistic rule. With the proposed model, it is possible to predict accurately all five physiological states in one run and it is possible to implement a huge amount of different buffer types. The most relevant problem of the Fuzzy Logic model consisted in the implementation to CFX. It seems to be difficult to develop a Fuzzy model as a finite differential code independent of time. Therefore, the Logistic equation was used for the implementation into CFX. The advantage of that system is the simple integration of the differential equation according to the Logistic equation. With this setting, it is possible to predict the inactivation of *L. Lactis* in dependence of the heterogeneous process. The disadvantage of that system is, that the additional implementation of a further buffer system is complex and time-consuming. Further on, the implementation of expert knowledge to such a model, e.g. describing the inactivation of the resistant fraction of the population, will end in the implementation of further equations resulting in elevated computational time and computational capacities.

### 4.5.4. Relevance for Industrial Practice

In general, it is known from previous contributions that microbial inactivation depends strongly on pressure, temperature and additives. However, only a few incomplete and empirical models exist accounting for these parameters in laboratory scale. Furthermore, no data or validated model exist for the process design of the inactivation of bacteria in a medium-scale high pressure autoclave taking into account the temperature heterogeneity as yet. In this work, clear effects of the heterogeneous temperature distribution were detected on the inactivation behaviour of *L. lactis*. In worst case, a difference of Δ-1-log cycles between the locally stored probes was detected. This effects on the population of *L. lactis* can be easily explained with the existing temperature gradient in the autoclave. In general, the fluid temperature is higher in the upper part and lower in the lower part of the autoclave. Therefore, in case of extrapolation on industrial-size-autoclaves, a much larger deviation of the inactivation behaviour has to be expected.

If this temperature gradient could be diminished, better product homogeneity can be secured. This can be achieved with several methods. The first method may be the insulation of the inner volume of the autoclave with some polymers like Polyetheretherketon (PEEK) or Polyoxymethylen (POM) reducing the heat transfer between the fluid and the steel wall. The numerical simulations by Hartmann et al. (2004) confirmed the positive effect of such heat insulation on the homogeneity of the system. Further on, for industrial applications the use of horizontal high pressure autoclaves should also be considered. The reduction of the total height of the autoclave by placing it horizontally should reduce the temperature gradient inside of the autoclave, leading to more product uniformity.

# 5. Summary

The aim of this thesis was to study the effect of temperature-co-solvent or combined pressure-temperature-co-solvent induced inactivation behaviour of bacteria. Therefore, the focus was set on the fermentative organism *Lactococcus lactis* ssp. *cremoris* MG 1363, which should be characterised on its physiological behaviour under extreme conditions. In addition, previously measured data sets were used (Molina-Höppner, 2002) to the pressure-temperature-co-solvent dependent inactivation kinetics that were determined in preparation of this work. Data Mining tools as well as differential equation tools have been used for this bacteria to extract as much information as possible out of the generated data and to describe its behaviour mathematically. The second part of the thesis represents a study about the detection of stress induced enzymes and their influence on the inactivation behaviour of contaminating *Escherichia coli* TMW 2.497.

The prolongation of temperature induced inactivation of *L. lactis* by the use of protective additives was verified by quantifying viable and stress resistant cell counts after the process as well as by the use of FT-IR spectroscopy during the temperature treatment. Therefore, different buffer systems namely milk bufffer, milk buffer 1.5M sucrose or milk buffer 4M NaCl and a temperature range between 40°C and 75°C was used to detect the protective effect of both additives. NaCl protects *L. lactis* more effective than sucrose. The inactivation kinetics followed the characteristics of sigmoid asymetric shapes with either with or without an initial shoulder effects. Nevertheless, a complete inactivation of the population was reached by the use of 65°C in each buffer. The protective effect was detected and assigned to the reduced $a_w$ in case of NaCl as well as the preferential hydration effect of proteins in carbohydrate solutions. These findings as well as the generated data were used to detect correlations between those physiological states as well as data describing protein unfolding behaviour under extreme temperature conditions. Therefore, FT-IR study was done using $D_2O$ and $D_2O$-1.5M sucrose. A powerful tool was found to describe the cumulative behaviour of all proteins in *L. lactis* and their conformational changes due to the process. The protective effect was proved by an D/H exchange as well as an advanced change from strucured to unstructered protein behaviour in the presence of $D_2O$. Sucrose hampered both reactions which were detected by amide I' and amide II and amide II' behaviour.

The effects of combined pressure-temperature and the above named buffer systems on the behaviour of *L. lactis* were characterised by the use of lethal and sublethal measurands,

namely viable cell counts, stress resistant cell counts, membrane integrity, metabolic activity and LmrP-activity.

The pressure-temperature kinetics differ from those obtained by the use of temperature alone. The inactivation kinetics followed the characteristics of sigmoid asymetric shapes with an initial shoulder and an inactivation phase followed by tailing. *L. lactis* exhibited maximum resistance to pressure when treated in milk buffer at a temperature that was approximately 6°C below the growth temperature. This temperature of maximum resistance was determined with all of the indicators of lethal or sublethal injury. Therefore, a complete inactivation of the population was only reached, if a temperature of higher or equal than 40°C was used. Temperatures below 30°C inhibit the inactivation of the complete population resulting in a resistant fraction of about $10^5$ bacteria. In the presence of 1.5M sucrose, the population was completely protected using temperatures below 20°C. At each pressure level and temperatures greater than 40°C, the population was sublethally injured after short pressurisation in the presence of this additive. The loss of viability just took place, if a pressure equal to 500 MPa or greater and temperatures equal or greater than 45°C were used. In case of 4M NaCl, *L. lactis* lost its ability to recover on the selective medium if temperatures below 20°C were used. Otherwise, the population was completely protected at elevated temperatures up to 400 MPa. In case of a pressure level greater than 400 MPa, the inactivation of *L. lactis* took place at each temperature, and it was strengthened by increasing temperatures.

The correlations detected in this work by PCA between viable cell counts and metabolic activity and LmrP and stress resistant cell counts were used in different ways.

First, a multi-layer Fuzzy Logic model was generated describing the pressure-temperature effects as well as the effect of 21 different varieties of milk buffer on *L. lactis*. Therefore, the autonomous output variables viable cell counts and LmrP activity have been defined. The remaining quantities were calculated mainly based on the autonomous output variables. Due to the fact, that the model accurately predicts all five physiological states, the detected findings by PCA were correct. These findings enable a more rapid data aquisition and additionally reduces computation time and computer capacities concerning industrial modelling. For example, the determination of viable and stress resistant cell counts provided information on the metabolic activity of the cells as well as the activity of MDR-transport enzymes involved in the resistance to bactericidal agents. Likewise, the determination of the

metabolic activity with tetrazolium salts can be used as a rapid screening of lethal pressure effects at various combinations of pressure, temperature, and co-solvents.

Second, inactivation data was recorded for the physiological states viable- and stress resistant cell counts in the presence of milk buffer, milk buffer 1.5M sucrose, or 4M NaCl in a 3.3-litre-medium-sized-high-pressure vessel at two different locations. Generated data out of the 10 ml vessel were used to establish a model using the Logistic equation. The time dependent first order differential equation of the Logistic function has then been used to describe the inactivation behaviour of *L. lactis*. Therefore, the focus was based on process induced spatiotemporal heterogeneties and their influence on the inactivation behaviour of *L. lactis*. The model was validated by microbiological data.

For the first time, the process heterogeneity of the mass conversion in an industrial-sized high-pressure autoclave could be confirmed both experimentally and numerically. Furthermore, the combination of this state-of-the-art modelling techniques and numerical simulations enabled highly precise prediction of the mass conversion process, i.e. inactivation process of microorganisms or enzymes. Overall, an excellent regression of $R^2$=0.95 or higher were achieved in this work.

The second part was focused on the behaviour of *Escherichia coli* and its ability to maintain a high intracellular pH to prevent damage to intracellular macromolecules, and to provide favourable conditions for intracellular enzymes. Three transport systems are known to contribute to the extrusion of protons in *E. coli*. Among these, the glutamate decarboxylation pathway is the most favourable because it stabilizes the internal pH without the expense of ATP, and neutralizes the external medium at low pH-values. The availability of glutamate strongly improved the survival of *E. coli* during post-pressure acid challenge. This improved acid tolerance correlated well to an improved ability of *E. coli* to restore a high intracellular pH after pressure treatment. Apparently, the enzymes required for the glutamate acid survival pathways remain functional even after pressure treatments that inactivate those enzymes, which are required to establish a transmembrane pH gradient with glucose as sole energy source. The utilisation of glutamate was enhanced in pressure treated cells compared to untreated cells, indicating induction or activation of the glutamate acid survival pathway. Adaptation of *E. coli* to mild acid conditions further improved the survival of *E. coli* to post-pressure acid exposure.

# 6. Zusammenfassung

Das Ziel der Arbeit stellte die Untersuchung temperatur- oder druck-temperatur- oder druck-pH-induzierter Inaktivierung von Bakterien in Abhängigkeit von verschiedenen Additiva zum Messsystem „Milchpuffer“ dar. Dabei kam der fermentative Organismus *Lactococcus lactis* ssp. *cremoris* MG 1363 sowie der Verderbsorganismus *Escherichia coli* TMW 2.497 zum Einsatz. Der Fokus der Arbeit lag auf *L. lactis* sowie der Analyse der druck-temperaturinduzierten Inaktivierung. Zusätzlich zu den in dieser Arbeit generierten Daten wurden Daten aus einer weiteren Doktorarbeit zur Hochdruckinaktivierung von *L. lactis* verwendet (Molina-Höppner, 2002). Beide Datensätze sollten mit Hilfe geeigneter Data Mining Methoden analysiert werden, um letztendlich weiteres Wissen aus den Daten zu extrahieren um ein Modell generieren zu können, welches die Detektion von thermisch induzierten Prozessungleichförmigkeiten bei der Hochdruckbehandlung von Lebensmitteln voraussagen kann. Der zweite Teil der Arbeit stellte die Detektion von stressinduzierter Resistenzmechanismen in *E. coli* und deren Einfluss auf die kombinierte Druck-pH-Inaktivierung dar.

Bei der Anlayse zur temperaturinduzierten Inaktivierung von *L. lactis* konnte durch den Zusatz von Protektiva wie Kochsalz bzw. Saccharose in molarer Konzentration ein Schutzeffekt im Vergleich zu Inaktivierungsdaten generiert in Milchpuffer bestätigt werden. Dabei bot die Zugabe von 4 M Kochsalz einen effektiveren Schutz wie der Zusatz von 1,5M Saccharose. Die dabei erzielten Kinetiken nahmen einen Verlauf an, bei dem entweder keine Inaktivierung und/oder eine Dezimierung der Population stattfanden. Eine komplette Reduktion der Population von *L. lactis* konnte in jedem Puffersystem ab 65°C beobachtet werden. Der Schutzeffekt lässt sich durch den reduzierten $a_w$-Wert in Gegenwart von Kochsalz sowie der Bildung einer proteinumlagerneden schützenden Hydrathülle in Gegenwart von Saccharose erklären. Dadurch musste in Gegenwart dieser Zusätze mehr Energie in Form von höheren Temperaturen aufgebracht werden, um den Zelltod von *L. lactis* zu forcieren. Weiterhin wurde die temperaturinduzierte Inaktivierung von *L. lactis* mit Hilfe der FT-IR-Spektroskopie untersucht. Dabei konnten konformationsspezifische Änderungen aller in *L. lactis* vorhandener Proteine detektiert werden. Der protektive Effekt von Saccharose konnte in der Form bestätigt werden, da erstens der D/H-Austausch und zweitens der Übergang des Ordnungsgrades der Proteine von strukturiert zu unstrukturiert durch den Zusatz verzögert werden konnte.

Die Effekte einer Druck-Temperaturbehandlung in den oben genannten Puffersystemen wurde mit Hilfe der physiologischen Parameter Anzahl überlebender Keime, Anzahl stressresistenter Keime, Metabolische Aktivität, Membranintegrität sowie der Aktivität von LmrP bestimmt. Die dabei erzielten Ergebnisse unterscheiden sich stark zu denen ermittelt bei der Temperaturinaktivierung. Die Inaktivierung lässt sich hierzu wie folgt beschreiben. In einem Temperaturbereich bis zu 30°C nehmen die Kinetiken einen sigmoiden Verlauf an. Dabei konnte immer eine Subfraktion von $10^5$-Keime detektiert werden, welche unabhängig von der Temperatur durch die Druckbehandlung in Milchpuffer erreicht wurde. Je nach angewandtem Druck- und Temperaturniveau konnte diese schneller erreicht werden. Wurde die Temperatur jedoch auf 40°C erhöht, so konnte dieses Phänomen nicht mehr gemessen werden. Somit konnte die Temperatur maximaler Resistenz von *L. lactis* gegen den angewandten Prozess durch Messung der physiologischen Parameter als auch durch die Modellierung bei einer spezifischen Temperatur von ca. 26-28°C ermittelt werden.

Durch den Zusatz von 1,5M Saccharose konnte die Population im Bereich von kleiner 40°C auf allen angewandten Druckebenen nahezu vollständig vor Inaktivierung bewahrt werden. Bei der Anwendung von 45°C und 50°C konnte ab 200 MPa eine subletale Schädigung und ab 500 MPa ein Verlust der Überlebensfähigkeit detektiert werden. In Gegenwart von 4M NaCl verliert *L. lactis* bei einer Temperatur von kleiner 20°C die Möglichkeit, auf Selektivmedium zu überleben. Andererseits konnte ab dieser Temperatur und bis 40°C ein kompletter Schutz der Anzahl überlebender Keime bis zu einem Druckniveau von 400 MPa gemessen werden. Im Bereich von 500 MPa oder mehr wird *L. lactis* in Gegenwart von 4M NaCl inaktiviert. Somit schützt der Zusatz von 1,5M Saccharose *L. lactis* effektiver vor einer Druck-Temperaturbehandlung.

Zur Anwendung von Data Mining sowie der Modellierung wurde der oben generierte Datensatz um einen existenten aus einer vorangehenden Doktorarbeit zu *L. lactis* erweitert (Molina-Höppner, 2002). Daraufhin wurden mit Hilfe einer Hauptkomponentenanlyse die relevanten physiologischen Parameter detektiert. Zusammenhänge konnten zwischen der Anzahl stressresisteneter Keime sowie der LmrP Aktivität als auch zwischen der Metabolischen Aktivität und der Anzahl überlebender Keime detektiert werden. Die Membranintegrität birgt keine weitere Information mit sich. Dieses Ergebnis wurde in zweifacher Hinsich genutzt.

Einerseits wurde ein mehrlagiges Fuzzy Logik Modell generiert. Dabei wurden die physiologischen Zustände LmrP-Aktivität als auch die Anzahl überlebender Keime mit Hilfe der Prozessparameter modelliert. Mit Hilfe der hierzu erzielten Ergebnisse konnten nahezu alle erzielten Ergebnisse zu den anderen gemessenen physiologischen Zuständen berechnet werden. Somit konnten letztendlich die Ergebnisse der Hauptkomponentenanalyse bestätigt werden, da die Validierungsdarten exzellent mit den gemessenen Daten übereinstimmten.

Andereseits wurde ein deterministisches Modell mit Hilfe der Logistischen Funktion für die Daten zu Milchpuffer und Milchpuffer 1,5M Saccharose als auch Milchpuffer 4M Kochsalz entworfen. Die hierbei gewonnen Parameter wurden zur Lösung der zugehörigen Differentialgleichung genutzt. Dabei konnte der Einfluss von thermisch induzierten Prozessungleichförmigkeiten bei der Hochdruckbehandlung auf Bakterien in einem 3,3-Liter Autoklaven gemessen als auch berechnet werden. Damit wurde erstmalig der Einfluss von Prozessungleichförmigkeiten auf das Inaktivierungsverhalten sowohl mathematisch als auch experimentell nachgewiesen. Dabei konnte eine Regression von $R^2$=0,95 oder besser erzielt werden.

Weiterhin wurde das Verhalten von *E. coli* sowie dessen Möglichkeit den intrazellulären pH-Wert zu stabilisieren analysiert, um prozessinduzierte Zellschädigung mit anschließendem Zelltod zu vermeiden. Dabei wurden drei Resistenzmechanismen analysiert. Als Ergebnis soll vermerkt werden, dass die Glutamatdecarboxylase nach der Hochdruckbehandlung den intrazellulären pH-Wert stabilisiert und somit ein Überleben von *E. coli* in pH 4 über 24h gewährleistet. Dabei wurde festgestellt, dass die glukose- als auch argininabhängigen Enzyme inaktiviert wurden, und keinen Beitrag am Überleben nach subletaler Druckbehandlung hatten. Weiterhin verlängerte die Adaption der *E. coli* Population an einen leicht sauren pH-Wert vor einer Druckbehandlung die Überlebensfähigkeit von *E. coli* wesentlich.

# 7. LITERATURE

Abee, T., Wouters, J. A. 1999. Microbial stress response in minimal processing. International Journal of Food Microbiology 50:65-91.

Aertsen, A., Vanoirbeek, K., De Spiegeleer, P., Sermon, J., Hauben, K., Farewell, A., Nystrom, T., Michiels, C. W. 2004. Heat shock protein-mediated resistance to high hydrostatic pressure in *Escherichia coli*. Applied and Environmental Microbiology 70:2660-2666.

Ahern, T. J., Klibanov, A. M. 1985. The mechanisms of reversible enzyme inactivation at 100°C. Science 228:1280-1284.

Alpas, H., Kalchayanand, N., Bozoglu, F., Sikes, A., Dunne, C. P., Ray, B. 1999. Variation in resistance to hydrostatic pressure among strains of food-borne pathogens. Applied and Environmental Microbiology 65:4248-4251.

Alpas, H., Kalchayanand, N., Bozoglu, F., Ray B. 2000. Interactions of high hydrostatic pressure, pressurization temperature and pH on death and injury of pressure-resistant and pressure-sensitive strains of foodborne pathogens. International Journal of Food Microbiology 60:33-42.

Ananta, E., Knorr, D. 2003. Pressure-induced thermotolerance of *Lactobacillus rhamnosus* GG. Food Research International 36:991-997.

Anonymous, 1997. Methodensammlung der Mitteleuropäischen Brautechnischen Analysenkomission (MEBAK) - Brautechnische Analysenmethoden, Selbstverlag der MEBAK, Band III, Freising, Germany.

Anonymous, 2001. Data Engine Überblick und Benutzerdokumentation. MIT GmbH Aachen, Germany.

Anonymous, 2003. Scientific criteria to ensure safe food. Committee on the review of the use of scientific criteria and performance standards for safe food, food and nutrition board, board on agriculture and natural resources. The national academic press, Washington, DC.

Arnold, S., Becker, T., Delgado, A., Emde, F., Enenkel, A. 2002. Optimizing high strength acetic acid bioprocess by cognitive methods in an unsteady state cultivation. Journal of Biotechnology 97: 133-145.

Asano, T., Le Noble W. J. 1978. Activation and Reaction Volumes in Solution. Chemical Reviews 78: 407-489.

Baars, A., Pereyra, N., Delgado, A., Margosch, D., Ehrmann, M., Vogel, R., Czerny, M., Schieberle, P., Meußdörffer, F. 2004. Adaptive High Hydrostatic Pressure Treatment – A Technique for Minimal Processing of Food. International Conference Engineering and Food, Montpellier, 07.03-11.03.2004.

Balny, C., Masson, P. 1993. Effects of High-Pressure on Proteins. Food Reviews International 9:611-628.

Barth, A., Zscherp, C. 2002. What vibrations tell us about proteins. Quarterly Reviews of Biophysics 35: 369-430.

Becker, T. M. 2002. Management of bioprocesses by means of modelling and cognitive tools. Habilitational Thesis, TU München.

Becker, T., Schmidt, H.-L. 2000. Data model for the elimination of matrix effects in enzyme-based flow injection systems. Biotechnology and Bioengineering 69: 377-384.

Bellgardt, K.-H. 2000. Some Modeling Basics. In: Bioreaction Engineering: Modeling and Control, K. Schügerl, K.-H. Bellgardt (eds.), Springer-Verlag Berlin Heidelberg New York, 3-5.

Benito, A., Ventoura, G., Casadei, M., Robinson, T., Mackey, B. 1999. Variation in resistance of natural isolates of *Escherichia coli* O157 to high hydrostatic pressure, mild heat, and other stresses. Applied and Environmental Microbiology 65:1564-1569.

Blackburn, C. D., Curtis, L. M., Humpheson, L., Billon, C., McClure, P. J. 1997. Development of thermal inactivation models for *Salmonella enteritidis* and *Escherichia coli* O157:H7 with temperature, pH and NaCl as controlling factors. International Journal of Food Microbiology 38:31-44.

Bolhuis, H., Molenaar, D., Poelarends, G., van Veen, H. W., Poolman, B., Driessen, A. J. M., Konings, W. N. 1994. Proton motive force–driven and ATP-dependent drug extrusion systems in multidrug resistant *Lactococcus lactis.* Journal of Bacteriology 176:6957-6964.

Bolhuis, H., Poelarends, G., van Veen, H. W., Poolman, B., Driessen, A. J. M., Konings, W. N. 1995. The lactococcal *lmrP* gene encodes a proton motive force-dependent drug transporter. Journal of Biological Chemistry 270:26092-26098.

Bolhuis, H., van Veen, H. W., Brands, J. R., Putman, M., Poolman, B., Driessen, A. J. M., Konings, W. N. 1996. Energetics and mechanism of drug transport mediated by the lactococcal multidrug transport LmrP. Journal of Biological Chemistry 271:24123-24128.

Brown, D., Rothery, P. 1993. Models in biology – Mathematics, Statistics and Computing. John Wiley, Chichester, UK.

Bryjak, J., Ciesielski, K., Zbicinski, I. 2004. Modelling of glucoamylase thermal inactivation in the presence of starch by artificial neural network. Journal of Biotechnology 114:177-185.

Buchner, J. 2005. Protein Folding Handbook. Wiley-VCH.

Butz, P., Edenharder, R., Garcia, A. F., Fister, H., Merkel, C., Tauscher, B. 2002. Changes in functional properties of vegetables induced by high pressure treatment. Food Research International 35:295-300.

Casadei, M. A., Manas, P., Niven, G., Needs, E., Mackey, B. M. 2002. Role of membrane fluidity in pressure resistance of *Escherichia coli* NCTC 8164. Applied and Environmental Microbiology 68:5965-5972.

Chang, Y. Y., Cronan Jr., J. E. 1999. Membrane cyclopropane fatty acid content is a major factor in acid resistance of *Escherichia coli*. Molecular Microbiology 33:249-259.

Cheftel, J. C. 1995. Review: High-pressure, microbial inactivation and food preservation. Food Science and Technology International 1:75-90.

Chen, Q., Mynett A. E. 2003. Integration of data mining techniques and heuristic knowledge in Fuzzy Logic modelling of eutrophication in Taihu Lake. Ecological Modelling 162:55-67.

Chilton, P., Isaacs, N. S., Manias, P., Mackey, B. M. 2001. Biosynthetic requirements for the repair of membrane damage in pressure-treated *Escherichia coli*. International Journal of Food Microbiology 71:101-104.

Choi, S. H., Baumler, D. J., Kaspar, C. W. 2000. Contribution of dps to acid stress tolerance and oxidative stress tolerance in *Escherichia coli* O157:H7. Applied and Environmental Microbiology 66:3911-3916.

Cody, S. H., Glynn, M. K., Farrar, J. A., Cairns, K. L., Griffin, P. M., Kobayashi, J., Fyfe, M., Hoffman, R., King, A. S., Lewis, J. H., Swaminathan, B., Bryant, R. G., Vugia, D. J. 1999. An outbreak of *Escherichia coli* O157:H7 infection from unpasteurized commercial apple juice. Annales of Internal Medicine 130:202-209.

Cole, M. B., Davies, K. W., Munro, G., Holyoak, C. D., Kilsby, D. C. 1993. A vitalistic model to describe the thermal inactivation of Lysteria monocytogenes. Journal of Industrial Microbiology 61:4389-4395.

Coroller, L., Leguerinel, I., Mafart, P. 2001. Effect of water activities of heating and recovery media on apparent heat resistance of Bacillus cereus spores. Applied and Environmental Microbiology 67:317-3122.

Crowe, J. H., Crowe, L. M., Chapman, D. 1984. Preservation of Membranes in Anhydrobiotic Organisms - the Role of Trehalose. Science 223:701-703.

Cui, S., Meng, J., Bhagwat, A. A. 2001. Availability of glutamate and arginine during acid challenge determines cell density-dependent survival phenotype of *Escherichia coli* strains. Applied and Environmental Microbiology 67:4914-4918.

Deboosere, N., Legeay, O., Caudrelier, Y., Lange, M. 2004. Modelling effect of physical and chemical parameters on heat inactivation kinetics of hepatitis A virus in a fruit model system. International Journal of Food Microbiology 93:73-85.

de Heij, W. B. C., van Schepdael, L. J. M. M., Moezelaar, R., Hoogland, H., Matser, A. M., van den Berg, R. W. 2003. High- Pressure Sterilization: Maximizing the Benefits of Adiabatic Heating. Food Technology 57:37-58.

Denys, S., van Loey, A. M., Hendrickx, M. E. 2000. A modelling approach for evaluating process uniformity during batch high hydrostatic pressure processing: combination of a numerical heat transfer model and enzyme inactivation kinetics. Innovative Food Science and Emerging Technologies 1:5-19.

Devlieghere, F., Francois, K., Vereecken, K. M., Geeraerd, A. H., Van Impe, J. F., Debevere, J. 2004. Effect of chemicals on the microbial evolution in foods. Journal of Food Protection 67:1977-1990.

Diels, A. M., Wuytack, E. Y., Michiels, C. W. 2003. Modelling inactivation of *Staphylococcus aureus* and *Yersinia enterocolitica* by high-pressure homogenisation at different temperatures. International Journal of Food Microbiology 87:55-62.

Diez-Gonzalez, F., Karaibrahimoglu, Y. 2004. Comparison of the glutamate-, arginine- and lysine-dependent acid resistance systems in *Escherichia coli* O157:H7. Journal of Applied Microbiology 96:1237-1244.

Ehrmann, M. A., Scheyhing, C. H., Vogel, R. F. 2001. *In vitro* stability and expression of green fluorescent protein under high pressure conditions. Letters in Applied Microbiology 32:230-234.

Erkmen, O. 2001. Mathematical modeling of *Escherichia coli* inactivation under high-pressure carbon dioxide. Journal of Bioscience and Bioengineering 92:39-43.

Esterl, S., Ozmutlu, O., Hartmann, C., Delgado, A. 2003. Three-dimensional numerical approach to investigate the substrate transport and conversion in an immobilized enzyme reactor. Biotechnology and Bioengineering 83:780-789.

Evans, M. G., Polanyi, M. 1935. Some applications of the transition state method to the calculation of reaction velocities, especially in solution. Transactions of the Faraday Society 31: 875.

Ewald, T., Delgado, A., Becker, T. 2003. Fuzzy state controller for the soft process drying of natural material foil. Engineering Life Science 3: 21-29.

Fachin, D., Van Loey, A., Indrawati, A., Ludikhuyze, L., Hendrickx, M. 2002. Thermal and high-pressure inactivation of tomato polygalacturonase: A kinetic study. Journal of Food Science 67:1610-1615.

Fayyad, U. M. 1996. Advances in knowledge discovery in data mining. AAAI Press. Menlo Park, Californien, USA.

Gänzle, M. G., Ulmer, H. M., Vogel, R. F. 2001. High pressure inactivation of *Lactobacillus plantarum* in a model beer system. Journal of Food Science 66:1174-1181.

Gänzle, M. G., Vogel, R. F. 2001. On-line fluorescence determination of pressure mediated outer membrane damage in *Escherichia coli*. Systematic and Applied Microbiology 24:477-85.

Garcia-Graells, C., Hauben, K. J., Michiels, C. W. 1998. High-pressure inactivation and sublethal injury of pressure-resistant *Escherichia coli* mutants in fruit juices. Applied and Environmental Microbiology 64:1566-1568.

Geeraerd, A. H., Herremanns, C. H., Ludikhuyze, L. R., Hendrickx, M. E., Van Impe, J. F. 1998. Modeling the kinetics of isobaric-isothermal inactivation of Bacillus subtilis α-amylase with artificial neural networks. Journal of Food Engineering 36:263-279.

Gervilla, R., Felipe, X., Ferragut, V., Guamis, B. 1997. Effect of high hydrostatic pressure on *Escherichia coli* and *Pseudomonas fluorescens* strains in ovine milk. Journal of Dairy Science 80:2297-2303.

Gilmanshin, R., Gulotta, M., Dyer, R. B., Callender, R. H. 2000. Structures of Apomyoglobin´s Various Acid-Destabilized Forms. Biochemistry 40:5127-5136.

Goh, S., Newman, C., Knowles, M., Bolton, F. J., Hollyoak, V., Richards, S., Daley, P., Counter, D., Smith, H. R., Keppie N. 2002. *E. coli* O157 phage type 21/28 outbreak in North Cumbria associated with pasteurized milk. Epidemiology and Infection 129:451-457.

Goosens, K., Smeller, L., Frank, J., Heremans, K. 1996. Pressure-tuning the conformation of bovine pancreatic trypsin inhibitor studied by Fourier-transform infrared spectroscopy. European Journal of Biochemistry 236:236-262.

Gross, M., Jaenicke, R. 1994. Proteins under Pressure - the Influence of High Hydrostatic-Pressure on Structure, Function and Assembly of Proteins and Protein Complexes. European Journal of Biochemistry 221:617-630.

Harte, F., Amonte, M., Luedecke, L., Swanson, B. G., Barbosa-Canovas, G. V. 2002. Yield stress and microstructure of set yogurt made from high hydrostatic pressure-treated full fat milk. Journal of Food Science 67:2245-2250.

Hartmann, C. 2002. Numerical Simulation of Thermodynamic and Fluiddynamic Processes during the High Pressure Treatment of Fluid Food Systems. Innovative Food Science and Emerging Technologies 3:11-18.

Hartmann, C., Delgado A. 2002. Numerical simulation of convective and diffusive transport effects on a high-pressure-induced inactivation process. Biotechnology and Bioengineering 79: 94-104.

Hartmann, C., Delgado, A. 2003. The influence of transport phenomena during high-pressure processing of packed food on the uniformity of enzyme inactivation. Biotechnology and Bioengineering 82:725-735.

Hartmann, C., Delgado, A. 2004. Numerical simulation of the mechanics of a yeast cell under high hydrostatic pressure. Journal of Biomechanics 37:977-987.

Hartmann, C., Schuhholz, J. P., Kitsubun, P., Chapleau, N., Le Bail, A., Delgado, A. 2004. Experimental and numerical analysis of the thermofluiddynamics in a high-pressure-autoclave. Innovative Food Science and Emerging Technologies 5:399-411.

Hauben, K. J., Bartlett, D. H., Soontjens, C. C., Cornelis, K., Wuytack, E. Y., Michiels, C. W. 1997. *Escherichia coli* mutants resistant to inactivation by high hydrostatic pressure. Applied and Environmental Microbioligy 63:945-950.

Hauben, K. J., Bernaerts, K., Michiels, C. W. 1998. Protective effect of calcium on inactivation of *Escherichia coli* by high hydrostatic pressure. Journal of Applied Microbiology 85:678-684.

Hawley, S. A. 1971. Reversible pressure-temperature denaturation of chymotrypsinogen. Biochemistry 10:2436-2442.

Heijnen, J. J. 1996. Macroscopic Approach and Mathematical Modelling of Microbial Processes. In: BODL-Advanced Course Microbial Physiology and Fermentation Technology, Delft.

Hendrickx, M., Ludikhuyze, L., Van den Broeck, I., Weemaes, C. 1998. Effects of high pressure on enzymes related to food quality. Trends in Food Science & Technology 9:197-203.

Hengge-Aronis, R. 2002. Signal transduction and regulatory mechanisms involved in control of the sigma(S) (RpoS) subunit of RNA polymerase. Microbiology and Molecular Biology Reviews 66:373-395.

Henrion, R., Henrion, G. 1995. Multivariate Datenanalyse. Springer-Verlag Berlin.

Huang, J., Nanami, H., Kanda, A., Shimizu, H., Shioya, S. 2002. Classification of fermentation performance by multivariate ananlysis based on mean hypothesis testing. Journal of Bioscience and Bioengineering 94:251-257.

Illeova, V., Polakovic, M., Stefuca, V., Acai, P., Juma, M. 2003. Experimental modelling of thermal inactivation of urease. Journal of Biotechnology 105:235-243.

imb Jena, w. D. Determination of Secondary Structure in Proteins by Fourier Transform Infrared Spectroscopy (FTIR), download 27.02.2005, URL: http://www.imb-jena.de/ImgLibDoc/ftir/IMAGE_FTIR.html.

Isaacs, N. S., Chilton, P., Mackey, B. 1995. Studies on the inactivation by high pressure of microorganisms, High Pressure Processing of Foods. Eds. D.A. Ledward, D.E. Johnston, R.G. Earnshaw, A.P.M. Hasting, Nottingham University Press, Nottingham.

Jischa, M. 1982. Konvektiver Impuls-, Wärme- und Stoffaustausch. Vieweg Braunschweig/Wiesbaden.

Jolliffe, I. T. 1986. Principal component analysis. Springer-Verlag, Berlin.

Jordan, S. L., Pascual, C., Bracey, E., Mackey, B. M. 2001. Inactivation and injury of pressure-resistant strains of *Escherichia coli* O157 and *Listeria monocytogenes* in fruit juices. Journal of Applied Microbiology 91:463-439.

Kalchayanand, N., Sikes, A., Dunne, C. P., Ray, B. 1998. Interaction of hydrostatic pressure, time and temperature of pressurization and pediocin AcH on inactivation of foodborne bacteria. Journal of Food Protection 61:425-431.

Karatzas, A. K., Kets, E. P. W., Smid, E. J., Bennik, M. H. J. 2001. The combined action of carvacrol and high hydrostatic pressure on *Listeria monocytogenes* Scott A. Journal of Applied Microbiology 90:463-469.

Kato, M., Hayashi, R., Tsuda, T., Taniguchi, K. 2002. High pressure-induced changes of biological membrane Study on the membrane bound Na+/K+-ATPase as a model system. European Journal of Biochemistry 269:110-118.

Kessler, H. G. 1996. Lebensmittel- und Bioverfahrenstechnik – Molkereitechnologie. Verlag A. Kessler. München.

Kiendl, H. 1997. Fuzzy Control methodenorientiert. Oldenbourg Verlag. München.

Kilimann, K. V., Hartmann, C., Delgado, A., Vogel, R. V., Gänzle M. G. 2005a. A Fuzzy Logic based model for the multi-stage high pressure inactivation of *Lactococcus lactis* ssp. *cremoris* MG 1363. International Journal of Food Microbiology 98:89-105.

Kilimann, K. V., Hartmann, C., Vogel, R. F., Gänzle, M. G. 2005b. Differential inactivation of glucose- and glutamate dependent acid resistance of *Escherichia coli* TMW 2.497 by high-pressure treatments, accepted in Systematic and Applied Microbiology.

Kim, B. H., Jang, A., Lee, S. O., Min, J. S., Lee, M. 2004. Combined effect of electron-beam (beta) irradiation and organic acids on shelf life of pork loins during cold storage. Journal of Food Protection 67:168-171.

Kitamura, Y., Itoh, R. 1987. Reaction volume of protonic ionization for buffering agents - prediction of pressure-dependence of pH and pOH. Journal of Solution Chemistry 16:715-725.

Kitsubun, P. 2005. Numerical Investigation of Thermofluiddynamical Heterogeneities during High Pressure Treatment of Biotechnological Substances. Doctoral thesis, Technische Universität München, Centre for Life and Food Sciences Weihenstephan.

Kneen, M., Farinas, J., Li, Y. X., Verkman, A. S. 1998. Green fluorescent protein as a noninvasive intracellular pH indicator. Biophysical Journal 74:1591-1599.

Knorr, D. 1996. Advantages, opportunities and challenges of high hydrostatic pressure application to food systems. High Pressure Bioscience and Biotechnology 279-287.

Kowalczyk, W., Hartmann, C., Delgado, A. 2004. Modelling and numerical simulation of convection driven high pressure induced phase changes. International Journal of Heat and Mass Transfer 47:1079-1089.

Krämer, J. 1997. Lebensmittel-Mikrobiologie. Ulmer Verlag. Stuttgart.

Krebbers, B., Matser, A. M., Koets, M., van den Berg, R. W. 2002. Quality and storage-stability of high-pressure preserved green beans. Journal of Food Engineering 54:27-33.

Krone, A., Kiendl, H. 1996. Rule based decision analysis with Fuzzy-ROSA method. Proceedings of European Workshop on Fuzzy Decision Analysis for Management, Dortmund 109-114.

Lanza, M., Priamo, W. L., Vladimir Oliveira, J., Dariva, C., de Oliveira, D. 2004. The effect of temperature, pressure, exposure time, and depressurization rate on lipase activity in SCCO2. Applied Biochemistry and Biotechnology 113-116:181-7.

Lee, D.-U., Heinz, V., Knorr, D. 2001. Biphasic Inactivation kinetics for *Escherichia coli* in liquid whole egg by high hydrostatic pressure treatments. Biotechnology Progress 1020-1025.

Linders, L. J. M., Wolkers, W. F., Hoekstra, F. A., Van ´t Riet, K. 1997. Effect of Added Carbohydrates on Membrane Phase Behavior and Survival of Dried *Lactobacillus plantarum*. Cryobiology 35:31-40.

Ludikhuyze, L. R., Van den Broeck, I., Weemaes, C. A., Herremans, C. H., Van Impe, J. F., Hendrickx, M. E., Tobback, P. P. 1997. Kinetics for isobaric-isothermal inactivation of Bacillus subtilis alpha-amylase. Biotechnology Progress 13:532-538.

Luo, S., Huang, C. F., McClelland, J. F., Graves, J. D. 1994. A Study of Protein Secondary Structure by Fourier Transform Infrared/Photoacoustic Spectroscopy and Ist Application for Recombinant Proteins. Analytical Biochemistry 216:67-76.

MacDonald, D. M., Fyfe, M., Paccagnella, A., Trinidad, A., Louie, K., Patrick, D. 1999. *Escherichia coli* O157:H7 outbreak linked to salami, British Columbia, Canada, 1999. Epidemiology and Infection 132:283-289.

Mackey, B. M., Forestiere, K., Isaacs, N. 1995. Factors Affecting the Resistance of *Listeria-Monocytogenes* to High Hydrostatic-Pressure. Food Biotechnology 9:1-11.

Mafart, P., Couvert, O., Leguerinel, I. 2001. Effect of pH on the heat resistance of spores comparison of two models. International Journal of Food Microbiology 63:51-6.

Mafart, P., Couvert, O., Gaillard, S., Leguerinel, I. 2002. On calculating sterility in thermal preservation methods: application of the Weibull frequency distribution model. International Journal of Food Microbiology 72:107-113.

Manas, P., Mackey, B. M. 2004. Morphological and physiological changes induced by high hydrostatic pressure in exponential- and stationary-phase cells of *Escherichia coli*: relationship with cell death. Applied and Environmental Microbiology 70:1545-1554.

Martens, H., Næs, T. 1989. Multivariate Calibration. Wiley. New York.

Masschalck, B., Van Houdt, R., Van Haver, E. G. R., Michiels, C. W. 2001a. Inactivation of gram-negative bacteria by lysozyme, denatured lysozyme, and lysozyme-derived peptides under high hydrostatic pressure. Applied and Environmental Microbiology 67:339-344.

Masschalck, B., Van Houdt, R., Michiels, C. W. 2001b. High pressure increases bactericidal activity and spectrum of lactoferrin, lactoferricin and nisin. International Journal of Food Microbiology 64:325-332.

Mattick, K. L., Jorgensen, F., Legan, J. D., Lappin-Scott, H. M., Humphrey, T. J. 2000. Habituation of *Salmonella* spp. at reduced water activity and its effect on heat tolerance. Applied and Environmental Microbiology 66:4921-4925.

Mattick, K. L., Jorgensen, F., Wang, P., Pound, J., Vandeven, M. H., Ward, L. R., Legan, J. D., Lappin-Scott, H. M., Humphrey, T. J. 2001. Effect of challenge temperature and solute type on heat tolerance of *Salmonella serovars* at low water activity. Applied and Environmental Microbiology 67:4128-4136.

McClements, J. M., Patterson, M. F., Linton, M. 2001. The effect of growth stage and growth temperature on high hydrostatic pressure inactivation of some psychrotrophic bacteria in milk. Journal of Food Protection 64:514-522.

Menter F. R. 1994. Two-Equation Eddy Viscosity Turbulence Model for Engineering Applications. AIAA Journal 32:1598-1605.

Mille, Y., Beney, L., Gervais, P. 2002. Viability of *Escherichia coli* after combined osmotic and thermal treatment: a plasma membrane implication. Biochimica et Biophysica Acta 1567:41-48.

Molina-Höppner, A. 2002. Physiological response of *Lactococcus lactis* to high pressure. Doctoral thesis, Technische Universität München, Centre for Life and Food Sciences Weihenstephan.

Molina-Höppner, A., Doster, W., Vogel, R. F., Gänzle, M. G. 2004. Protective effect of sucrose and sodium chloride for *Lactococcus lactis* during sublethal and lethal high-pressure treatments. Applied and Environmental Microbiology 70:2013-2020.

Molina-Gutierrez, A., Stippl, V., Delgado, A., Ganzle, M. G., Vogel, R. F. 2002. In situ determination of the intracellular pH of *Lactococcus lactis* and *Lactobacillus plantarum* during pressure treatment. Applied and Environmental Microbiology 68:4399-4406.

Motshwene, P., Karreman, R., Kgari, G., Brandt, W., Lindsey, G. 2004. LEA (late embryonic abundant)-like protein Hsp 12 (heat-shock protein 12) is present in the cell wall and enhances the barotolerance of the yeast *Saccharomyces cerevisiae*. Biochemical Journal 377:769-774.

Mozhaev, V. V., Heremans, K., Frank, J., Masson, P., Balny, C. 1994. Exploiting the Effects of High Hydrostatic-Pressure in Biotechnological Applications. Trends in Biotechnology 12:493-501.

Murnleitner, E., Becker, T., Delgado, A. 2002. State Detection and Control of Overloads in the Anaerobic Wastewater Treatment using Fuzzy Logic. Water Research 36: 201-211.

Noma, S., Hayakawa, I. 2003. Barotolerance of *Staphylococcus aureus* is increased by incubation at below 0 degrees C prior to hydrostatic pressure treatment. International Journal of Food Microbiology 80:261-264.

Olsen, K. N., Budde, B. B., Siegumfeldt, H., Rechinger, K. B., Jakobsen, M., Ingmer, H. 2002. Noninvasive measurement of bacterial intracellular pH on a single-cell level with green fluorescent protein and fluorescence ratio imaging microscopy. Applied and Environmental Microbiology 68:4145-4147.

O'Sullivan, F., O'Sullivan, J., Bull, A. M., McGregor, A. H. 2003. Modelling multivariate biomechanical measurements of the spine during a rowing exercise. Clinical Biomechanics (Bristol, Avon) 18:488-493.

Özmutlu, Ö. 2005. Visualization of temperature and velocity fields during phase change of water under high hydrostatic pressure. Doctoral thesis, Technische Universität München, Centre for Life and Food Sciences Weihenstephan.

Pagan, R., Mackey, B. 2000. Relationship between membrane damage and cell death in pressure-treated *Escherichia coli* cells: Differences between exponential- and stationary-phase cells and variation among strains. Applied and Environmental Microbiology 66:2829-2834.

Pagan, R., Jordan, S., Benito, A., Mackey, B. 2001. Enhanced acid sensitivity of pressure-damaged *Escherichia coli* O157 cells. Applied and Environmental Microbiology 67:1983-1985.

Park, S. W., Sohn, K. H., Shin, J. H., Lee, H. J. 2001. High hydrostatic pressure inactivation of *Lactobacillus viridescens* and its effects on ultrastructure of cells. International Journal of Food Science and Technology 36:775-781.

Pehl, M., Werner F., Delgado A. 2000. First Visualisation of Temperature Fields in Liquids at High-pressure Using Thermochromic Liquid Cristals. Experiments in Fluids 29:302-304.

Pehl, M., Delgado, A. 2002. Experimental Investigation on Thermofluiddynamical Processes in Pressurized Substances, In: Hayashi R, editor. Trends in High Pressure Biosci Biotechnol. Amsterdam: Elsevier, 429-435.

Penniston, J. T. 1971. High hydrostatic pressure and enzymic activity: inhibition of multimeric enzymes by dissociation. Arch Biochem Biophys 142:322-332.

Periago, P. M., Fernandez, P. S., Salmeron, M. C., Martinez, A. 1998. Predictive model to describe the combined effect of pH and NaCl on apparent heat resistance of *Bacillus stearothermophilus*. International Journal of Food Microbiology 44:21-30.

Petermeier, H., Benning, R., Delgado, A., Kulozik, U., Hinrichs, J., Becker, T. 2002. Hybrid Model of the fouling process in tubular heat exchangers for the dairy industry. Journal of Food Engineering 55:9-17.

Planck, M. 1887. Über das Prinzip der Vermehrung der Entropie Annalen der Physikalischen Chemie 32:426-503.

Port, M., Abend, M., Romer, B., Van Beuningen, D. 2003. Influence of high-frequency electromagnetic fields on different modes of cell death and gene expression. International Journal of Radiation Biology 79:701-708.

Rasanayagam, V., Balasubramaniam, V. M., Ting, E., Sizer, C. E., Bush, C., Anderson, C. 2003. Compression heating of selected fatty food materials during high-pressure processing. Journal of Food Science 68:254-259.

Reis, O., Winter, R., Zerda, T. W. 1996. The effect of high external pressure on DPPC-cholesterol multilamellar vesicles: a pressure-tuning Fourier transform infrared spectroscopy study. Biochimica et Biophysica Acta 1279:5-16.

Richard, H. T., Foster, J. W. 2003. Acid resistance in *Escherichia coli*. Advances in Applied Microbiology 52:167-186.

Robey, M., Benito, A., Hutson, R. H., Pascual, C., Park, S. F., Mackey, B. M. 2001. Variation in resistance to high hydrostatic pressure and rpoS heterogeneity in natural isolates of *Escherichia coli* O157:H7. Applied and Environmental Microbiology 67:4901-4907.

Rohsenow, W. M., Hartnett, J. P., Ganić, E. N. 1973. Handbook of Heat Transfer Fundamentals. McGraw-Hill Book Company, New York.

Saad-Nehme, J., Bezerra, A. L., Fornells, L. A., Silva, J. L., Meyer-Fernandes J. R. 1997. A contribution of the mitochondrial adenosinetriphosphatase inhibitor protein to the thermal stability of the $F_0F_1$-ATPase complex. Zeitschrift für Naturforschung 52c:459-465.

Saad-Nehme, J., Silva, J. L., Meyer-Fernandes, J. R. 2001. Osmolytes protect mitochondrial $F(_0)F(_1)$-ATPase complex against pressure inactivation. Biochimica et Biophysica Acta 1546:164-170.

Scheyhing, C. H., Hörmann, S., Ehrmann, M. A., Vogel, R. F. 2004. Barotolerance is inducible by preincubation under hydrostatic pressure, cold-, osmotic- and acid-stress conditions in *Lactobacillus sanfranciscensi*s DSM 20451T. Letters in Applied Microbiology 39:284-289.

Schlegel, H. G. 1992. Alllgemeine Mikrobiologie. Thieme Verlag. Stuttgart.

Silvius, J. R., McElhaney, R. N. 1980. Membrane lipid physical state and modulation of the Na+,Mg2+-ATPase activity in Acholeplasma laidlawii B. Proceedings of the National Academy of Science USA 77:1255-1259.

Small, P., Blankenhorn, D., Welty, D., Zinser, E., Slonczewski, J. L. 1994. Acid and base resistance in *Escherichia coli* and *Shigella flexneri*: Role of rpoS and growth pH. Journal of Bacteriology 176:1729-1737.

Smeller, L., Rubens, P., Frank, J., Fidy, J., Heremans, K. 2000. Two-dimensional Fourier-transform infrared correlation spectroscopy study of the high-pressure tuning of proteins. Vibrational Spectroscopy 22:119-125.

Smeller, L., Meersman, F., Fidy, J., Heremans, K. 2002. High-Pressure FTIR Study of the Stability of Horseradish Peroxidase. Effect of Heme Substitution, Ligand Binding, Ca++ Removal and Reduction of the Disulfide Bonds. Biochemistry 42:553-561.

Smeller, L. 2002. Pressure-temperature phase diagrams of biomolecules. Biochimica et Biophysica Acta 1595:11-29.

Smelt, J. P., Hellemons, J. C., Wouters, P. C., van Gerwen, S. J. 2002. Physiological and mathematical aspects in setting criteria for decontamination of foods by physical means. International Journal of Food Microbiology 78:57-77.

Snyder, G. R. 1961. Vibrational spectra of crystalline n-paraffins. Journal of Molecular Spectroscopy 7:116-144.

Sola-Penna, M., Meyer-Fernades, J. R. 1994. Protective role of trehalose in thermal denaturation of yeast pyrophosphatase. Zeitschrift für Naturforschung 49c:327-330.

Somero, G. N. 1995. Proteins and temperature. Annual Review of Physiology 57:43-68.

Sonoike, K., Setoyama, T., Kuma, Y., Kobayashi, S. 1992. Effect of pressure and temperature on the death rates of *Lactobacillus casei* and *Escherichia coli*. Balny, C., Hayashi, R., Heremans, K., Masson, P. (eds.). High pressure and Biotechnology 224:279-301.

Spurk, J. H. 2004. Strömungslehre, Einführung in die Theorie der Strömungen. 5. Auflage, Springer-Verlag, Berlin Heidelberg.

Stephens, P. J., Cole, M. B., Jones, M. V. 1994. Effect of heating rate on the thermal inactivation of *Listeria monocytogenes*. Journal of Applied Bacteriology 77:702-708.

Stewart, C. M., Jewett, F. F., Dunne, C. P., Hoover, D. G. 1997. Effect of concurrent high hydrostatic pressure, acidity and heat on the injury and destruction of *Listeria monocytogenes*. Journal of Food Safety 17:23-36.

Stippl, V., Delgado, A., Becker, T. 2002. Optical Method for the in-situ measurement of pH-value during high pressure treatment of foods. High Pressure Research 22: 757-761.

Stippl, V. 2005. Optical In-Situ Measurement of the pH-Value During High Pressure Treatment of Fluid Food. Doctoral thesis, Technische Universität München, Centre for Life and Food Sciences Weihenstephan.

Takeda, N., Kato, M., Taniguchi, Y. 1995a. Pressure-Induced Secondary Structure Changes of Ribonuclease A and Ribonuclease S Studied by FTIR Spektroskopy. Biospectroskopie 1:207-216.

Takeda, N., Kato, M., Taniguchi, Y. 1995b. Pressure and Thermally-Induced Reversible Changes in the Secondary Structure of Ribonuclease A Studied by FTIR Spektroskopie. Biochemisrtry 34:5980-5987.

ter Steeg, P. F., Hellemons, J. C., Kok, A. E. 1999. Synergistic actions of nisin, sublethal ultrahigh pressure, and reduced temperature on bacteria and yeast. Applied and Environmental Microbiology 65:4148-4154.

Timasheff, S. N. 1993. The Control of Protein Stability and Association by Weak-Interactions with Water - How Do Solvents Affect These Processes. Annual Review of Biophysics and Biomolecular Structure 22:67-97.

Ulmer, H. M., Gänzle, M. G., Vogel, R. F. 2000. High pressure effects on survival and metabolic activity of *Lactobacillus* p*lantarum* TMW 1.460. Applied and Environmental Microbiology 66: 3966-3973.

Ulmer, H. M., Heinz, V., Ganzle, M. G., Knorr, D., Vogel R. F. 2002a. Effects of pulsed electric fields on inactivation and metabolic activity of *Lactobacillus plantarum* in model beer. Journal of Applied Microbiology 93:326-335.

Ulmer, H. M., Herberhold, H., Fahsel, S., Gänzle, M. G., Winter, R., Vogel, R. F. 2002b. Effects of pressure-induced membrane phase transitions on inactivation of HorA, an ATP dependent multidrug resistance transporter, in *Lactobacillus plantarum*. Applied and Environmental Microbiology 68:1088-1095.

Vaidyanathan, S., White, S., Harvey, L. M., McNeil, B. 2003. Influence of morphology on the near-infrared spectra of mycelial biomass and its implications in bioprocess monitoring. Biotechnology and Bioengineering 82:715-724.

Vandeginste, B. G. M., Massart, D. L., Buydens, L. M. C., De Yong, S., Lewi, P., Smeyers-Verbeke, J. 1998. Data handling in science and technology. Handbook of chemometrics and qualimetrics Part A/Part B. Elsevier Science B.V.

Van den Broeck, I., Ludikhuyze, L. R., Van Loey, A. M., Weemaes, C. A., Hendrickx, M. E. 1999. Thermal and combined pressure-temperature inactivation of orange pectinesterase: influence of pH and additives. Journal of Agriculture and Food Chemistry 47:2950-2958.

Van Opstal, I., Vanmuysen, S. C., Michiels, C. W. 2003. High sucrose concentration protects *E. coli* against high pressure inactivation but not against high pressure sensitization to the lactoperoxidase system. International Journal of Food Microbiology 88:1-9.

Vogel, R. F., Ehrmann, M. A., Gänzle, M. G., Kato, C., Scheyhing, C., Molina-Gutierrez, A., Ulmer, H. M., Winter, R. 2003. Advances in High Pressure Response of Lactic Acid Bacteria. in: Winter, R. (ed.), High Pressure Bioscience and Biotechnology II, Springer Verlag, Berlin. 249-254.

Winter, R. 2002. Synchrotron X-ray and neutron small-angle scattering of lyotropic lipid mesophases, model biomembranes and proteins in solution at high pressure. Biochimica et Biophysica Acta 1595:160-184.

Wollenweber, M., Polster, J., Becker, T., Schmidt, H.-L. 1997. Application of Fuzzy Logic in multicomponent analysis by optodes. Biosensors & Bioelectronics 12: 917-923.

Wouters, P. C., Glaasker, E., Smelt, J. P. P. M. 1998. Effects of high pressure on inactivation kinetics and events related to proton efflux in *Lactobacillus plantarum*. Applied and Environmental Microbiology 64:509-514.

Wuytack, E. Y., Phuong, L. D., Aertsen, A., Reyns, K. M., Marquenie, D., De Ketelaere, B., Masschalck, B., Van Opstal, I., Diels, A. M., Michiels, C. W. 2003. Comparison of sublethal injury induced in *Salmonella enterica serovar Typhimurium* by heat and by different nonthermal treatments. Journal of Food Protection 66:31-37.

Xiong, R., Xie, G., Edmondson, A. E., Sheard, M. A. 1999. A mathematical model for bacterial inactivation. International Journal of Food Microbiology 46:45-55.

Yokota, A., Veenstra, M., Kurdi, P. van Veen, H. W., Konings, W. N. 2000. Cholate resistance in *Lactococcus lactis* is mediated by an ATP-dependent multispecific organic anion transporter. Journal of Bacteriology 182:5196-5201.

Yoo, C. K., Vanrolleghem, P. A., Lee, I. B. 2003. Nonlinear modeling and adaptive monitoring with fuzzy and multivariate statistical methods in biological wastewater treatment plants. Journal of Biotechnology 105:135-163.

Zimmermann, H. J. 1993. Fuzzy Technologien. VDI Verlag, Düsseldorf.

Mein besonderer Dank gilt:

Meinen beiden Betreuern Herrn Prof. Michael G. Gänzle und Herrn Prof. Christoph Hartmann für die hervorragende Betreuung, die zahlreichen Diskussionen, die „gute Laune“ Stimmung sowie die kritischen als auch humorvollen Korrekturen zu allen Veröffentlichungen.

Herrn Prof. Antonio Delgado und Herrn Prof. Rudi F. Vogel für die Überlassung des Themas sowie des Arbietsplatzes an beiden Instituten, die zahlreichen Anregungen, die fachlichen Diskussionen, das entgegengebrachte Vertrauen sowie der partnerschaftlichen Zusammenarbeit.

Herrn Priv. Doz. Dr. Wolfgang Doster für die Überlassung des Arbietsplatzes am Lehrstuhl für Experimentalphysik IV zur Messung der FT-IR Spektren, seine zahlreichen Anregungen und kritischen Beiträge, die Ermutigungen weiter zu machen, sowie der partnerschaftlichen Zusammenarbeit.

Herrn Prof. Alain Le Bail und Nicolas Chapleau für die Überlassung sowie die Unterstützung bei der Aufnahme der Daten zur Inaktivierung von *L. lactis* im 3,3 Liter Autoklaven sowie allen Mitarbeitern von ENITIAA für die freundliche Aufnahme sowie den sehr schönen Aufenthalt in Nantes.

Frau Dr. Adriana Molina-Höppner für die mikrobiologische Einarbeitung, ihrem Fachwissen sowie dem generierten Datensatz. Weiterhin soll Herrn Prof. Thomas Becker an dieser Stelle für die hervorragenden Diskussionen, die aufmunternden als auch aufbauenden Worte sowie der erbrachten fachlichen Unterstützung in jeglicher Hinsicht gedankt werden.

Allen Lehrstuhlangestellten des LFP/ITW sowie der TMW, all meinen Mathe-Studenten, Biotechnologie Studenten und studentischen Mitarbeitern für die wunderbaren Jahre, die gute kollegiale Zusammenarbeit, die lustigen Abende und Nächte.

Allen technischen Angestellten beider Institute: Walter Seidl, Joseph Rohrer, den Lehrlingen, Monika Hadek, Eva Leitner und Georg Maier für Ihre Unterstützung.

Freising, 25.07.2005 Klaus Valentin Kilimann